UNIVERSITAT ROVIRA I VIRGILI

ECONOMIC AND ENVIRONMENTAL VIABILITY OF CENTRAL SOLAR HEATING PLANTS WITH SEASONAL STORAGE IN THE EUROPEAN RESIDENTIAL SECTOR: A SYSTEMATIC MULTI-OBJECTIVE OPTIMIZATION APPROACH

Victor Tulus

UNIVERSITAT
ROVIRA i VIRGILI

Economic and environmental viability of central solar heating plants with seasonal storage in the European residential sector: A systematic multi-objective optimization approach

Victor Tulus

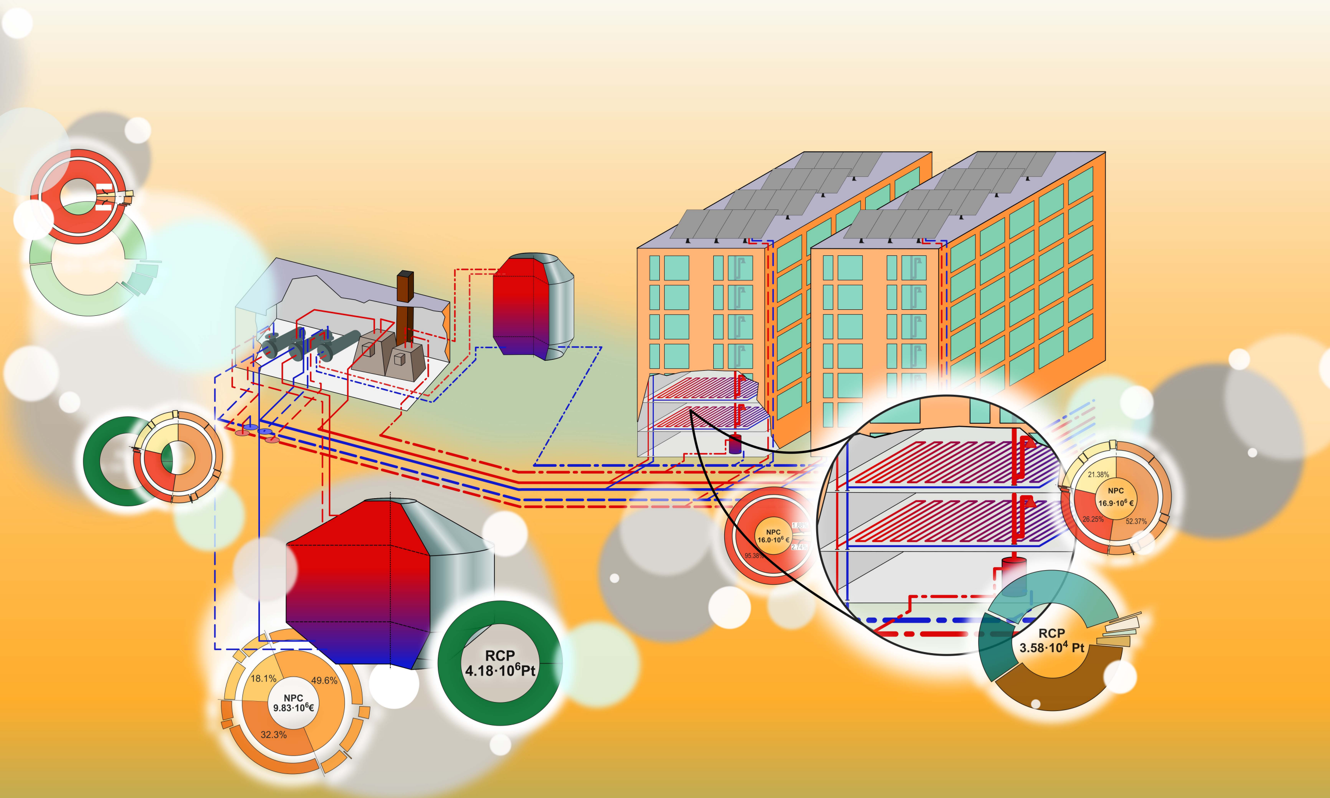

DOCTORAL THESIS
2018

Victor Tulus

Economic and environmental viability of central solar heating plants with seasonal storage in the European residential sector: A systematic multi-objective optimization approach

Doctoral Thesis

Supervised by:

Dr. Dieter-Thomas Boer

Dr. Laureano Jiménez Esteller

Dr. Gonzalo Guillén Gosálbez

DEPARTMENT OF CHEMICAL ENGINEERING

SUSCAPE RESEARCH GROUP

University Rovira i Virgili

Tarragona

2018

UNIVERSITAT ROVIRA i VIRGILI

We state that the present study, entitled "Economic and environmental viability of central solar heating plants with seasonal storage in the European residential sector: A systematic multi-objective optimization approach", presented by Victor Tulus for the award of the degree of Doctor, has been carried out under our supervision at the Department of Chemical Engineering of this university.

Tarragona, September 3rd 2018

Doctoral Thesis Supervisors:

Dr. Dieter-Thomas Boer

Dr. Laureano Jiménez Esteller

Dr. Gonzalo Guillén Gosálbez

ACKNOWLEDGEMENTS

Firstly, I would like to express my gratitude to my supervisors, Dr. Dieter Boer, Dr. Laureano Jiménez and Dr. Gonzalo Guillén Gosálbez for providing me with the opportunity to access the PhD program and being supportive, comprehensive and patient with me in the moments of difficulty.

I am grateful to my colleagues from SUSCAPE research group (fulltime members and visitors) for intellectually stimulating discussions, helpful advices, and for all the fun we have had in the last years. Special thanks go to Daniel, Ángel, Carlos, Claudia, Lucas.

I would like to extend my gratitude to all the doctorate students I had the pleasure to meet from other research groups at the University Rovira i Virgili, Manchester University, Imperial College and Carnegie-Mellon University.

I would like to express my very great appreciation to my dear friends, the ones I had before I started this chapter of my life and the ones I made during the journey. Thank you all, you are making me a better person.

I wish to thank my family, especially my parents, Vera and Grisha, and my sister Tanya for their immense support and encouragement throughout all these years of studying. Without you none of this would be possible. *Без вас ничего из этого не было бы возможным, я перед вами в огромнейшем долгу. Спасибо.*

Finally, I would like to thank those who started this journey with me or were close to me part way through and, unfortunately, did not finish it by my side. I like to believe that things happen for a reason and this is how it had to be.

Yours sincerely,

Victor/Vitěk/Витя

September 2nd, 2018

SUMMARY

With the start of the Anthropocene era, human-driven actions became noticeable on the scale of the planet; many of our unsustainable activities cause significant changes to the Earth's environment. Four of the nine planetary boundaries for sustainable development have already been overpassed, among them the most important are the climate change and biodiversity loss. To return to safe operating zone the scientists have established 6 key structural transformations to be tackled in the next decades. In this thesis we point to two of them: i) energy transformation, ii) urban sustainable transformation.

The global tendency for changing the world energy map is a booming topic, and more efforts should be scaled up to shift the current energy production systems towards the use of cleaner and less carbon-intensive sources. Currently, fossil fuels share about 80% of the primary energy use. Their high specific energy density and combustion temperatures up to 2500 ºC make them excellent energy carriers capable of meeting extreme energy demands. But unfortunately, large amounts of fossil fuels are used inefficiently to cover energy demands below 260 ºC, a large fraction of which belongs to the residential-commercial sector. According to the European Environment Agency, in 2013 this sector represented 40% of the total final energy consumption. In order to improve its energy efficiency, this sector should use alternative energy sources, particularly for space heating.

On top of that United Nations expects a global fast growing of the cities, with the urbanization reaching 66% by 2050. This will provoke significant increases in the world energy demands. The International Energy Outlook projects that the global energy consumption will evolve by 48% in 2040 with a growth in the usage of crude oil and natural gas by 30% and 53.2%, respectively. This outlook trend leads to serious environmental problems such as more greenhouse gas emissions and the subsequent impact on the climate.

Europe is one of the relevant players in this scenario contributing 21.6% to the overall energy consumption. Additionally, in the European Union the building stock

accounts for about 40% of the total energy demand, while the residential sector consumes 63% of this energy. According to estimations of the US Energy Information Administration, the energy consumption demand for the residential section in the EU increases by an average of 0.9% per year. Along with all these figures, the residential buildings are the fourth most important source of GHG in the EU and it accounted for about 10% of the total GHG in 2016. In response to this challenge, the EU has adopted the 2020 climate and energy package which includes a set of requisite legislation to tackle the environmental concerns and support the energy security and independence. The package sets three main targets: (i) reduce by 20% the GHG emissions compared to the 1990 levels, (ii) increase the renewable energy share and (iii) improve its energy efficiency by 20%. In 2013, the EU approved a new ambitious framework for the climate and energy between 2020 and 2030. This strategy plans to cut the GHG emissions by 40%, to achieve a share of at least 27% of renewable energies, and to improve the energy efficiency by at least 27%.

Over the past decades, various technologies based on renewable energy sources have been put forward as viable alternatives to the use of fossil fuels, including wind power, hydropower, waste energy, geothermal energy, bio energy, solar energy and energy storage. In the residential-commercial sector, and especially in large cities or inner city areas, these technologies can become even more competitive if they are integrated in an existing district heating network.

Among all the renewable energy resources, the solar thermal energy obtained a considerable attention since it is a CO_2 neutral and it can be used for both space and water heating. Apparently, the solar thermal technologies could satisfy substantially the heat demand in the residential sector in many countries. Furthermore, it has several advantages which include (i) savings in the primary energy consumption at the end user and country planning level, (ii) increase in energy security against the fluctuations in the prices of the conventional energy resources, (iii) decrease the dependency on the electricity from the network, and (iv) contribute to the network stabilization. These solar thermal energy systems continue to increase their market share across whole Europe. More than 1.2 $GW_{thermal}$ was installed within 2015 to raise the total installed capacity to 34.4 $GW_{thermal}$.

However, the solar thermal systems are facing a great challenge of intermittency and predictability, which cause a gap between the supply and the energy demand. The thermal energy storage (TES) systems can effectively solve this issue. There are three main categories of the TES. These categories include the sensible TES through a temperature gradient, the latent TES based on the phase change materials, and the thermo-chemical TES through chemical reactions. Currently, sensible storage is the most common system to be used in the residential sector, while latent and chemical systems are promising technologies under development.

To maximize the benefits from the central solar heating plants with seasonal and short-term storages in the residential sector, the optimal sizing of the system components and their operation should be planned properly. This can turn into a computationally requesting task.

The aim of this work was to develop a systematic multi-objective optimization (MOO) framework for optimizing the design of CSHPSS plants considering economic and environmental aspects simultaneously. To this end, a simulation-optimization methodology was developed based on a CSHPSS plant modeled in TRNSYS 18 that was optimized by a generic optimization tool (i.e. GenOpt) according to economic and environmental indicators. The latter objective was assessed through LCA principles, which quantify the impact caused in all the stages in the life cycle of the energy system. The inspiring numerical results showed that improvements in cost and environmental impact can be achieved simultaneously, comparing to a conventional heating system. With this knowledge we amplified the range of our study and investigated the optimal configurations of CSHPSS in different EU member states and identified forecast models for the cases which predict reductions in the cost of the installation of such systems in the near future. Moreover, with the expected growth of the prices of the primary non-renewable sources makes this type of plants even more attractive with the years.

In summary, the proposed methodology can serve as a supportive tool for decision- and policy-makers helping them assess the potential of the CSHPSS plants in Europe and subsequently, promote a clear statement towards the possibility of achieving the 2030 European climate and energy framework targets, and sustainable development.

Contents

LIST OF FIGURES

LIST OF TABLES

I OVERVIEW

1. BACKGROUND AND MOTIVATION

The world we are living in has always been going through series natural changes. Historically human-kind had no significant effect on the course of the events, on the global scale. Until recently, when the human-driven actions started to cause noticeable changes to the Earth's environment. This determined the beginning of a new era, the Anthropocene [1]. Since the beginning of this epoch (scientists arguable affirm that the Anthropocene started in the 1800's with the rise of the Industrial Revolution) the effects of humans have escalated drastically. The atmospheric carbon dioxide concentration is used by specialists to quantify the progression of the Anthropocene [2]. Its concentration went from the preindustrial value of 270 ppm to about 310 ppm by 1950. But the Great Acceleration occurred in the next 30 years; the CO_2 concentration reached 380 ppm. Almost 40 years later, the panorama has not changed significantly; on the contrary, continuous population growth and increase in the demands of primary resources together with the climatic problems ring the bell for immediate actions which should lead the modern society to a sustainable development. This development, defined by Brundtland Commission as the development "that meets the needs of the present without compromising the ability of future generations to meet their own needs" [3], represents a real challenge with not trivial steps to be taken. Usually these steps constitute tough sustainable challenges which should simultaneously satisfy three goals: the economic, environmental and social. The goals together represent the main pillars of sustainability [4] and their achievement requires initiatives, concrete actions, strong strategies, plans and policies to be generated. The decision- and policy-makers oversee the solution of these types of complex multi-stakeholder problems. In this context, unbiased, scientifically backed up information becomes a valuable argument capable of giving the push towards a faster transition to a sustainable future.

The impacts on the Earth system derived from human activities are putting our future at risk. To reverse the negative tendencies of the last decades, Rockström et al. [5] and Steffen et al. [2] suggested to impose planetary boundaries (see the current situation in Fig. I-1) which can be seen as global sustainable challenges. These 9 boundaries extend to: chemical pollution, load of atmospheric aerosols, biodiversity loss, change in land use,

use of global freshwater, biogeochemical flows (nitrogen and phosphorus cycles), stratospheric ozone depletion, ocean acidification, and climate change. According to the authors, 4 of the boundaries have already exceeded the safe operating zone. Two of those boundaries are considered of core importance for the maintenance of the current stable state, they are the climate change and the biodiversity loss. A significant perturbation of any of the planetary boundaries may provoke a chain reaction and destabilize the whole Earth system taking us to a new state.

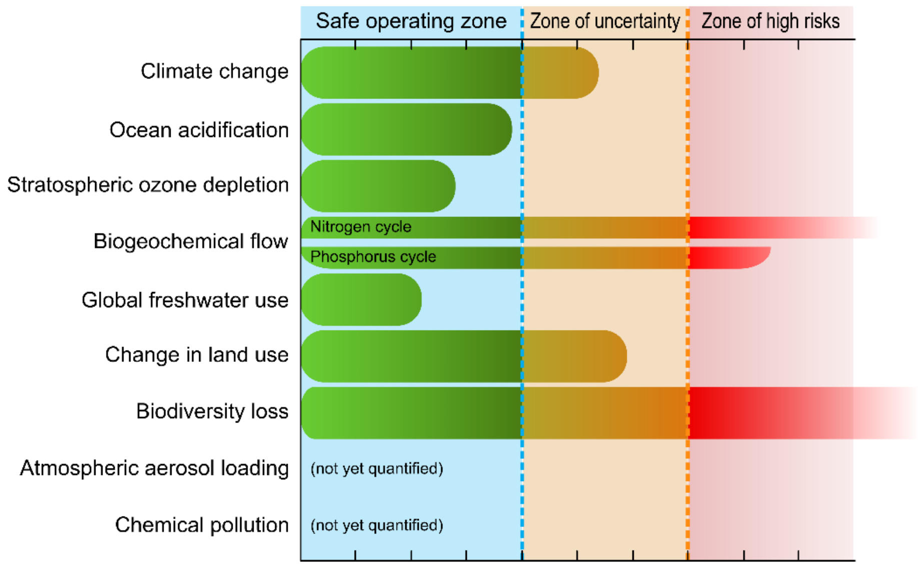

Fig. I-1. Current picture of the planetary boundaries suggested by Rockström [5].

The whole society must take responsibility in the transition to sustainable development, however, the key role on designing and promoting the strategies and policies lays on the governments and legislative bodies and businesses of all levels (local, national or international). Making wise decisions on all the types of complex problems arisen from that matter is extremely difficult since most likely the alternatives will affect multiple stakeholders with conflicting interests. The need of developing systematic tools to ease the decision-making process served as the main motivation for the realization of this thesis.

Rockström et al. [6] proposed 6 key structural transformations to be applied worldwide to move in the sustainable development trajectory. In this work, we point to two of those transformations:

i) Energy transformation, through installation of heating systems which help to shift towards a low-carbon economy;

ii) Urban sustainability transformation, supporting the installation of centralized heating systems in the residential sector.

The trends indicate that these two key structural transformations may become relevant in the near future as many of the global energy-related challenges will be solved in an urban context [7]. In the context of this thesis, the two transformations make reference to centralized solar heating plants with seasonal storage (CSHPSS). In section 1 of Chapters II and III the reader can find detailed information about CSHPSS systems and their background.

The use of technology in general can reverse the negative environmental trends by attacking the problem at its origin and alleviating the pressure over the environment [8]. This technology in particular helps in the transition towards a renewable energy use in the residential sector and the centralization of the equipment units provides a better use of the urban infrastructure and helps in the achievement of better managed cities. Since it is expected the global urbanization to grow up to 66% by 2050 [9], the installation of CSHPSS systems may cover the increase in energy demand by the new users. And providing renewable energy in a centralized manner can potentially increase the global effectiveness of the technology.

In this work the attention is centered in providing the best configurations of CSHPSS plants depending on the climatic conditions and the sizes of heating demands. Selection of the best configurations is done by the means of mathematical simulation-based optimization. The approach is based on the development of simulation models which are optimized using metaheuristic algorithms. A sensitivity analysis is performed on four of the case studies to give a deeper insight in the stability of the simulation-optimization model. Finally, a forecasting technique is applied in an attempt to provide future trends of deployment of CSHPSS plants in the European climates. Fig. I-2 summarizes the work developed in this thesis.

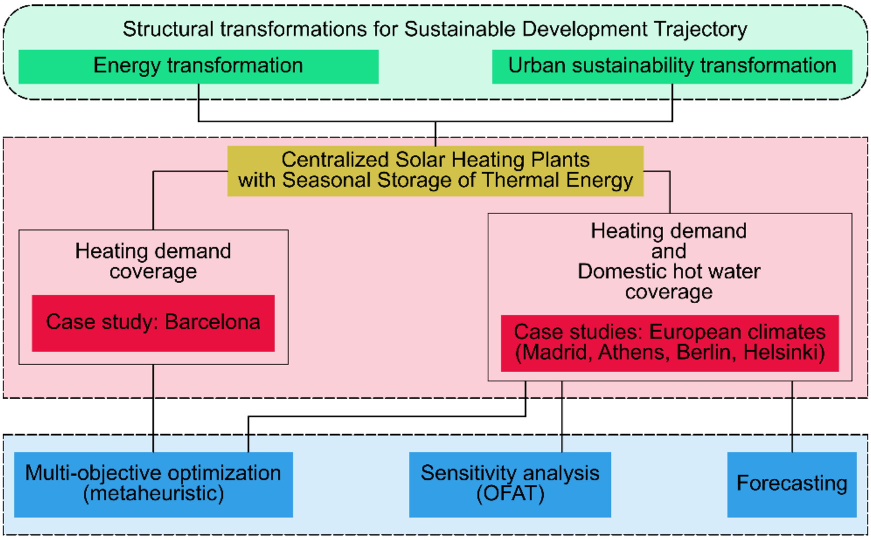

Fig. I-2. Thesis roadmap: the green rectangle shows the addressed structural transformations; the red rectangle includes tackled problems and the blue rectangle shows the used mathematical techniques.

This thesis is structured in 6 chapters. Chapter I show an overview of the whole work by introducing the sustainable challenges which act as a motivation, following with the general objectives of the thesis and background on the applied computational techniques. The chapter ends with a general outline of the case studies. Chapters II, III provide detailed information about the modeling of the CSHPSS, its optimization and discuss the proposed case studies. In the Chapter IV is briefly discussed the ongoing work on combi-systems similar to CSHPSS but in much smaller scale. In this case we are trying to optimize a system coupled to a single-family building constructed following the technology of Passivhaus. The model we have is based on a pilot plant and properly validated. Internal convergence issues with some equipment units did not allow us to follow with the optimization of this model. Chapter V covers the main conclusions and the future work. Finally, Chapter VI includes the appendices with the information about the author and his academic activities.

2. GENERAL OBJECTIVES

This work intends to bring a small contribution to the combat against challenging sustainability problems. The main goal is to generate systematic tools based on mathematical programming and optimization methods which can be used by decision-makers to address sustainability problems in the residential energy sector.

The following objectives have been accomplished in order to achieve the main goal:

- To develop systematic simulation-based multi-objective optimization approach for the designing of central solar heating plants with seasonal storage capable of simultaneously minimizing the overall cost of the system and its environmental impact.
- To study the suitability of central solar heating plants with seasonal storage for different European climatic conditions by generating and solving representative case studies.
- To determine the sensitivity of the developed simulation-optimization model to economic fluctuations.
- To provide future trends on the implementation of central solar heating plants with seasonal storage in Europe.

3. MATHEMATICAL PROGRAMMING

Mathematical programming refers to the building of mathematical models which describe real-world problems of different complexity and the designing of algorithms capable of finding the optimal solutions for those problems. In other words, mathematical programming provides the evaluation of a problem with the purpose of minimizing (or maximizing) a function by systematically identifying the best values for the variables of the model. Nowadays, the mathematical programming expanded beyond the academic interests and is widely used in engineering to provide scientifically based information for decision-making purposes. In process systems engineering (PSE) we distinguish two main modelling approaches: i) simultaneous approach (algebraic-based) and ii) sequential approach (simulation-based). For detailed review on simulation-based optimization methods which were predominantly used in this thesis, the reader is referred elsewhere [10].

The mathematical models for optimization problems following the simultaneous approach include a set of explicit algebraic equations which represent short-cut equipment units to simplify the optimization process and, to the maximum possible extent, avoid nonlinearities which are numerically challenging to solve. If the right assumptions were made, these simplifications show good approximations to the behavior of the real-world problems.

In the recent decades, the sequential approach started gaining importance due to the exponentially growing computational power and appearing of new simulation software. The simulations are capable of handling complex engineering problems with fewer simplifications, solving numerically nonlinear equations.

Simulation-optimization methods decompose the problem in two sub-problems: the simulation is performed by the specific software (e.g. TRNSYS) and the optimization is carried out by an external optimizer with an algorithm (e.g. GenOpt) which iterates with the simulation model until the termination criteria is met. Fig. I-3 shows an illustrative example of the connection between the different software in simulation-based optimization modelling. In some cases, to automate even further the connection between the simulator and the optimizer, MATLAB environment can be used.

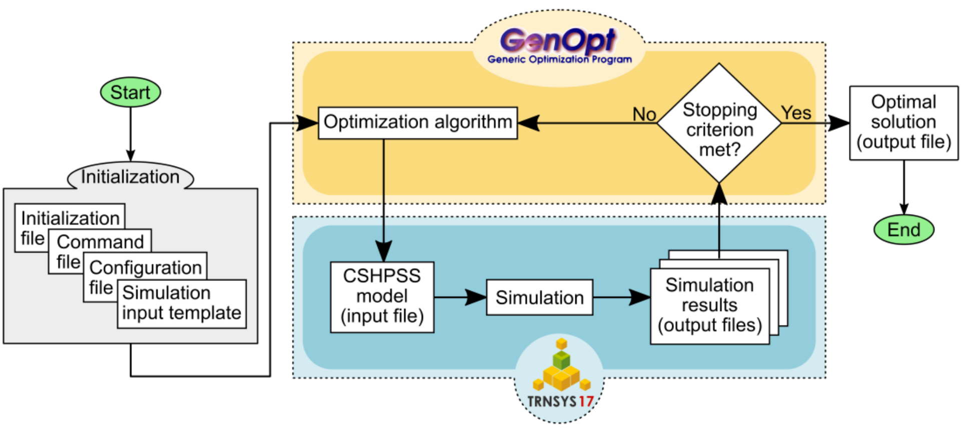

Fig. I-3. Connection between the simulation software TRNSYS and the optimization ‘engine’, GenOpt for the simulation-based optimization methodology.

Both types of mathematical models require explicit equations for the objective function (one or several) and the constraints (which can be implicitly defined in the case of simulation modelling). The objective function is the explicit equation which measures the quality of the proposed solutions. This is the main goal of the optimization. In engineering the objective function usually is an economic criterion (e.g. minimizing the cost), an environmental criterion (e.g. minimizing environmental impact) or social criterion (e.g. maximizing personal satisfaction). The constraints impose bounds on the variables (e.g. in simulation models nonnegative sizes of the equipment units).

In the next subsections we show the mathematical programming techniques which constitute the basis of this thesis. They are single-objective optimization (SOO) and multi-objective optimization (MOO).

3.1. Single-objective optimization problems

A generic single-objective optimization problem is generally stated in compact form [11] as follows:

$$\begin{aligned} \min \quad & f(x,y) \\ s.t. \quad & h(x,y) = 0 \\ & g(x,y) \leq 0 \\ & x \in \mathbb{R},\ y \in \mathbb{Z} \end{aligned} \qquad \text{(M I-1)}$$

where *f(x,y)* represents the objective function to be minimized and *x* and *y* represent the vectors of continuous and integer decision variables (if any), respectively. The feasible set of solutions is defined by the set of constraints imposing restrictions on variables where h(x,y) represents equality constraints whereas g(x,y) refers to inequality constraints.

A point (*x,y*) satisfying all constraints is a feasible solution to the problem. All feasible solutions constitute the feasible regions. The aim of the optimization is to satisfy the optimality criteria by selecting the best point from available feasible solutions. A point (x^*,y^*) from the feasible region ω is deemed as local minimum if the objective function takes the smallest value in some feasible neighborhood, that is, there exists a δ>0 such that $f(x^*,y^*) \leq f(x,y) \forall x,y \in \{\omega: |x-x^*| \leq \delta\}$. Often, in an optimization problem, there can be many local minima but only one global minimum is possible. A point (x^*,y^*) is a global minimum when the objective function takes the smallest value in all the feasible region, that is, $f(x^*,y^*) < f(x,y) \forall x,y \in \omega$.

3.2. Multi-objective optimization problems

The decision-making problems often consider several criteria simultaneously. A generic multi-objective optimization problem includes a simultaneous optimization of conflicting objective functions. In compact form the MOO problem can be presented as follows:

$$\begin{aligned} \min \quad & F = \{f_1, \ldots, f_n\} \\ s.t. \quad & h(x,y) = 0 \\ & g(x,y) \leq 0 \\ & x \in \mathbb{R},\ y \in \mathbb{Z} \end{aligned} \qquad \text{(M I-2)}$$

where F is the vector of n objective functions ranging from f_1 to f_n. The ideal solution containing the individual minimum of all objectives is referred to as the utopian point which is in general impossible to achieve due to the existing trade-off between the objectives. The worse value of all objectives is the nadir point. MOO offers a set of optimal solutions called Pareto frontier [12] with different trade-offs among the conflicting objectives, on the contrary of SOO which gives a single solution. A solution is said to be Pareto optimal when it is impossible to improve one of the objectives without worsening at least another objective. In essence, a set of solution x^* is said to be Pareto optimal for a MOO, if there is no other x in the feasible region such that $f_n(x) \leq f_n(x^*)$ for all $n \in \{1, \ldots, n\}$.

Fig. I-4 shows the concept of Pareto multi-objective optimality based on an illustrative optimization example where two objectives functions are simultaneously minimized. The green points constitute the Pareto frontier. Any point lying above the curve is sub-optimal since it can be improved in both objectives simultaneously. The unfeasible solutions are found below the Pareto curve, since none of those points perform better than the Pareto solutions in both indicators simultaneously. The anchor points are obtained by giving the full priority to one of the objectives at a time, they are (f_1^*, f_2^{1*}) and (f_1^{2*}, f_2^*). Moreover, the utopian and nadir points are referred as (f_1^*, f_2^*) and (f_1^{2*}, f_2^{1*}), respectively.

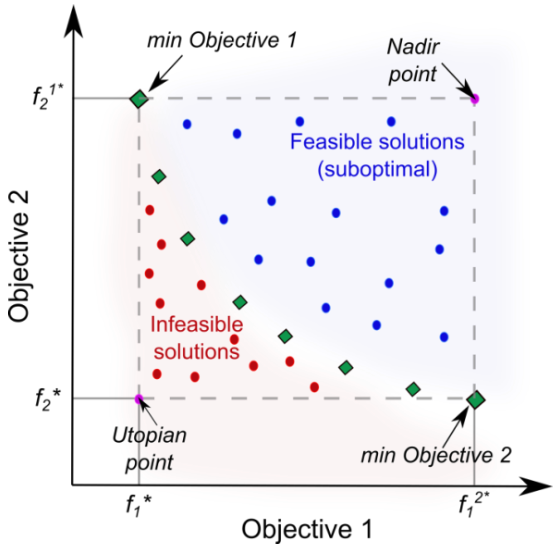

Fig. I-4. Schematic representation of the Pareto frontier for a two criteria multi-objective optimization problem.

The most commonly used methods for obtaining the set of Pareto optimal solutions are the weighted-sum and the epsilon constraint methods. In the weighted-sum method the weighted sums of the objectives constitute a new function which is optimized exploring the space of possible weights [13]. In the epsilon constraint method one objective is kept as a main objective function while the others act as auxiliary constraints which impose bounds on the main objective [13,14]. In this thesis we used the weighted-sum method due to an easy implementation, but it is worth noting that any other method could be implemented as well.

3.2.1. Weighted-sum method

The weighted-sum method consists of solving an auxiliary SOO model (M I-3) derived from the original MOO model. The auxiliary SOO model optimizes a lineal weighted sum of the original objectives which are previously normalized as shown in Eq. I-1.

$$\begin{aligned} \min_{x} \quad & WS = (1-\lambda)\overline{f}_1(x) + \dots + \lambda \overline{f}_n(x) \\ \text{s.t.} \quad & h(x) = 0 \\ & x^L \le x \le x^U \\ & 0 \le \lambda \le 1 \\ & x \in \mathbb{R}, \lambda \in \mathbb{R} \end{aligned} \qquad \text{(M I-3)}$$

Here, $\bar{f}_1(x)$ to $\bar{f}_n(x)$ are all the normalized objectives, and λ is the non-negative weight given to $\bar{f}_n(x)$.

$$\bar{f}_c(x) = \frac{f_c(x) - f_c^{UT}}{f_c^{PN} - f_c^{UT}} \quad \forall c = 1,2 \qquad \text{(I-1)}$$

where, f_c^{UT} denotes the c[th] coordinate of the utopia point and f_c^{PN} denotes the c[th] coordinate of the pseudo nadir point. These points, f^{UT} and f^{PN}, are the anchor points.

3.3. Optimization algorithms: Metaheuristics

Since the simulation-based optimization models heavily rely on the simulation part which can be seen as black-box function generator, the information about the gradients required by some rigorous optimization algorithms is unavailable. On the other side, the discontinuities in the objective functions make unsuitable the use of derivative based algorithms [15]. Metaheuristic algorithms are recommended as first option in these cases [10].

Metaheuristic algorithms are approximate algorithms that combine basic heuristics to explore a discrete search-space in a more effective way than the heuristics and the local search. The metaheuristics are defined as strategies that “guide” the search process efficiently exploring the search space in order to provide (near)optimal solutions [16].

We provide a brief classification of the metaheuristics, but it should be noticed that they are not problem specific. Many times, the algorithm selection and the configuration of its settings require a tedious trial and error process.

3.3.1. Classification of metaheuristics

Below are presented several types of classification of metaheuristics according to Blum [17].

i) Nature-inspired or non-nature inspired.

There are nature-inspired algorithms, such as ant colony optimization and evolutionary algorithms. The non-nature inspired ones are the local search and tabu search. This is the most intuitive way of classifying, referring to the origins of the metaheuristics. However, many recently developed hybrid algorithms cannot be assigned to any of those groups.

ii) Single point or population-based search.

The number of solutions attained by the algorithm at the same time can be the other characteristic of classification. The algorithms which work on single solutions are also referred to as trajectory methods. Here are included all the metaheuristics based on local search. On the other hand, population-based metaheuristics perform search processes similar to the evolution of the set of points in the search space.

iii) Dynamic or static objective function.

Some algorithms use static objective functions during run-time, others (e.g. guided local search) modify the objective function during the search. The idea behind the dynamic approach is to escape from local minimum by modifying the search “landscape”.

iv) One or various neighborhood structures.

Many algorithms use one invariable neighborhood structure during the optimization. Some metaheuristics (e.g. variable neighborhood search) use different landscape topologies which make them more likely to escape the local minimum solutions.

v) Memory-based or memory-less methods.

The use of memory is recognized as one of the most important elements of a powerful metaheuristic. Memory-less algorithms perform a Markov process, they use memory slots only to decide the next action. There are also short-term algorithms which refer to recently performed moves or recently taken decisions. The long-term algorithms accumulate information about the whole search.

4. ENVIRONMENTAL IMPACT ASSESSEMENT

The second pillar of sustainability, environmental, is addressed in this thesis by appending the environmental impact as an additional objective function in the optimization models. Environmental impact assessment is traditionally applied in the scientific and political spheres to systematically evaluate the potential impacts that a system may have on the environment. Life Cycle Assessment (LCA) is one of the methodologies broadly applied in decision-making contexts [18–22].

4.1. Life cycle assessment

LCA is a methodology used to quantify and assess the inputs and outputs and potential environmental impacts of goods and processes throughout their life cycle [23,24]. In practice, LCA has been developed to improve product systems, to identify impact drivers on corporate strategies, to provide hotspot analysis of consumption life styles, etc. [22].

Combination of LCA with mathematical programming is a powerful tool to assist sustainable decision-making which was used since the middle of 1990s [25] in many engineering areas. The strengths of the combined approach guide practitioners and provide useful insights for decision- and policy-makers [18–22,26]. This framework consists of two steps. First, an LCA study is carried out to determine the impacts along the entire life cycle. Next, these impacts are used as inputs in the optimization model.

An LCA study generally includes four main phases: i) goal and scope definition, ii) inventory analysis, iii) impact assessment, and iv) interpretation. The detailed description of the phases is provided by the ISO: 14044 standards [23]. Full LCA study is a time-consuming process where attention should be paid to many details. To facilitate the search of information, several LCA databases are available (unfortunately none of them is open source). The most popular database (and used in this thesis) is Ecoinvent [27].

The four phases of an LCA study are described below:

i) Goal and scope definition.

The decisions taken in this phase will affect the results of the whole study. In this phase, the system under study, its boundaries, and the functional unit are established. Next the practitioner has to choose between attributional or consequential modelling approaches [28,29]. And finally, select the method of partitioning of environmental burdens among the products of the same process.

ii) Life cycle inventory analysis (LCI)

In this phase all the inputs and outputs of the system are quantified along the life cycle by performing material and energy balances. Mathematically, the inventory can be defined as follows:

$$LCI_i^{TOT} = \sum_j LCI_{i,j} \quad \forall i \qquad \text{(I-2)}$$

where LCI_i^{TOT} is the total LCI entry corresponding to the elementary flow *i* which is computed as the summation of all the flows *i* for all the system units *j.*

iii) Life cycle impact assessment (LCIA)

In this phase, the LCI data are converted into impact indicators using a specific methodology. Several LCIA methodologies are available but no agreement is achieved in the scientific community on which one to prioritize above the others. In this work we followed the recommendations of the EU Commission [30] (use of the ReCiPe 2008 methodology [31]). ReCiPe 2008 uses midpoint and endpoint levels of aggregation. The characterization at the endpoint level can be carried out by either using or not midpoints.

First, the LCI data are converted into impacts:

$$IMP_e = \sum_i \theta_{ei} LCI_i^{TOT} \quad \forall e \tag{I-3}$$

where θ_{ei} is the characterization factor that connects the elementary flow *i* with endpoint impact category *e*, and IMP_e is the indicator result for endpoint impact category *e*. A further aggregation leads to three damage categories: human health, ecosystems and resources. Each damage category is a combination of different endpoint impacts:

$$DAM_d = \sum_{e \in ID_d} IMP_e \quad \forall d \tag{I-4}$$

where ID_d denotes the set of endpoint impacts *e* that contribute to damage *d*, and DAM_d is the indicator result for damage category *d*.

Moreover, the ReCiPe methodology incorporates three different time perspectives which are based on the three archetypes used in Cultural Theory [31]. These perspectives are the Egalitarian (long-time perspective), the Individualist (short-time perspective), and the Hierarchist (balanced time perspective). In this work, we apply the Hierarchist model, which is the most commonly used.

Finally, the three damages are normalized and aggregated into a single final score (RCP), as follows:

$$RCP = \sum_d \delta_d \cdot \xi_d \cdot DAM_d \tag{I-5}$$

where *RCP* is the ReCiPe 2008 aggregated metric, while δ_d and ξ_d are the normalization and weighting factors, respectively. The normalization factors are estimated based on damage calculations of relevant European emissions, extractions and land uses. Regarding the set of weighting factors, we use the recommended averaged factors defined in the ReCiPe 2008.

iv) Interpretation

The interpretation phase draws conclusions of the study and provides recommendations for performance improvement. The decision-makers can easily identify weak points of the process where extra effort should be made to reduce the environmental impact. However, no clear guidelines are provided on how to achieve the reduction. Moreover, the interpretation is usually complex due to the number of available alternatives and the conflicting objectives (i.e. impact categories) in many scenarios.

To overcome these limitations, the results of the LCA can be included as parameters in the mathematical model and the optimization process will identify in systematic way the best alternative (i.e. optimal solution).

5. OUTLINE OF THE CASE STUDIES

The simulation-based optimization methods have a great potential for solving computationally expensive real-world sustainability problems. These methods can aid decision-makers and policy-makers in their struggle of taking correct actions towards a more sustainable future. In the next lines we briefly comment on the problems we have addressed in this thesis (Fig. I-2). For detailed information the reader is referred to Chapters II, III and IV.

5.1. Case study: Barcelona

Central solar heating plants with seasonal storage (CSHPSS) are among the most promising technologies to save energy in the industrial and residential-commercial building sectors. This work introduces a systematic approach to optimize these systems according to economic and environmental criteria.

Our method combines the TRNSYS 17 simulation software with life cycle costing and life cycle assessment equations together with a multi-objective optimization. As a result of this connection, optimal CSHPSS designs for any climatic condition and heating demand profiles can be identified considering economic and environmental criteria simultaneously.

The capabilities of this approach are illustrated through its application to a case study of a CSHPSS located in Barcelona (Spain), which satisfies a heating demand for neighborhood of 1120 dwellings. Numerical results show that the CSHPSS plant leads to significant environmental and economic improvements compared to the use of a conventional natural gas heating system.

Our tool can guide engineers and architects in the transition towards a more sustainable residential sector. In Fig. I-5 we graphically summarize the outline of the work, for details follow to Chapter II.

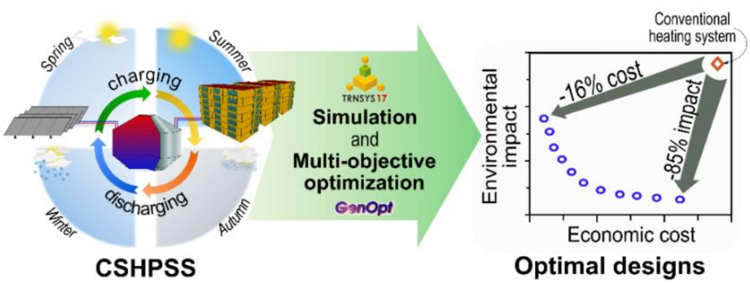

Fig. I-5. Graphical abstract of “Enhanced thermal energy supply via Central Solar Heating Plants with Seasonal Storage: A multi-objective optimization approach”.

5.2. European case studies

Aligning with the ambitious EU 2030 climate and energy package for cutting the greenhouse emissions and replacing conventional heat sources through the presence of renewable energy share inside efficient district heating fields, central solar heating plants coupled with seasonal storage (CSHPSS) can have a viable contribution to this goal. However, the technical performance uncertainty combined with inadequate financial assessment and deficient environmental impact data associated with the deployment of those innovative district heating systems represents a big challenge for the wide implementation of CSHPSS in Europe.

In this context, our paper presents a comprehensive evaluation for the possibility of integrating CSHPSS in the residential sector in various EU member states through the formulation of a multi-objective optimization problem. This problem comprises simultaneously the life cycle cost analysis for the economic evaluation and the life cycle assessment for the environmental impact estimation with technical consideration of satisfying both the space heating demand and the domestic hot water services. The methodology framework is applied to residential neighborhood community of 1120 apartments in various EU climate zones with Madrid, Athens, Berlin, and Helsinki acting as proxy for the Mediterranean continental, Mediterranean, central European, and Nordic climates, respectively.

The environmental assessment shows a significant improvement when using the CSHPSS in comparison to a natural gas heating system, in those cases the environmental impact is reduced up to 82-87%. On the other hand, an extensive economic improvement is especially limited in the Mediterranean climate zone (Athens) due to low heating demands and the prices of the non-renewable resources, there the total economic cost of the CSHPSS plants can increase up to 50.8% compared to a natural gas heating system.

However, considering the incremental tendency in natural gas prices all over EU nowadays, the study of future plant costs confirms its favorable long term economic feasibility. In Fig. I-6 we graphically summarize the outline of the work, for details follow to Chapter III.

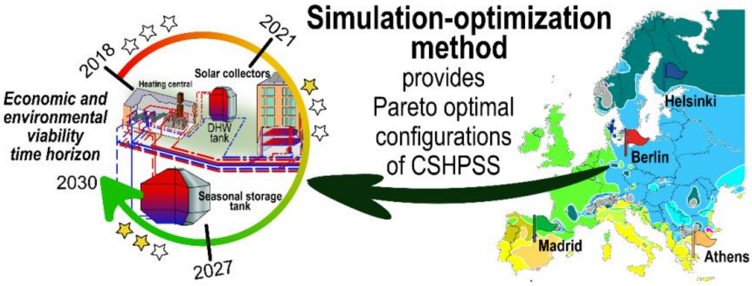

Fig. I-6. Graphical abstract of "Economic and environmental potential for solar assisted central heating plants in the EU residential sector: Roadmap to the 2030 climate and energy EU targets".

5.3. Case study: Passivhaus

Climate and energy framework of the European Commission for 2030 keeps motivating a significant research effort in the area of storage of renewable energy sources and its utilization in a variety of industrial, building and transport sectors. Around forth part of all final energy consumption belongs to the building sector. Significant research was done on low-energy consumption houses which were built following the Passivhaus standard. The next logical step was to cover part of the demand of a Passivhaus with renewable energy, for example solar energy. Due to a significant shift between the availability of solar energy and the demand generated by the Passivhaus users, a seasonal solar thermal energy storage system appeared to be an interesting option.

Some previous works developed a simulation model based on a pilot plant of a seasonal thermal energy store (STES) installed next to a single-family house which was built under the standard of low-energy Passivhaus in Galway, Ireland. The STES system was intended to cover part of the space heating demand of the house and part of the domestic hot water demand.

In this chapter, we move a step forward and want to introduce a systematic approach to finding the optimal equipment designs for a solar assisted seasonal thermal energy storage system coupled to the demand of a single-family passive house. The optimal designs are expected to provide a simultaneous improvement on the economic and environmental criteria on long-term period over the existing electric heating systems.

Our method is based on a simulation-optimization approach which includes the combined use of TRNSYS 18, transient simulation software, and GenOpt, generic optimization toolbox. The TRNSYS 18 incorporates a validated simulation model of the STES system, based on an existing pilot plant. On the other hand, in GenOpt is performed the multi-objective optimization (MOO) process, which combines the economic and environmental indicators. The economic indicators are obtained following the life cycle costing methodology developed by Kalogirou and the environmental indicators follow the life cycle assessment principles.

This study will propose a systematic approach to facilitate the discovery of optimal configurations of a solar assisted seasonal thermal energy storage system connected to a demand generated by a single-family passive house. As a result of the multi-objective optimization the economic cost of the installation and the total environmental impact will be minimized simultaneously generating a set of Pareto optimal solutions. These alternatives could be offered to the decision-makers to select the best configurations based on their priorities.

At the moment of writing this thesis no conclusive results are achieved but the reader is referred to Chapter IV for further details on the topic and the discussion of the possible drawbacks.

REFERENCES

[1] Crutzen PJ. Geology of mankind. Nature 2002;415:23. doi:10.1038/415023a.

[2] Steffen W, Crutzen PJ, McNeill JR. The Anthropocene: Are Humans Now Overwhelming the Great Forces of Nature. AMBIO A J Hum Environ 2007;36:614–21. doi:10.1579/0044-7447(2007)36[614:TAAHNO]2.0.CO;2.

[3] Brundtland G. Report of the World Commision on Environement and Development: Our Common Future. vol. Report of. Oxford University Press, USA; 1987. doi:10.2307/2621529.

[4] Todorov V, Marinova D. Modelling sustainability. Math Comput Simul 2011;81:1397–408. doi:10.1016/j.matcom.2010.05.022.

[5] Rockström J, Steffen W, Noone K, Persson Å, Chapin FS, Lambin E, et al. Planetary boundaries: Exploring the safe operating space for humanity. Ecol Soc 2009;14. doi:10.5751/ES-03180-140232.

[6] Rockström J, Sachs JD, Öhman MC, Schmidt-Traub G. Sustainable Development and Planetary Boundaries. Backgr Res Pap UN High-Level Panel Eminent Pers Post-2015 Dev Agenda 2013:45.

[7] Mavromatidis G, Orehounig K, Carmeliet J. Design of distributed energy systems under uncertainty: A two-stage stochastic programming approach. Appl Energy 2018;222:932–50. doi:10.1016/j.apenergy.2018.04.019.

[8] Steffen W. Will Technology Spare the Planet? In: Steffen W, Jäger J, Carson DJ, Bradshaw C, editors. Challenges a Chang. Earth, Berlin, Heidelberg: Springer Berlin Heidelberg; 2002, p. 189–91. doi:10.1007/978-3-642-19016-2.

[9] United Nations, Department of Economic and Social Affairs PD. World Urbanization Prospects. United Nations 2014;12:32. doi:10.4054/DemRes.2005.12.9.

[10] Nguyen A-TT, Reiter S, Rigo P. A review on simulation-based optimization methods applied to building performance analysis. Appl Energy 2014;113:1043–58. doi:10.1016/j.apenergy.2013.08.061.

[11] Grossmann IE, Caballero JA, Yeomans H. Advances in mathematical

programming for the synthesis of process systems. Lat Am Appl Res 2000;30:263–84.

[12] Ehrgott M. Multiobjective Optimization. AI Mag 2009;29:47. doi:10.1609/aimag.v29i4.2198.

[13] Ehrgott M. Multicriteria optimization. Heidelberg: Springer; 2005.

[14] Haimes, Y., Lasdon, L., Wismer D. On a bi-criterion formulation of the problems of integrated system identification and system optimization. IEEE Trans Syst Man Cybern 1971;1 (3):296–297.

[15] Wetter M, Wright J. A comparison of deterministic and probabilistic optimization algorithms for nonsmooth simulation-based optimization. Build Environ 2004;39:989–99. doi:10.1016/j.buildenv.2004.01.022.

[16] Blum C. Ant colony optimization: Introduction and recent trends. Phys Life Rev 2005;2:353–73. doi:10.1016/j.plrev.2005.10.001.

[17] Blum C. Theoretical and Practical Aspects of Ant Colony Optimization. vol. 282. 2004.

[18] Azapagic A, Clift R. Life cycle assessment and multiobjective optimisation. J Clean Prod 1999;7:135–43. doi:10.1016/S0959-6526(98)00051-1.

[19] Grossmann IE. Challenges in the new millennium: product discovery and design, enterprise and supply chain optimization, global life cycle assessment. Comput Chem Eng 2004;29:29–39. doi:10.1016/j.compchemeng.2004.07.016.

[20] Pieragostini C, Mussati MC, Aguirre P. On process optimization considering LCA methodology. J Environ Manage 2012;96:43–54. doi:10.1016/j.jenvman.2011.10.014.

[21] Azapagic A, Clift R. The application of life cycle assessment to process optimisation. Comput Chem Eng 1999;23:1509–26. doi:10.1016/S0098-1354(99)00308-7.

[22] Hellweg S, Milà i Canals L. Emerging approaches, challenges and opportunities in life cycle assessment. Science (80-) 2014;344:1109 LP-1113.

[23] ISO. Standardization, International Organization for Standardization. The New International Standards for Life Cycle Assessment: ISO 14040 and ISO 14044.

Geneva, Switzerland: 2006.

[24] Guinée J. Handbook on life cycle assessment — operational guide to the ISO standards. Int J Life Cycle Assess 2001;6:255. doi:10.1007/BF02978784.

[25] Azapagic A, Clift R. Life cycle assessment and linear programming environmental optimisation of product system-. Comput Chem Eng 1995;19:229–34. doi:10.1016/0098-1354(95)87041-5.

[26] Grossmann IE, Guillén-Gosálbez G. Scope for the application of mathematical programming techniques in the synthesis and planning of sustainable processes. Comput Chem Eng 2010;34:1365–76. doi:10.1016/j.compchemeng.2009.11.012.

[27] Frischknecht R, Rebitzer G. The ecoinvent database system: a comprehensive web-based LCA database. J Clean Prod 2005;13:1337–43. doi:http://dx.doi.org/10.1016/j.jclepro.2005.05.002.

[28] Frischknecht R, Stucki M. Scope-dependent modelling of electricity supply in life cycle assessments. Int J Life Cycle Assess 2010;15:806–16. doi:10.1007/s11367-010-0200-7.

[29] Finnveden G, Hauschild M, Ekvall T. Recent developments in life cycle assessment. J Environ … 2009;91:1–21. doi:10.1016/j.jenvman.2009.06.018.

[30] Hauschild M, Goedkoop M, Guinee J, Heijungs R, Huijbregts M, Jolliet O, et al. Recommendations for Life Cycle Impact Assessment in the European context - based on existing environmental impact assessment models and factors (International Reference Life Cycle Data System - ILCD handbook). 2011. doi:10.2788/33030.

[31] Goedkoop M, Heijungs R, De Schryver A, Struijs J, van Zelm R, Huijbregts M, et al. ReCiPe 2008. A LCIA method which comprises harmonised category indicators at the midpoint and the endpoint level. Report I: Characterisation 2009:1–133. doi:http://www.lcia-recipe.net.

II CASE STUDY: BARCELONA

Enhanced thermal energy supply via Central Solar Heating Plants with Seasonal Storage: A multi-objective optimization approach‡

Victor Tulus [a], **Dieter Boer** [b,*], **Luisa F. Cabeza** [c], **Laureano Jiménez** [a], **Gonzalo Guillén-Gosálbez** [a,d]

[a] Departament d'Enginyeria Química, Universitat Rovira i Virgili, Av. Països Catalans 26, 43007 Tarragona, Spain

[b] Departament d'Enginyeria Mecànica, Universitat Rovira i Virgili, Av. Països Catalans 26, 43007 Tarragona, Spain

[c] GREA Innovació Concurrent, Edifici CREA, Universitat de Lleida, Pere de Cabrera s/n, 25001 Lleida, Spain

[d] Department of Chemical Engineering, Centre for Process Systems Engineering, Imperial College, South Kensington Campus, SW7 2AZ London, UK

** Corresponding author: dieter.boer@urv.cat*

‡ Published article (November 2016), DOI: 10.1016/j.apenergy.2016.08.037

Keywords:
central solar heating plant with seasonal storage
thermal energy storage
solar district heating
multi-objective optimization
life cycle assessment
TRNSYS modeling

1. INTRODUCTION

Due to their high specific energy density and combustion temperatures ranging from 1000 to 2500 ºC, fossil fuels are excellent energy carriers able to meet extreme energy demands. Unfortunately, large amounts of fossil fuels are used inefficiently to cover energy demands below 260 ºC [1], a large fraction of which belongs to the residential-commercial sector. According to the European Environment Agency, in 2013 this sector represented 40% of the total final energy consumption [2]. To improve its energy efficiency, this sector should use alternative energy sources, particularly for space heating.

Over the past decades, various technologies based on renewable energy sources have been put forward as viable alternatives to the use of fossil fuels, including wind power, hydropower, waste energy, geothermal energy, bio energy, solar energy and energy storage. In the residential-commercial sector, and especially in large cities or inner city areas, these technologies can become even more competitive if they are integrated in an existing district heating (DH) network [3]. Several authors have investigated the use of renewables in the residential sector. Ostergaarg *et al.* studied a geothermal energy based technology coupled to a DH network [4], concluding that in combination with an absorption heat pump it could be a promising technology in the current situation. Nuytten *et al.* assessed the flexibility of a combined heat and power (CHP) system with thermal energy storage (TES) for DH [5]. Sartor *et al.* developed a simple model of a CHP plant connected to a DH [6]. Wang *et al.* optimized a CHP-DH plant combined with energy storage [7]. Bouro *et al.* optimized different configurations of renewable energy technologies, finding that the minimum heat costs are achieved when the CHP system, DH network, solar field, and energy storage are all integrated in the energy supply [8]. Renaldi *et al.* proposed an optimization framework for a heat pump heating system integrated with TES [9]. More recently, Liu *et al.* studied a ground-source heat pump system with seasonal storage [10]. Furthermore, biomass district heating in rural communities was studied by Hendricks *et al.* [11].

In this work, we focus on centralized solar heating plant with seasonal storage (CSHPSS), which are at present among the most promising technologies to save energy in the industrial and residential-commercial building sectors. Different review papers [12–15] discuss in detail several configurations for the CSHPSS technology. These alternative configurations differ in the type of thermal energy storage implemented, a topic widely studied since the 1960s. Due to the intermittent nature of solar radiation, the energy source in a CSHPSS system does not fully match the energy demand profile. Hence, it is necessary to store energy in periods with high radiation to use it in other periods with low radiation and/or high energy demand (see Fig. II-1).

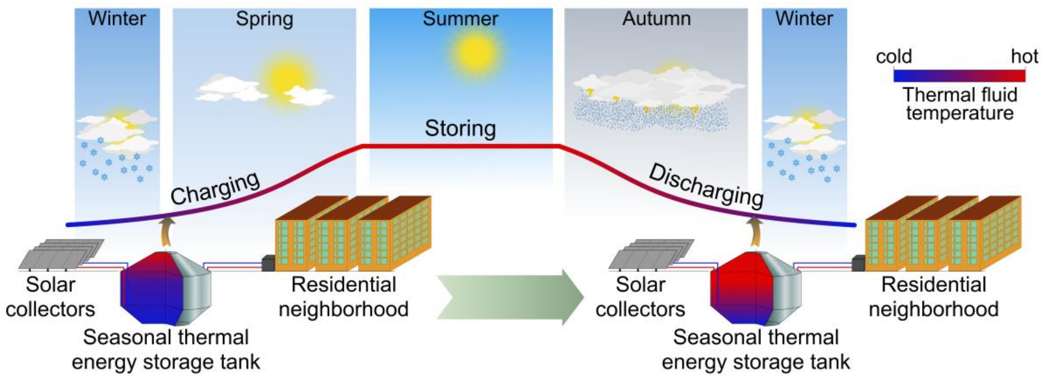

Fig. II-1. General overview of the seasonal thermal energy storage technology.

In the early 1980s, the first proof-of-concept CSHPSS plants were built in Sweden and Denmark, followed by Germany in the 1990s. Since then, the list of pilot and fully operating CSHPSS plants has been continuously growing [16], particularly in Northern and Central European countries. Recently, CSHPSS plants have gained interest in the residential-commercial sector as a viable alternative for meeting the energy demand in a highly effective manner [13].

In Southern European countries, following the minimum requirements of renewable energy use imposed by their legislations (*i.e.* the Spanish legislation [17]), solar thermal energy is mainly used to cover part of the domestic hot water demand. In this context, energy storage technologies offer a unique opportunity to exploit the solar energy surplus during specific periods of the year, thereby leading to environmental and economic savings. According to Novo *et al.* [13], the use of CSHPSS in the residential-commercial sector could save more than 50% of the non-renewable energy consumed for heating. Hence, the study and implementation of CSHPSS systems is of great interest from the economic and sustainability perspective, aligning very well with the “20-20-20” targets of the European Commission for 2020 [18].

Some useful guidelines have been defined for designing CSHPSS pilot plants [19–22]. For the European climate, Argiriou [23] simulated CSHPSS plants with storage tanks in Greece. Ucar *et al.* [24] studied several configurations of storage tanks in a CSHPSS plant in four climatically different Turkish locations. In a later work, Ucar *et al.* [25] optimized a CSHPSS model from the economic point of view. Pahud [26] provided guidelines for the design of a CSHPSS plant using boreholes in Switzerland. Sibbitt *et al.* [27] presented a simulation model of a CSHPSS with a borehole storage, which was validated using data from five years of operation of a plant built in Alberta, Canada. For the climatic conditions of Virginia, USA, Terziotti *et al.* [28] simulated a CSHPSS with a sand bed storage. Chung *et al.* [29] presented a simulation model for a CSHPSS plant with a medium-sized storage tank located in Cheju, Korea. For the Mediterranean region, Lozano *et al.* [30], Frago-Moreno [31], and Guadalfajara *et al.* [32] demonstrated that CSHPSS is a promising and economically viable alternative for covering the heating demand of residential buildings in a number of Spanish regions.

All of the previous authors studied the economic viability of CSHPSS plants in different locations. On the other hand, Raluy *et al.* [33] studied the environmental performance of these systems by applying the Life Cycle Assessment (LCA) methodology. To the best of our knowledge, however, no work has studied simultaneously the economic and environmental performance of CSHPSS plants.

The aim of this work is to develop a systematic multi-objective optimization (MOO) framework for optimizing the design of CSHPSS plants considering economic and environmental aspects simultaneously. To this end, a simulation-optimization methodology was developed based on a CSHPSS plant modeled in TRNSYS 17 [34] that was optimized by a generic optimization tool (*i.e.* GenOpt [35]) according to economic and environmental indicators. The latter objective was assessed through LCA principles, which quantify the impact caused in all of the stages in the life cycle of the energy system

[36]. Numerical results show that improvements in cost and environmental impact can be achieved simultaneously, comparing to a conventional heating system.

The chapter is organized as follows: section 2 provides a general overview of the CSHPSS plant and describes how to model it in TRNSYS. The mathematical formulation and optimization methodology to obtain the Pareto frontier is discussed in section 3. To highlight the potential of the methodology, in section 4 we introduce a case study for the city of Barcelona (Spain). In the following section 5, the results of the case study are presented and discussed. Finally, in section 6, we draw the conclusions of this work.

2. OVERVIEW OF THE INSTALLATION

In this section, we provide an overview of CSHPSS facilities. CSHPSS are large scale systems designed to cover thermal energy demands along the year. The main components of a CSHPSS are the solar collectors and the storage tank. The field of solar collectors can be either installed on the ground in relative proximity to the storage and distribution system, or (in the case of the residential sector) on the roofs of the buildings. The storage tank is a large-scale insulated reservoir, usually half-buried, which accumulates thermal energy during long periods. The performance of CSHPSS plants strongly depends on the profiles of incident solar radiation and heating demand, which show continuous variations on an hourly basis and also from day to day. The energy simulation software TRNSYS 17 enables the modelling of this transient behavior shown by CSHPSS facilities. A sketch of the plant we analyze in this work with the main inputs and outputs is shown in Fig. II-2. The simulation model developed here is based on the work by Guadalfajara *et al.* [32], where the reader will find further details on the simulation approach.

The CSHPSS plant we consider is composed of a set of closed pipe loops designed to transport thermal energy. These loops can be visually divided in four circuits (primary, secondary, tertiary, and distribution), as shown in Fig. II-2. The solar radiation is collected in the field of solar collectors and transported from the primary to the secondary loop. Part of this energy is transferred directly to the DH network (through the tertiary and distribution loops) to cover the instant daily heating demands, while the surplus is stored inside the seasonal storage tank.

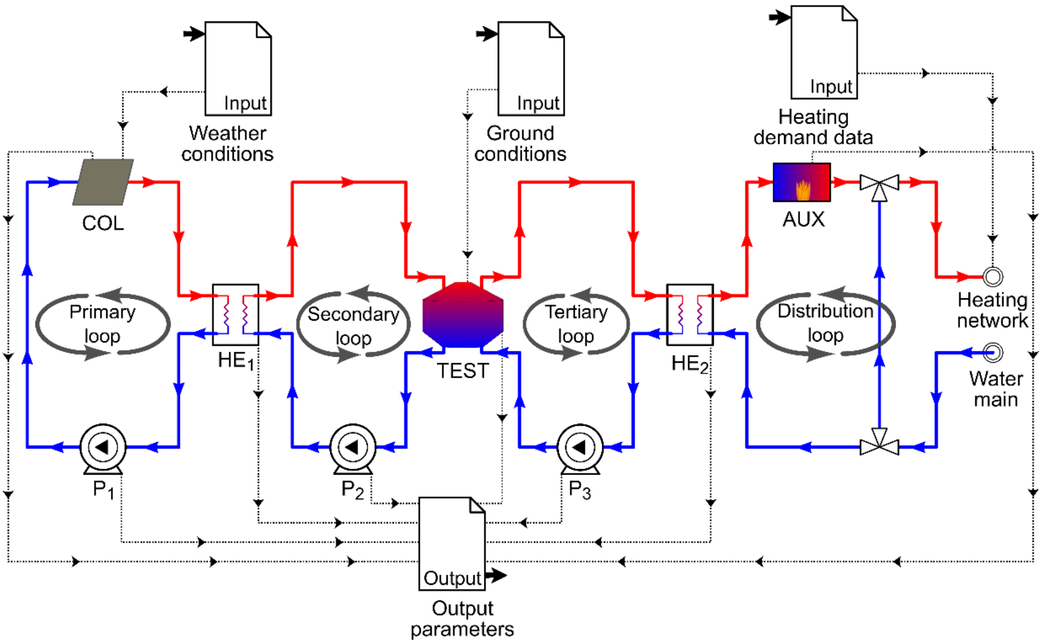

Fig. II-2. Process flow diagram of the CSHPSS model simulated in TRNSYS 17, where COL is the field of solar collectors, TEST is the thermal energy storage tank, AUX is the auxiliary heater, HE_i are the heat exchangers, and P_i are the centrifugal pumps.

A pump (P_1) impulses the fluid of the primary circuit through the field of solar collectors (COL) to finally reach a heat exchanger (HE_1). In this heat exchanger HE_1, thermal energy is transferred to the fluid of the secondary loop, which is displaced by another pump (P_2). This heated fluid is pumped to a specific height in the thermal energy storage tank (TEST), while the cold fluid is returned to the HE_1 from the bottom of the TEST. The pumping height is established depending on the temperature of the entering fluid and the temperature profile in the tank. No mixing between fluids at different temperatures is allowed in the simulation due to a stratification device.

During the periods of heating demand, the pump of the tertiary loop (P_3) pumps the cold fluid to the bottom of the TEST and discharges the hot fluid from the top of it. The hot fluid is sent to a heat exchanger (HE_2) that connects the tertiary and distribution loops. In the HE_2, the cold water provided by the district water supply network is heated. The heated water flow passes through an auxiliary heater (AUX), which operates when the temperature of the water cannot reach the set point. When the temperature after the AUX exceeds the set point, a bypass loop is activated to supply fresh cold water from the main water supply.

The fluid for the primary loop is usually a water-glycol mixture, which protects the expensive solar collector equipment from potential damages caused by low ambient temperatures. The secondary and tertiary loops (including the TEST) operate with water due to its good thermal properties and low cost [13].

Our model implements a controlling system to regulate the performance of the pumps, the auxiliary heater and other components of the plant, similarly as was done by Guadalfajara *et al.* [32]. Control loops are omitted in Fig. II-2 for the sake of clarity. One of the controllers regulates the synchronic activation of the pumps P_1 and P_2 when the temperature of the water-glycol mixture in the primary loop reaches the predefined value. The same pumps are controlled by another selective control loop with high selector switch that keeps the temperature in the TEST within the desired limits. When the temperature at the top of the TEST reaches its set point, the pumps are stopped to avoid malfunctioning of the equipment. Another control loop regulates the operation of pump P_3 according to the amount of heating demanded by the network. An extra thermostat-type controller regulates the intermittent operation of the AUX, which supplies auxiliary heat to meet the fixed temperature set point. Finally, the bypass loop is regulated by another controller, which monitors the output temperature of the AUX.

3. METHODOLOGY

Our methodology is based on a simulation-optimization approach [37–39] that integrates a CSHPSS simulation model with an external MOO algorithm. The plant model is implemented in the transient simulation software (TRNSYS 17), which incorporates a palette of standard equipment units that can be easily combined to model more complex systems. On the other hand, the optimization is carried out by an external optimizer using a generic optimization tool, GenOpt. The general overview of the methodology is summarized in Fig. II-3. In the ensuing sections, we describe in detail each of the components of our approach.

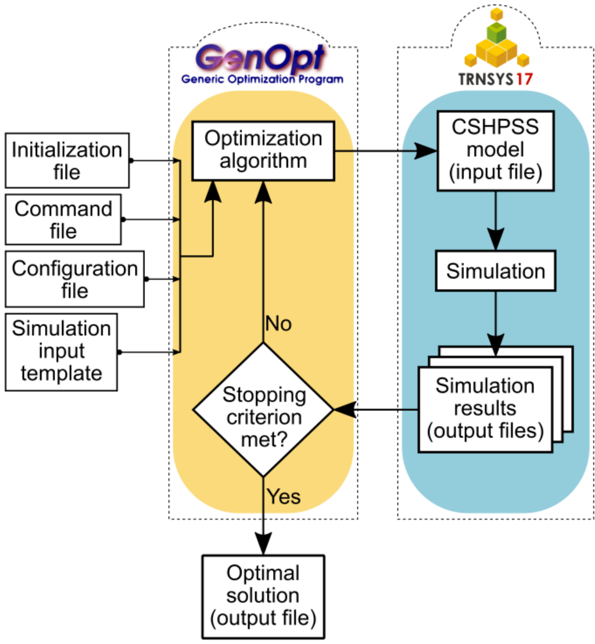

Fig. II-3. Overview of the optimization methodology indicating the connection between GenOpt and TRNSYS software environments.

3.1. Mathematical model

The mathematical model of the CSHPSS plant is simulated with TRNSYS 17. This software, which is based on first principles, solves partial differential equations representing mass and energy balances applied within the boundaries of the plant.

The dynamic nature of the software is an important advantage, as it makes the simulation of the CSHPSS plant more realistic. To simplify the calculations, we simulate a typical year of operation using averaged data expressed on an hourly timescale. The results for this year are then extrapolated to the whole plant life assuming that the same radiation pattern is repeated over time.

The main goal in this design task is to reduce the total cost of the installation and its environmental impact simultaneously, being the total area of solar collectors (A_{COL}) and the volume of the storage tank (V_{TEST}) the main decision variables (note that the sizes of the other equipment units are closely related to the values of these variables). Note, however, that the methodology is general enough to work with any others decision variables.

3.2. Objective functions

In this section, we describe in detail how the economic and environmental performance of the CSHPSS is computed. The economic objective is represented by the total cost, whereas the environmental objective is calculated as a linear weighted sum of a set of environmental indicators (each of them determined following LCA principles).

3.2.1. Economic indicators

The economic indicators are estimated based on the life cycle cost analysis methodology developed by Kalogirou [40]. The net present cost of the CSHPSS plant (*NPC*) is determined as the summation of the discounted expenses generated during the lifetime of the installation, as follows:

$$NPC = C_C + C_O + C_R \qquad \text{(II-1)}$$

In Eq. II-1, C_C, C_O, and C_R denote the initial capital cost, the total discounted operating cost, and the total discounted cost related to the equipment replacement, respectively. Each of these terms is described in detail in the next subsections.

3.2.1.1. Initial capital cost

The initial capital cost (C_C) is the investment outlay at the starting point of the project. This outlay takes into consideration the purchase, transportation and installation of the equipment, along with the expenses for any possible contingencies and fees:

$$C_C = (1+\alpha_{CF})\cdot\sum_k PEC_k \cdot FBM_k \qquad \text{(II-2)}$$

Here, PEC_k denotes the purchase cost of equipment unit *k*, parameter FBM_k is the bare module factor, which represents the costs of transportation and installation of the purchased unit *k*, and parameter α_{CF} is the factor of contingency charges and fees.

The purchase equipment cost (PEC_k) is updated from a base year (year A) to the year of the installation (year B) using the Chemical Engineering Plant Cost Index (CEPCI) [41] as follows:

$$PEC_k = PEC_k^{year\ \mathrm{A}} \frac{CEPCI^{year\ \mathrm{B}}}{CEPCI^{year\ \mathrm{A}}} \quad \forall k \qquad \text{(II-3)}$$

The purchase cost of unit *k* in the base year ($PEC_k^{year\ A}$) is estimated via Eqs. II-4 to II-6.

$$PEC_k^{year\ A} = \alpha_k \cdot CAP_k^{\beta_k} \quad \forall k = \text{COL, TEST, AUX} \tag{II-4}$$

$$PEC_k^{year\ A} = CAP_k \cdot 10^{\left[\alpha_k \cdot \log_{10} CAP_k^{\ \beta_k}\right]} \quad \forall k = \text{HE}_1, \text{HE}_2 \tag{II-5}$$

$$PEC_k^{year\ A} = \alpha_k \cdot \ln\left(\frac{CAP_k}{1000}\right) + \beta_k \quad \forall k = \text{P}_1, \text{P}_2, \text{P}_3 \tag{II-6}$$

where α_k and β_k are equipment cost parameters, and CAP_k is the design variable of unit k. In our case, the design variables are the aperture area for the solar collectors (A_{COL}), the storage volume for the seasonal storage tank (V_{TEST}), the duty for the auxiliary boiler (Q_{AUX}), the heat transfer area for the heat exchangers (A_{HE1}, A_{HE2}), and the mass flow rate for the pumps ($\dot{m}_{P1}$, $\dot{m}_{P2}$, $\dot{m}_{P3}$).

3.2.1.2. Operating cost

The total operating cost (C_O) is the discounted summation of all annual operating costs:

$$C_O = C_M \cdot PWF_M + C_P \cdot PWF_P + C_{AUX} \cdot PWF_{AUX} \tag{II-7}$$

where C_M, C_P, and C_{AUX} are the annual costs of the equipment maintenance, the electric consumption of the pumps, and the energy consumption of the auxiliary heater, respectively. The term *PWF* is the present worth factor determined via Eq. II-11, which is specific to each type of operating cost.

The annual maintenance cost (C_M) is proportional to the initial purchase equipment cost, as shown in the next equation, where f_m is the maintenance factor.

$$C_M = f_m \cdot \sum_k PEC_k \tag{II-8}$$

The annual cost of electricity consumed by the pumps (C_P) is calculated as follows:

$$C_P = c_E \int_0^t L_P dt \tag{II-9}$$

where parameter c_E is the cost of electricity during time period t and L_p is the load of electricity consumed by the pump in that time period.

Finally, the annual cost of energy consumed by the auxiliary heater (C_{AUX}) is obtained as stated in Eq. II-10.

$$C_{AUX} = c_F \int_0^t L_{AUX} dt \tag{II-10}$$

Here, c_F is the cost of fuel during time period t and L_{AUX} is the load of fuel consumed by the auxiliary heater in the same time period.

The present worth factor (*PWF*), which captures the time value of money, is defined as the present worth of one Euro paid periodically in the future. Eq. II-11 takes into consideration the market discount rate (d) and the inflation rate (i), as shown below:

$$PWF = \begin{cases} \dfrac{1}{d-i}\left(1-\left[\dfrac{1+i}{1+d}\right]^{N_e}\right) & \forall\ i \neq d \\ \dfrac{N_e}{1+i} & \forall\ i = d \end{cases} \tag{II-11}$$

where the selection of the inflation rate value depends on the analyzed cost (i for C_M, i_e for C_P, and i_f for C_{AUX}), while parameter N_e represents the time period over which the economic analysis is performed (*i.e.* lifespan of the system).

3.2.1.3. Replacement cost

Typically, some of the equipment units (for example, solar collectors, auxiliary heaters, and heat exchangers) are replaced before reaching the total life time of the plant (*i.e.* the life time of some units will be shorter than that of the plant). The replacement of an equipment unit is modeled as a future cash flow that is discounted to the present using Eq. II-12.

$$C_R = PVF_n \cdot \sum_k PEC_k \cdot FBM_k \tag{II-12}$$

In the previous equation, parameter FBM_k is the bare module factor, which is multiplied with the purchase cost of equipment unit k (PEC_k) to model the combined costs of the purchase, transportation, and installation of unit k. Parameter PVF_n denoting the present value factor of a single future cash flow in year n is determined as follows:

$$PVF_n = \frac{1+i^{\;n}}{(1+d)^n} \qquad \text{(II-13)}$$

where i is the inflation rate, d is the market discount rate, and n is the nth year of operation of the plant in which an equipment unit must be replaced.

3.2.2. Environmental indicators

The environmental indicators are quantified based on LCA principles in a similar way as done before by Guillén-Gosálbez *et al.* [42]. LCA is a procedure standardized by the International Organization for Standardization [43] that estimates the total environmental impact of products and services throughout their whole life cycle. Thus, LCA assesses the impacts from the “cradle” of primary resources to the “grave” of the final disposed wastes. Moreover, LCA implements a damage model which links released emissions and waste materials to meaningful environmental damages reflecting important environmental problems.

The general LCA methodology includes four main phases [44]: goal and scope definition, inventory analysis, impact assessment, and interpretation. These phases are described in detail in the next subsections.

3.2.2.1. Goal and scope definition

In this phase, the system under study, its boundaries, and the functional unit are established. In our case, the system of interest is the CSHPSS plant. The LCA boundaries defined here focus on the CSHPSS itself, excluding the distribution network that delivers hot water to final customers (note that the CSHPSS is connected to an existing DH network). Thereby, the boundaries of the plant are drawn from “cradle-to-gate”, starting from the extraction of the necessary amount of raw materials required to manufacture the equipment units and ending with the delivery of thermal energy (in the form of hot water) to the piping network. The amount of hot water generated by the plant defines the functional unit (*i.e.* we assess the impact associated with the generation of a given amount of energy in the form of hot water demanded by the customers over the entire time horizon).

3.2.2.2. Inventory analysis

In the second phase, material and energy balances are performed in order to determine the life cycle inventory entries from where to assess the impacts. The following sources of impact are considered:

- the equipment manufacturing (industrial and on-site manufacturing) and generation of utilities (electricity and natural gas) consumed during the whole life time (LCI_i^{MP})
- the transportation of the materials and manufactured units to the site (LCI_i^{TR})
- the operation of the plant during the whole time-horizon (LCI_i^{OP})

The relevant information required to compute the life cycle inventory (LCI) of the whole spectrum of elementary flows has been retrieved from the Ecoinvent 3.0 database [45]. These elementary flows refer to resources consumption (*i.e.* feedstock and energy requirements), emissions of chemicals to air, water and soil, and waste generated.

Mathematically, the inventory of each of the aforementioned LCI contributors can be defined as follows:

$$LCI_i^{TOT} = LCI_i^{MP} + LCI_i^{TR} + LCI_i^{OP} \quad \forall i \tag{II-14}$$

where LCI_i^{TOT} is the total LCI entry corresponding to the elementary flow *i*. The parameters LCI_i^{MP}, LCI_i^{TR}, and LCI_i^{OP} are the LCI entries corresponding to the elementary flow *i*, which are related to the manufacturing processes (and utilities generation), the transportation tasks, and the plant operation, respectively.

3.2.2.3. Impact assessment

In the impact assessment phase, the LCI data are converted into impact indicators using a specific methodology. There are several life cycle impact assessment methodologies available with no general agreement on which one to use. We follow here the recommendations made by the EU Commission [46], which promote the use of the ReCiPe 2008, a scientifically robust endpoint method based on LCA principles. The ReCiPe 2008 framework, which is thoroughly discussed in [47], uses midpoint and endpoint levels of aggregation. The characterization at the endpoint level can be carried out by either using or not midpoints. The LCI data is first converted into impacts, as stated in Eq. II-15.

$$IMP_e = \sum_i \theta_{ei} LCI_i^{TOT} \quad \forall e \tag{II-15}$$

where θ_{ei} is the characterization factor that connects the elementary flow i with endpoint impact category e, and IMP_e is the indicator result for endpoint impact category e. A further aggregation leads to three damage categories: human health, ecosystems and resources. Each damage category is a combination of different endpoint impacts:

$$DAM_d = \sum_{e \in ID_d} IMP_e \quad \forall d \tag{II-16}$$

where ID_d denotes the set of endpoint impacts e that contribute to damage d, and DAM_d is the indicator result for damage category d.

Moreover, the ReCiPe methodology incorporates three different time perspectives which are based on the three archetypes used in Cultural Theory [47]. These perspectives are the Egalitarian (long-time perspective), the Individualist (short-time perspective), and the Hierarchist (balanced time perspective). In this work, we apply the Hierarchist model, which is the most commonly used.

Finally, the three damages are normalized and aggregated into a single final score (RCP), as follows:

$$RCP = \sum_{d} \delta_d \cdot \xi_d \cdot DAM_d \tag{II-17}$$

where RCP is the ReCiPe 2008 aggregated metric, while δ_d and ξ_d are the normalization and weighting factors, respectively. The normalization factors are estimated based on damage calculations of relevant European emissions, extractions and land uses. Regarding the set of weighting factors, we use the recommended averaged factors defined in the ReCiPe 2008.

3.2.2.4. Interpretation

The interpretation phase identifies the main sources of impact and provides recommendations as well to improve the performance of the system. In this LCA phase, impact indicators are used to compare different design alternatives. In order to generate these alternatives in a systematic way, the LCA methodology is coupled with a MOO tool [48]. The resulting framework optimizes simultaneously environmental and economic criteria. The MOO algorithm provides as output a number of Pareto optimal solutions from which decision-makers should identify the one that best reflects their preferences.

3.3. Solution procedure

The TRNSYS simulation model is therefore coupled with the GenOpt optimization tool, which incorporates various optimization algorithms suitable for a wide variety of problems. The overall simulation-optimization model can be written as follows:

$$\begin{aligned} \min_{x} \quad & f_1(x), f_2(x) \\ \text{s.t.} \quad & h(x) = 0 \\ & x^L \leq x \leq x^U \\ & x \in \mathbb{R} \end{aligned} \qquad \text{(M II-1)}$$

where $f_1(x)$ and $f_2(x)$ are the objective functions, in this case net present cost, *NPC(x)*, and ReCiPe 2008 aggregated impact factor, *RCP(x),* and x denotes the continuous variables of the simulation model, which are allowed to vary between their lower and upper bounds x^L and x^U, respectively. The equality constraints $h(x)=0$, which model mass and energy balances as well as thermodynamic correlations, are solved implicitly in TRNSYS.

The solution of the multi-objective problem introduced in model M II-1 is given by a set of Pareto points, which represent the optimal trade-off between economic and environmental objectives. The extreme points of this Pareto frontier are the so-called anchor points, which correspond to the individual minimum of each objective. The Pareto solutions are calculated here via the weighted-sum method [49], which relies on formulating an auxiliary single-objective model that optimizes a linear weighted-sum (*WS*) of the original objectives (M II-2).

$$\begin{aligned} \min_{x} \quad & WS = (1-\lambda)\bar{f}_1(x) + \lambda \bar{f}_2(x) \\ \text{s.t.} \quad & h(x) = 0 \\ & x^L \leq x \leq x^U \\ & 0 \leq \lambda \leq 1 \\ & x \in \mathbb{R}, \lambda \in \mathbb{R} \end{aligned} \qquad \text{(M II-2)}$$

Here, $\bar{f}_1(x)$ and $\bar{f}_2(x)$ are the normalized objectives, and λ is the non-negative weight given to $\bar{f}_2(x)$, *i.e.* the normalized *RCP(x)* function. We normalize the objectives as shown below:

$$\bar{f}_c(x) = \frac{f_c(x) - f_c^{UT}}{f_c^{PN} - f_c^{UT}} \qquad \forall c = 1,2 \qquad \text{(II-18)}$$

where, f_c^{UT} denotes the cth coordinate of the utopia point and f_c^{PN} denotes the cth coordinate of the pseudo nadir point. These points, f^{UT} and f^{PN}, are the anchor points.

The solution procedure starts with the determination of the anchor points. To obtain the individual minimum of the RCP(x) function, M II-2 is solved for λ=1. Next, to determine the individual minimum of the NCP(x) function, M II-2 is solved for λ=0. Then M II-2 is solved a finite number of times for different weight values between 0 and 1 (see details in Fig. II-4) to generate a sufficient number of Pareto points. Note that the weighted-sum method cannot generate solutions lying on the nonconvex part of the Pareto set.

3.3.1. Optimization algorithm

Each single-objective optimization is carried out using a hybrid metaheuristic optimization algorithm based on the work by Wetter [35]. This metaheuristic algorithm, known as the Generalized Pattern Search algorithm with Particle Swarm Optimization with Construction Coefficient and Hooke-Jeeves (GPSPSOCCHJ), combines the Particle Swarm Optimization (PSO) algorithm [50,51] with the Hooke-Jeeves (HJ) algorithm [52]. The formulation of this hybrid algorithm is described in deeper detail in [35].

The PSO algorithm is a population-based probabilistic optimization algorithm that performs a global search by generating numerous particles (potential optimal solutions) over the entire feasible space. The HJ algorithm is a generalized pattern search algorithm that examines the search space following directions that can potentially minimize the objective function. The HJ algorithm cannot guarantee the global optimality of the solutions found, so it is regarded as a local optimization algorithm. We used this algorithm with multiple starts in an attempt to minimize the probability of getting trapped in a local optimum.

The hybrid GPSPSOCCHJ algorithm combines the global features of the PSO algorithm with the strong convergence properties of the HJ algorithm. Here, the PSO is initialized using randomly generated numbers to spread the particles uniformly over the feasible region. After generating the particles, the best point is passed to the HJ algorithm as starting point to perform an exhaustive inspection of its neighborhood. This architecture is developed to avoid (to the maximum extent possible) locally optimal solutions that may arise due to the nonconvex nature of the problem. Note that our approach can easily work with any other optimization algorithm.

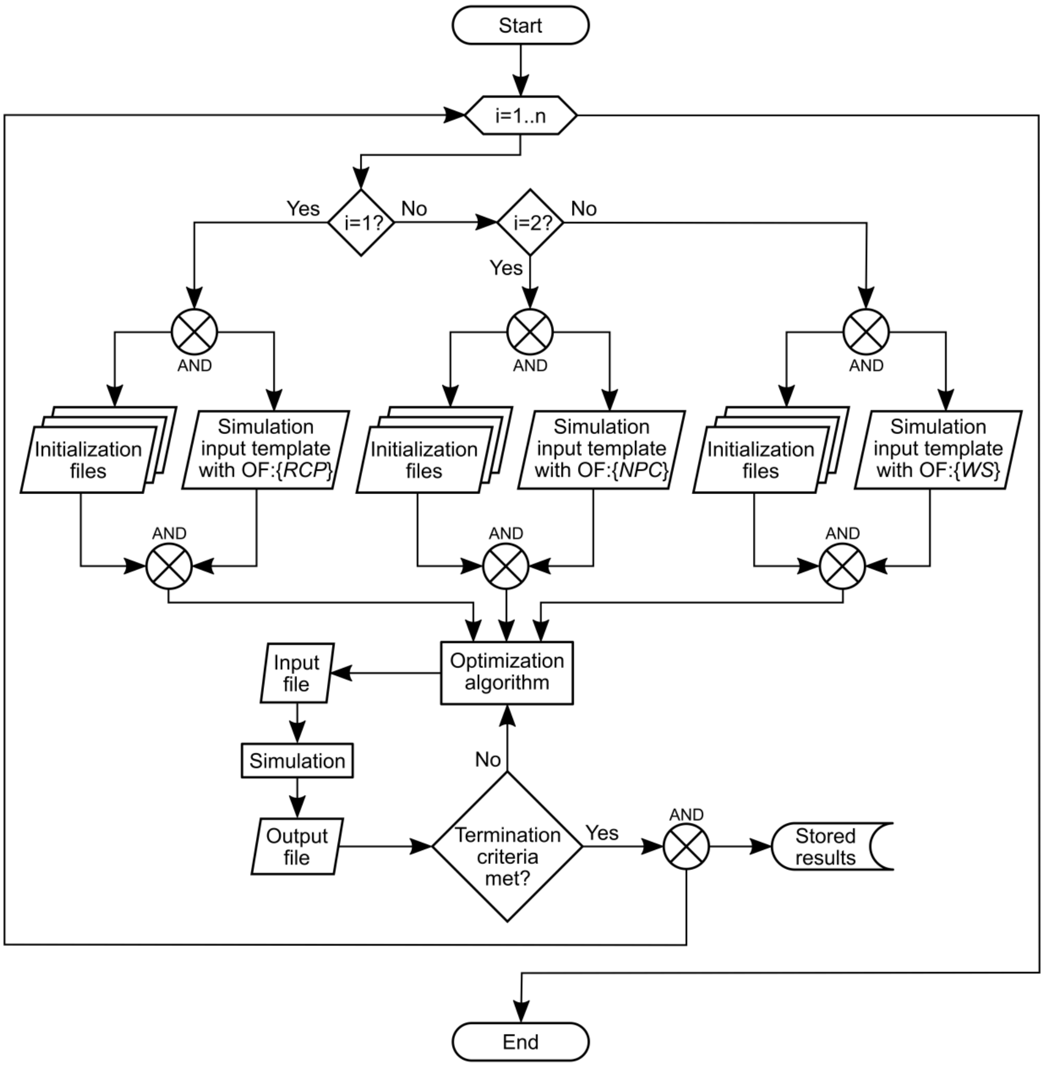

Fig. II-4. Flow chart of the solution procedure, where *OF: {RCP}* and *OF: {NPC}* are the original objective functions (environmental impact and total cost functions, respectively), and *OF:{WS}* is the objective function of the auxiliary single-objective model (weighted-sum function).

4. CASE STUDY

A case study is presented next to illustrate the application of the proposed methodology. A CSHPSS system located in Barcelona (Spain) is considered, which meets the heating demand of a neighborhood community of 1120 apartments (each with 90 m^2 of useful area [53]) and equipped with a radiant underfloor heating system and requiring 50 ºC hot water.

For comparison purposes, we consider a conventional heating system with no collectors as base case solution. This base case consists of a boiler of 93% of efficiency fueled with natural gas. This boiler is designed to heat the cold water to the established 50 ºC set-point. The validation of the CSHPSS model and the necessary heating demand data are performed comparing with the work by Guadalfajara *et al.* [32] and Guadalfajara [54].

4.1. <u>CSHPSS model specifications</u>

The field of solar collectors of the CSHPSS model consists of flat-plate type ARCON HT-SA 28/10 collectors [55] designed for large applications. These collectors, with 12.52 m^2 aperture area, are coupled in series, tilted 45º and oriented towards South. The working fluid, passing through the field of solar collectors (primary loop), is a $67/33_{w/w}$ mixture of water and glycol with a nominal flow rate of 20 kg/h-m^2 [32]. The secondary and tertiary loops as well as the storage tank operate with water. The distribution loop is fed with 30 ºC water coming from the central supply network.

The seasonal storage tank is a partially buried water tank built of reinforced concrete and insulated with 0.5 m of extruded polystyrene [32,33]. The tank has a cylindrical form with a constant height to diameter ratio of 0.6 and 20 levels of stratification.

The auxiliary heater is a natural gas fueled boiler with 93% efficiency able to heat the water until it reaches the 50 ºC set-point [32]. The boiler is properly designed to be able to deliver 100% of the heat when required.

All the TRNSYS simulations were performed using a 15 min time-step in order to reproduce precisely the temporal variation of the thermal processes [26]. Moreover, we use the results of the third year of the simulation to predict the plant performance during all the years of operation. This is because at the beginning of the first year of the simulation, the temperature inside the storage tank is defined as homogeneous and equal to 30 ºC. Hence, the simulation results of the first two years are used to eliminate the initial assumption about the water temperate inside the TEST.

The energy flow profiles of the simulated CSHPSS model are consistent with those reported by Guadalfajara [54]. The CSHPSS efficiency, defined as the fraction between the supplied solar energy and the total heating demand, differs in only 3% from the one obtained by Guadalfajara [54].

The plant operates 40 years [56], but the following equipment units need to be replaced after 20 years of operation: solar collectors, the auxiliary boiler and the heat exchangers [57]. The life span of the storage tank is 80 years [57].

4.2. Climatic and heating demand input data

The detailed climatic data for Barcelona have been obtained from the EnergyPlus database [58]. These data include solar radiation, ambient temperature, and air humidity, among other relevant information. In Fig. II-5 we show the average monthly values for the ambient temperature and the incident radiation per area of solar collector.

To generate the heating demand for the residential sector in Spain, we have followed the work by Guadalfajara [54] in order to reproduce a 7-story building that meets the minimum requirements of the Spanish regulation [17]. The 3-D sample building was developed using the graphical tool SketchUp [59], and later imported to TRNSYS, where the profiles of occupation of the apartments and the physical properties of the materials of the walls and windows were added. Thus, by simulating this building model, we generated a typical year heating demand on an hourly timescale. The monthly values of the demand per useful area of an apartment are presented in Fig. II-5.

The profiles generated following the approach described above differ in no more than 0.6% from those reported by Guadalfajara [54]. The demand profiles of the validated model were extrapolated to 40 buildings, with a total demand of 4225 MWh/year of heating demand.

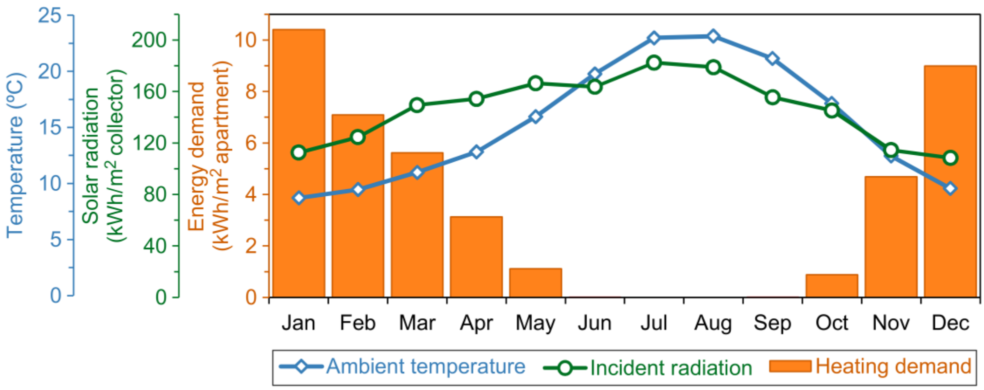

Fig. II-5. Climatic conditions in Barcelona (Spain) and energy demand of the sample building.

4.3. Economic and environmental data

The data used in the economic analysis (*i.e.* the parameters for the initial capital cost estimation and the data used to calculate the base year cost of the main equipment units) are summarized in Table II-1.

Table II-1. Equipment cost parameters.

Unit	α_k	β_k	CAP_k	**Range**	**Base year**	**Ref.**	FBM_k [60]
Solar collector	974.15	0.833	Aperture area (m^2)	4,000 – 15,000 m^2	2007	[61]	1
Storage tank	3955.3	0.650	Volume (m^3)	1 – 100,000 m^3	2007	[62]	1
Auxiliary boiler	225.01	0.746	Duty (kW)	600 – 10,000 kW	2001	[60]	2.1
Heat exchangers	3.1332	-0.331	Exchange area (m^2)	10 – 1,000 m^2	2001	[60]	3.29
Pump (P_1,P_2)	389	-283.15	Mass flow rate (kg/h)	15,000 – 100,000 kg/h	2009	[63]	3.24
Pump (P_3)	389	717	Mass flow rate (kg/h)	15,000 – 100,000 kg/h	2009	[63]	3.24

Table II-2 presents the CEPCI indices needed to update the purchase cost of the equipment from the base year to the year of installation of the CSHPSS.

Table II-2. Chemical engineering plant cost indices [41].

Year	2001	2007	2009	2015
CEPCI	394.3	525.4	521.9	547.2

The operating costs for this case study were estimated as follows. Following the work by Kalogirou [40], the costs of maintenance are assumed to be 1.5% of the total initial purchase cost of the equipment. The costs of natural gas and electricity for 2015 are 0.039 €/kWh [64] and 0.1735 €/kWh [65], respectively. Furthermore, we consider annual inflation rates for natural gas, electricity use and the purchase of goods. The annual rate of natural gas inflation (i_f) is set to 5.9%, and the rate of electricity inflation (i_e) to 5.0%. These percentages are defined from the average annual change of the consumer price index between 2004 and 2014 in Spain [66]. Additionally, the general inflation rate (i) is assumed to be 2.3%, which is the average annual change of the harmonized indices of consumer prices for the period between 2004 and 2014 in Spain [67]. Moreover, a 3.5% annual market discount rate (d) has been considered [68].

The LCA data were taken from the work by Raluy *et al.* [33], where the authors applied LCA to a CSHPSS plant simulated in Zaragoza (Spain). Table II-3 shows the impact of the main equipment units and utilities (based on ReCiPe 2008 methodology), with the former being expressed in relation to the size of the corresponding equipment (*i.e.* area of solar collector, inner surface of storage tank, etc.).

Table II-3. Specific ReCiPe 2008 aggregated impact factor for the main equipment units and utilities, in ReCiPe points (Pt) per characteristic dimension.

Unit/Utility	**Specific ReCiPe 2008 impact factor (final score)**
Solar collector	17 Pt/m^2
Storage tank	117 Pt/m^2
Auxiliary boiler	1570 Pt/unit
Heat exchangers	9 Pt/m^2
Pumps	82 Pt/unit
Electricity	0.04 Pt/kWh
Natural gas	0.02 Pt/kWh

4.4. Optimization parameters

The optimization parameters required to adjust the GPSPSOCCHJ algorithm were taken from Wetter [35]. The decision variables and their upper and lower bounds were incorporated to a command file, which was used by GenOpt during the optimization process. The bounds of the decision variables are defined as follows:

- Ratio between A_{COL} and total heating demand (ADR),
- Ratio between V_{TEST} and ACOL (VAR).

The starting points, the optimization step and the lower and upper bounds on variables are given in Table II-4.

Table II-4. Specifications of the upper and lower bounds of the decision variables.

Variable	**Parameter**	**Value**
ADR	Initial	2
	Step	0.05
	Minimum	0.003
	Maximum	3
VAR	Initial	5
	Step	0.05
	Minimum	0.01
	Maximum	20

5. RESULTS AND DISCUSSIONS

The solution of the multi-objective optimization model is given by a set of points that define the Pareto frontier of the problem (see Fig. II-6). Each optimal solution corresponds to a fully-defined configuration of a CSHPSS plant. It took 2500 CPU seconds on average to generate each of the Pareto solutions on a computer with an Intel® Core™ i5-4570 3.20GHz processor with 16 GB RAM. The GenOpt-TRNSYS platform iteratively simulated the TRNSYS model (spending around 30 CPU seconds per simulation) until the optimal solution was identified for each combination of weights.

The optimal solutions calculated following our approach improve clearly the base case alternative, which lies on the sub-optimal region of the search space. Thus, by choosing the proper Pareto point, the environmental impact can be reduced in as much as 85% (24.75 Pt/MWh in the base case and 3.83 Pt/MWh in solution B) and the total cost in as much as 16% (69.54 €/MWh in the base case and 58.17 €/MWh in solution A).

Starting from the minimum cost solution A, with the NPC equal to 58.17 €/MWh and the RCP equal to 4.53 Pt/MWh (see Fig. II-6), it is possible to reduce the impact by 15% by sacrificing the cost in as much as 5% compared to solution B (NPC is equal to 61.20 €/MWh and RCP is equal to 3.83 Pt/MWh). Solution C, with the NPC equal to 58.79 €/MWh and the RCP equal to 3.98 Pt/MWh, increases the cost by 1% with respect to the anchor point A, but at the same time reduces the impact by 12%. Without loss of generality, we will consider solution C, that was obtained with λ=0.5, as intermediate solution and use it throughout the analysis of the results. Note however, that any other intermediate solution would be equally valid for such an analysis, since all the Pareto points are optimal.

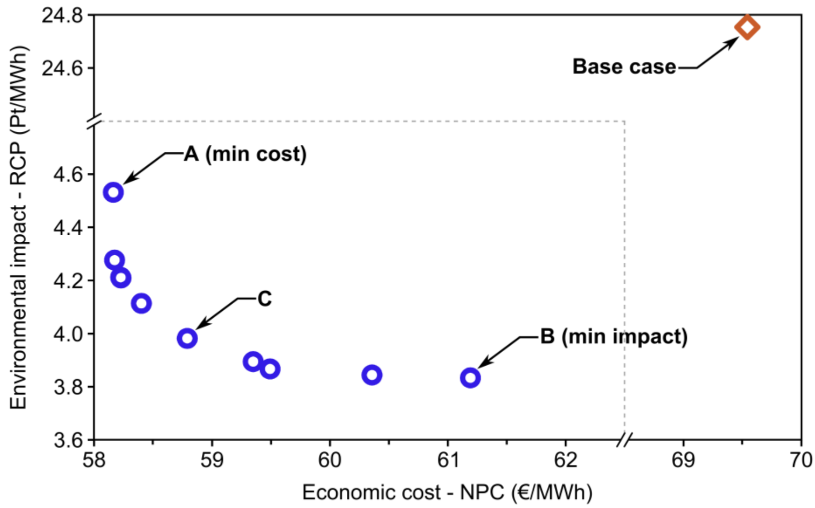

Fig. II-6. Pareto set of optimal configurations of a CSHPSS plant in Barcelona which meets the heating demand of 4225 MWh/year during its lifetime. Anchor points A and B are the minimum cost and minimum impact solutions, respectively; solution C is an intermediate CSHPSS design obtained with λ=0.5; base case represents a conventional heating system.

Recall that each of the proposed solutions represents a different configuration of the CSHPSS plant. The proposed methodology enables an in-depth analysis of each configuration to help decision-makers chose the most attractive alternative. We next analyze the economic cost (Fig. II-7) and environmental impact breakdown (Fig. II-8) of the anchor points (solutions A and B in Fig. II-6) and compare them with those corresponding to the base case.

In Fig. II-7, the capital cost in A and B solutions is quite large compared to that associated with the base case and might therefore be considered as a major financial bottleneck (the initial capital represents around 50% of the total net present cost). This issue is common to any CSHPSS configuration, as they require large investments to purchase the equipment units. More precisely, the solar collectors and the storage tank represent around 60% of the capital cost, whereas in the base case this percentage is 2.8%, the heater is the most expensive unit and 95% of the NPC is mainly due to the natural gas cost.

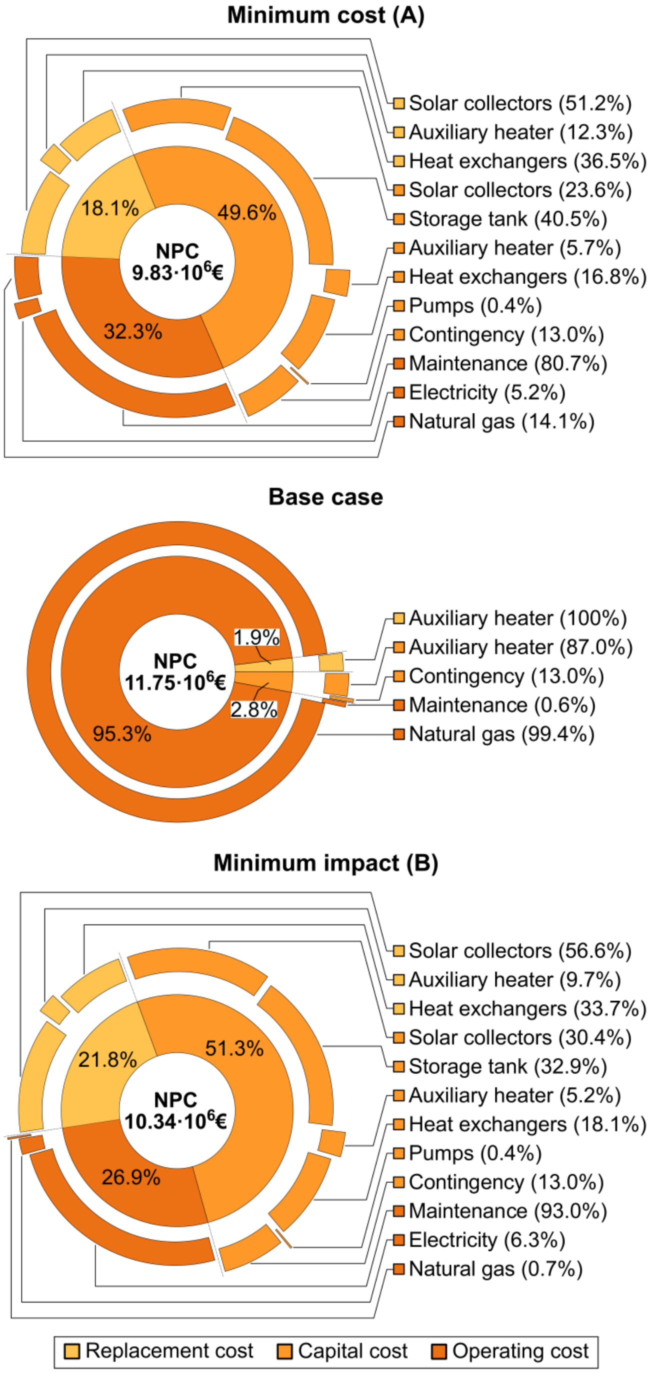

Fig. II-7. Breakdown of the net present costs of two Pareto optimal solutions (solution A and B in Fig. II-6) for a CSHPSS plant which meets the heating demand of 4225 MWh/year during its lifetime and the base case, which represents a conventional heating system.

Solutions A and B show a similar distribution of costs. However, A has slightly higher operating cost due to the cost of natural gas consumed during short periods along the year. On the other hand, natural gas consumption is drastically reduced in solution B.

The anchor points A and B can reduce the impact in as much as 6 times compared to the base case by diminishing the amount of natural gas used as main fuel (see Fig. II-8). In the base case, natural gas consumption represents almost 100% of the total impact ($4.18 \cdot 10^6$ Pt), whereas in the minimum cost solution (A) it represents 22% of the total impact ($0.17 \cdot 10^6$ Pt over $0.77 \cdot 10^6$ Pt). Moreover, in the minimum impact solution (B), natural gas consumption is almost negligible (1% of the total impact, $0.007 \cdot 10^6$ Pt over $0.65 \cdot 10^6$ Pt).

Comparing solutions A and B, we see that in both cases the solar collectors and the storage tank have a predominant share of the total impact. Hence, we can confirm the importance of the solar collectors and the storage tank from both, the economic and environmental points of view. In both anchor points, the storage tank is responsible for half of the damage to the environment. On the other hand, the fraction of the impact caused by the solar collectors increases from 21% in solution A ($0.16 \cdot 10^6$ Pt over $0.77 \cdot 10^6$ Pt) to 38% in solution B ($0.24 \cdot 10^6$ Pt over $0.65 \cdot 10^6$ Pt), while the consumption of non-renewable energy sources is reduced (from $0.17 \cdot 10^6$ Pt to $0.007 \cdot 10^6$ Pt).

Our analysis reveals that the solar collectors and storage tank are the main equipment units taking in consideration the tendencies observed in the previous economic cost and environmental impact breakdown figures. The proposed methodology provides the optimal sizing of the main equipment units for each optimal configuration (see Fig. II-9). The minimum cost solution (A) includes a field of solar collectors of 4600 m^2 and a storage tank of about 38700 m^3. On the other hand, the minimum impact configuration (B) has a larger field of solar collectors of 7000 m^2 and a storage tank of around 32100 m^3. The dimensions of each of the equipment units vary approximately by 20% to 30% between the extreme solutions of the Pareto frontier.

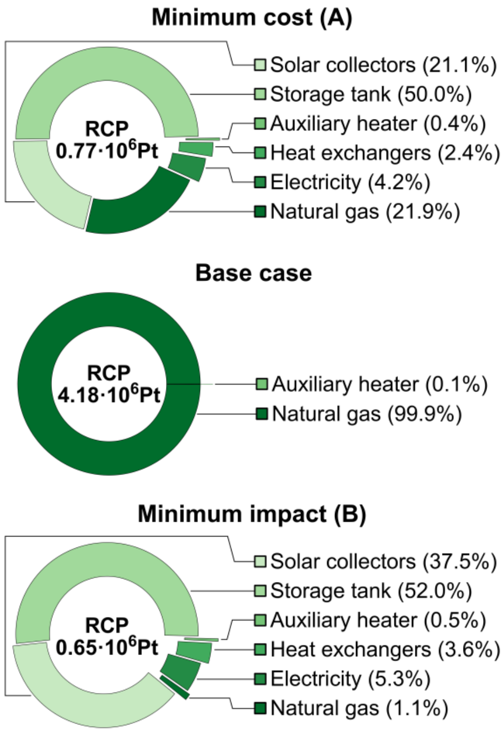

Fig. II-8. Breakdown of the environmental impact of two Pareto optimal solutions (solution A and B in Fig. II-6) for a CSHPSS plant which meets the heating demand of 4225 MWh/year during its lifetime and the base case, which represents a conventional heating system.

The environmental impact reduction from solution A to C occurs at the expense of increasing the area of solar collectors and the volume of the storage tank (Fig. II-9). Higher capacities of the main equipment units lead to larger cost but favor the reduction of non-renewable energy (*i.e.* natural gas and electricity) consumption, by replacing it by solar thermal energy. The move from solution C to B leads to more significant structural changes in the CSHPSS design. The area of the solar collectors is increased, while the volume of the storage tank is reduced (Fig. II-9), reflecting the necessity to satisfy the heating demand and reduce the environmental impact. Thus, a smaller fraction of the demand is covered by the thermal energy stored, favoring the transfer of direct energy from the solar collectors.

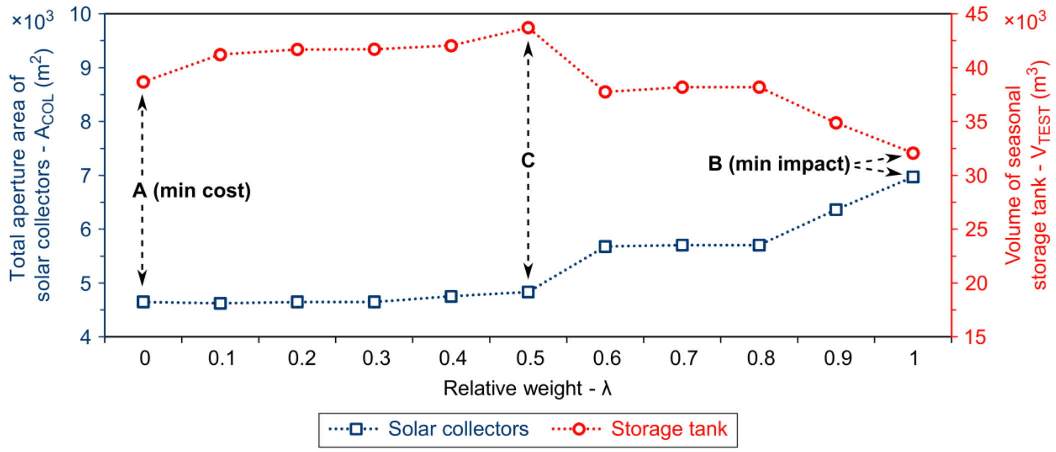

Fig. II-9. Optimal dimensions of solar collectors and storage tank for CSHPSS designs able to meet the heating demand of 4225 MWh/year during their lifetime. Anchor points A and B are the minimum cost and minimum impact solutions, respectively; solution C is an intermediate CSHPSS design obtained with λ=0.5.

Finally, our methodology enables the analysis of the optimal configurations of a CSHPSS plant from the thermodynamic point of view. We present in Fig. II-10 the thermal energy profiles of a typical year of operation for the intermediate solution (solution C in Fig. II-6). The monthly values of heating demand are fulfilled either by the instant solar radiation coming directly from the solar collectors or by the thermal energy stored in the TEST. In extreme cases, when the instant solar radiation and the stored energy are not able to cover the demand, the auxiliary heater provides the necessary energy. These extreme cases occur mostly during February and March, when the storage tank is almost discharged. Between April and September, the surplus of solar radiation is stored inside the TEST in order to be consumed during the coldest months of the year. The amount of energy stored is represented as negative input in Fig. II-10.

The incident solar radiation depicted in Fig. II-10 shows the availability of solar energy over the year and how it is used by the CSHPSS plant. The use of radiation is maximal in March, while in October it reaches its minimum level. This is due to several factors, including high heating demand, availability of storage space, and the combination of both.

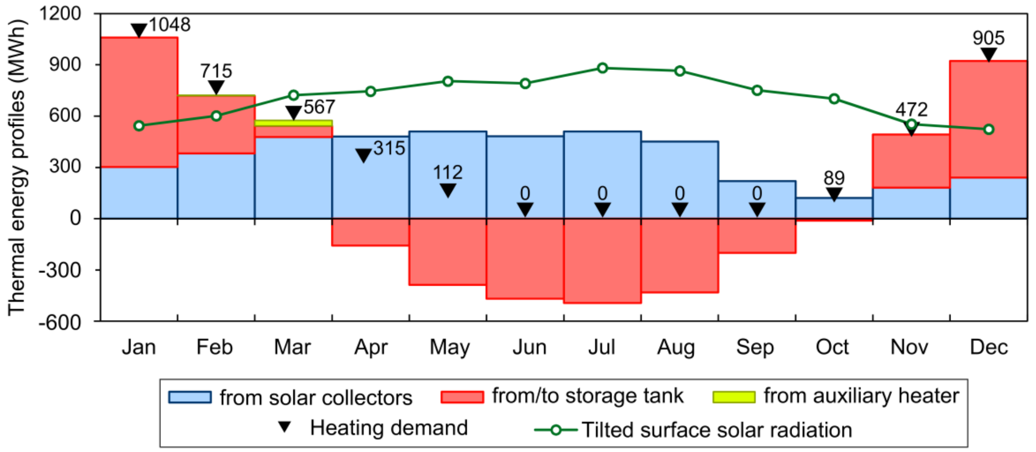

Fig. II-10. Thermal energy profiles for the intermediate CSHPSS design (solution C in Fig. II-6), where heating demand of 4225 MWh/year is satisfied by energy transfer from solar collectors, storage tank, and auxiliary heater. Surplus of thermal energy is sent to storage tank (negative values) to be used in the future.

6. CONCLUSIONS

In this study we developed a multi-objective optimization approach to design complex central solar heating plants with seasonal storage that considers economic and environmental objectives simultaneously. The methodology integrates simulation software with an optimization algorithm: the objectives are evaluated through a full TRNSYS simulation, while the optimization is carried out by GenOpt tool, which implements a hybrid metaheuristic algorithm.

We tested the capabilities of this approach in a case study of a CSHPSS located in Barcelona (Spain) that is able to supply 4225 MWh/year required for heating 1120 apartments. The main finding of this work is that it is possible to find a solution based on a CSHPSS with better cost and environmental performance than the base case (conventional heating system), in other words, CSHPSS can bring both economic and environmental benefits simultaneously, provided one is willing to invest in the capital cost required to build the facility. In the case study, the minimum cost solution reduces by 16% the net present cost and by 82% the environmental impact compared to a conventional heating system. This solution implements a total area of 4600 m^2 of solar collectors and a seasonal storage tank of 38700 m^3. Moreover, the minimum environmental impact solution reduces by 12% the net present cost and by 85% the environmental impact compared also to the base case design. This Pareto solution would require 7000 m^2 of solar collectors and a storage tank of 32100 m^3.

Overall, the CSHPSS technology is an economic and environmentally viable alternative in Mediterranean climate regions that can lead to significant benefits. While competitive optimal solutions can be identified, the high initial investments may act as a financial bottleneck that can eventually slow down the implementation of such plants. Hence, Government subsides might play a key role in promoting this technology. It is therefore important to define effective policies based on a longer-term view of the problem and the need to transition towards a more sustainable energy infrastructure.

Finally, the developed methodology can virtually offer a set of optimal CSHPSS plant designs for any climatic conditions and heating demand profiles. Through a detailed analysis of each optimal solution, decision-makers can choose the most convenient alternative to move towards a more sustainable energy system.

ACKNOWLEDGEMENTS

The authors would like to acknowledge financial support from the Spanish Government (CTQ2012-37039-C02-01, ENE2015-64117-C5-3-R, ENE2015-64117-C5-1-R, MINECO/FEDER, UE) and to thank the Catalan Government for the quality accreditation given to the research group GREA (2014 SGR 123). The research leading to these results has received funding from the European Commission Seventh Framework Programme under grant agreement no. PIRSES-GA-2013-610692 (INNOSTORAGE).

NOMENCLATURE

A_{COL} total aperture area of the solar collectors (m^2)

$A_{HE1\ or\ 2}$	heat transfer area of the heat exchanger 1 or 2 (m^2)
ADR	ratio between the area of solar collectors and the total heating demand (m^2/(MWh/year))
CAP_k	design variable of equipment unit k
C_{AUX}	annual operation cost of auxiliary heater (€)
C_C	initial capital cost (€)
$CEPCI^{year\ A}$	Chemical Engineering Plant Cost Index in base year (-)
$CEPCI^{year\ B}$	Chemical Engineering Plant Cost Index in installation year (-)
c_E	cost of electricity (€/kWh)
c_F	cost of natural gas (€/kWh)
C_M	annual cost of equipment maintenance (€)
C_O	total discounted operating cost (€)
C_P	annual operation cost of pumps (€)
C_R	total discounted equipment replacement cost (€)
d	market discount rate (%)
DAM_d	indicator result for damage category d
FBM_k	bare module factor of equipment unit k(-)
$f_c(x)$	original objective function (NPC(x) or RCP(x))
$\bar{f_c}(x)$	normalized objective function (NPC(x) or RCP(x))
f_m	maintenance factor (-)
$f^{PN}(x)$	pseudo nadir point
$f^{UT}(x)$	utopia point
i	annual inflation rate (%)
i_e	annual electricity inflation rate (%)
i_f	annual natural gas inflation rate (%)
IMP_e	indicator result for endpoint impact category e
L_{AUX}	annual natural gas load consumed by the auxiliary heater (MWh)
LCI_i^{MP}	life cycle inventory of the elementary flow i related to manufacturing process
LCI_i^{OP}	life cycle inventory of the elementary flow i related to operation activities
LCI_i^{TOT}	total life cycle inventory of the elementary flow i
LCI_i^{TR}	life cycle inventory of the elementary flow i related to transportation
L_P	annual electricity load consumed by pumps (MWh)
$\dot{m}_{P1\ or\ P2\ or\ P3}$	mass flow rate pumped through P_1, P_2 or P_3 (kg/h)

N_e	period of economic analysis (year)
NPC	net present cost of CSHPSS (€)
PEC_k	purchase cost of the equipment unit k in installation year (€)
$PEC_k^{year\ A}$	purchase cost of the equipment unit k in base year (€)
PVF_n	present value factor of a single future cash flow at the beginning of n^{th} time period (-)
PWF	present worth factor of periodic future cash flows (-)
Q_{AUX}	duty of auxiliary heater (kW)
RCP	ReCiPe 2008 aggregated impact factor (Pt)
t	time period (h)
V_{TEST}	volume of the thermal energy storage tank (m^3)
VAR	ratio between the volume of storage tank and the area of solar collectors (m^3/m^2)
WS(x)	weighted-sum objective function (-)
x	continuous variables of the simulation model
x^L	lower bounds of the continuous variables of the simulation model
x^U	upper bounds of the continuous variables of the simulation model
α_{CF}	factor of contingency charges and fees (-)
α_k	purchase cost coefficient of equipment unit k
β_k	purchase cost exponent of equipment unit k (-)
δ_d	normalization factor for damage category d
θ_{ei}	characterization factor that connects the elementary flow i with endpoint impact category e
λ	non-negative weight for the weighted-sum method
ξ_d	weighting factor for damage category d

Abbreviations

AUX	auxiliary heater
COL	solar collector
CHP	combined heat and power
CSHPSS	central solar heating plant with seasonal storage
DH	district heating
GenOpt	generic optimization program
GPSPSOCCHJ	generalized pattern search algorithm with particle swarm optimization

	with construction coefficient and Hooke-Jeeves algorithm
HE	heat exchanger
HJ	Hooke-Jeeves algorithm
LCA	life cycle assessment
MOO	multi-objective optimization
P	centrifugal pump
PSO	particle swarm optimization algorithm
TES	thermal energy storage
TEST	thermal energy storage tank
TRNSYS	transient system simulation program

Indices

c	objective function
d	damage category
e	endpoint impact category
i	elementary flow
k	units

Sets

ID_d set of endpoint impact categories e that contribute to damage d

REFERENCES

[1] Fox DB, Sutter D, Tester JW. The thermal spectrum of low-temperature energy use in the United States. Energy Environ Sci 2011;4:3731. doi:10.1039/c1ee01722e.

[2] European Environment Agency (EEA). Final energy consumption by sector and fuel (CSI 027/ENER 016) 2015. http://www.eea.europa.eu/data-and-maps/indicators/final-energy-consumption-by-sector-9/assessment (accessed February 14, 2016).

[3] Persson U, Werner S. Heat distribution and the future competitiveness of district heating. Appl Energy 2011;88:568–76. doi:10.1016/j.apenergy.2010.09.020.

[4] Ostergaard PA, Lund H. A renewable energy system in Frederikshavn using low-temperature geothermal energy for district heating. Appl Energy 2011;88:479–87. doi:10.1016/j.apenergy.2010.03.018.

[5] Nuytten T, Claessens B, Paredis K, Van Bael J, Six D. Flexibility of a combined heat and power system with thermal energy storage for district heating. Appl Energy 2013;104:583–91. doi:10.1016/j.apenergy.2012.11.029.

[6] Sartor K, Quoilin S, Dewallef P. Simulation and optimization of a CHP biomass plant and district heating network. Appl Energy 2014;130:474–83. doi:10.1016/j.apenergy.2014.01.097.

[7] Wang H, Yin W, Abdollahi E, Lahdelma R, Jiao W. Modelling and optimization of CHP based district heating system with renewable energy production and energy storage. Appl Energy 2015;159:401–21. doi:10.1016/j.apenergy.2015.09.020.

[8] Buoro D, Pinamonti P, Reini M. Optimization of a Distributed Cogeneration System with solar district heating. Appl Energy 2014;124:298–308. doi:10.1016/j.apenergy.2014.02.062.

[9] Renaldi R, Kiprakis A, Friedrich D. An optimisation framework for thermal energy storage integration in a residential heat pump heating system. Appl Energy 2015. doi:10.1016/j.apenergy.2016.02.067.

[10] Liu L, Zhu N, Zhao J. Thermal equilibrium research of solar seasonal storage system coupling with ground-source heat pump. Energy 2016;99:83–90. doi:10.1016/j.energy.2016.01.053.

[11] Hendricks AM, Wagner JE, Volk TA, Newman DH, Brown TR. A cost-effective evaluation of biomass district heating in rural communities. Appl Energy 2016;162:561–9. doi:10.1016/j.apenergy.2015.10.106.

[12] Fisch MN, Guigas M, Dalenbäck JO. A review of large-scale solar heating systems in Europe. Sol Energy 1998;63:355–66. doi:10.1016/S0038-092X(98)00103-0.

[13] Novo A V., Bayon JR, Castro-Fresno D, Rodriguez-Hernandez J. Review of seasonal heat storage in large basins: Water tanks and gravel–water pits. Appl Energy 2010;87:390–7. doi:10.1016/j.apenergy.2009.06.033.

[14] Pinel P, Cruickshank CA, Beausoleil-Morrison I, Wills A. A review of available

methods for seasonal storage of solar thermal energy in residential applications. Renew Sustain Energy Rev 2011;15:3341–59. doi:10.1016/j.rser.2011.04.013.

[15] Xu J, Wang RZ, Li Y. A review of available technologies for seasonal thermal energy storage. Sol Energy 2014;103:610–38. doi:10.1016/j.solener.2013.06.006.

[16] Dalenbäck JO. Large Scale Solar Heating Plants n.d. http://solar-district-heating.eu/ServicesTools/Plantdatabase.aspx (accessed February 14, 2016).

[17] Spanish Ministry of Housing. RD 314/2006, of March 28th, on approval of Spanish Technical Building Code - CTE (BOE n.74) 2006:11816–31.

[18] European Commission. The 2020 climate and energy package. Policies n.d. http://ec.europa.eu/clima/policies/strategies/2020/index_en.htm (accessed July 22, 2015).

[19] Meliß M, Späte F. The solar heating system with seasonal storage at the Solar-Campus Jülich. Sol Energy 2000;69:525–33. doi:10.1016/S0038-092X(00)00116-X.

[20] Schmidt T, Mangold D, Müller-Steinhagen H. Central solar heating plants with seasonal storage in Germany. Sol Energy 2004;76:165–74. doi:10.1016/j.solener.2003.07.025.

[21] Bauer D, Marx R, Nußbicker-Lux J. German central solar heating plants with seasonal heat storage. Sol Energy 2010;84:612–23. doi:10.1016/j.solener.2009.05.013.

[22] Pauschinger T. Solar district heating with seasonal thermal energy storage in Germany. Fact sheet. 2011.

[23] Argiriou AA. CSHPSS systems in Greece: Test of simulation software and analysis of typical systems. Sol Energy 1997;60:159–70. doi:10.1016/S0038-092X(96)00154-5.

[24] Ucar A, Inalli M. Thermal and economical analysis of a central solar heating system with underground seasonal storage in Turkey. Renew Energy 2005;30:1005–19. doi:10.1016/j.renene.2004.09.015.

[25] Ucar A, Inalli M. A thermo-economical optimization of a domestic solar heating plant with seasonal storage. Appl Therm Eng 2007;27:450–6. doi:10.1016/j.applthermaleng.2006.06.010.

[26] Pahud D. Central solar heating plants with seasonal duct storage and short-term water storage: design guidelines obtained by dynamic system simulations. Sol Energy 2000;69:495–509. doi:10.1016/S0038-092X(00)00119-5.

[27] Sibbitt B, McClenahan D, Djebbar R, Thornton J, Wong B, Carriere J, et al. The performance of a high solar fraction seasonal storage district heating system - Five years of operation. Energy Procedia 2012;30:856–65. doi:10.1016/j.egypro.2012.11.097.

[28] Terziotti LT, Sweet ML, McLeskey Jr. JT. Modeling seasonal solar thermal energy storage in a large urban residential building using TRNSYS 16. Energy Build 2012;45:28–31. doi:10.1016/j.enbuild.2011.10.023.

[29] Chung M, Park J-U, Yoon H. Simulation of a central solar heating system with seasonal storage in Korea. Sol Energy 1998;64:163–78. doi:10.1016/S0038-092X(98)00101-7.

[30] Lozano MA, Anastasia A, Palacín F, Serra LM. Simulation study and economic analysis of large-scale solar heating plants in Spain. EUROSUN 2010:1–8.

[31] Frago-Moreno J. Análisis Económico y geográfico de sistemas de calefacción de distrito con acumulación estacional. Proyecto final de carrera. 2011.

[32] Guadalfajara M, Lozano MA, Serra LM. Evaluation of the potential of large solar heating plants in Spain. Energy Procedia 2012;30:839–48. doi:10.1016/j.egypro.2012.11.095.

[33] Raluy R, Serra L, Guadalfajara M, Lozano M. Life Cycle Assessment of Central Solar Heating Plants with Seasonal Storage. Energy Procedia 2014;48:966–76. doi:10.1016/j.egypro.2014.02.110.

[34] Klein SA, Beckham WA, Mitchell DW. TRNSYS 17.1: A Transient System Simulation Program, Solar Energy Laboratory, University of Wisconsin, Madison, USA, 2010.

[35] Wetter M. GenOpt. Generic Optimization Program. User Manual. Berkeley Lab 2011:1–108.

[36] Azapagic A, Clift R. Life cycle assessment and multiobjective optimisation. J Clean Prod 1999;7:135–43. doi:10.1016/S0959-6526(98)00051-1.

[37] Carreras J, Boer D, Guillén-Gosálbez G, Cabeza LF, Medrano M, Jiménez L.

Multi-objective optimization of thermal modelled cubicles considering the total cost and life cycle environmental impact. Energy Build 2015;88:335–46. doi:10.1016/j.enbuild.2014.12.007.

[38] Torres CM, Gadalla M, Mateo-Sanz JM, Jiménez L. An automated environmental and economic evaluation methodology for the optimization of a sour water stripping plant. J Clean Prod 2013;44:56–68. doi:10.1016/j.jclepro.2012.12.002.

[39] Brunet R, Cortés D, Guillén-Gosálbez G, Jiménez L, Boer D. Minimization of the LCA impact of thermodynamic cycles using a combined simulation-optimization approach. Appl Therm Eng 2012;48:367–77. doi:10.1016/j.applthermaleng.2012.04.032.

[40] Kalogirou SA. Chapter twelve - Solar Economic Analysis. Sol. Energy Eng., Academic Press; 2009, p. 665–701. doi:10.1016/B978-0-12-374501-9.00012-1.

[41] Chemical Engineering Plant Cost Index (CEPCI): Economic Indicator. Chem Eng J 2015. http://www.chemengonline.com/pci-home (accessed July 13, 2015).

[42] Guillén-Gosálbez G, Grossmann IE. Optimal design and planning of sustainable chemical supply chains under uncertainty. AIChE J 2009;55:99–121. doi:10.1002/aic.11662.

[43] ISO/TC 207/SC 5, International Organization for Standardization (ISO). ISO 14040:2006 Environmental management — Life cycle assessment — Principles and framework. Geneva: 2006. doi:10.1002/jtr.

[44] ISO/TC 207/SC 5. ISO 14044:2006 Environmental management — Life cycle assessment — Requirements and guidelines 2006.

[45] Weidema BP, Bauer C, Hischier R, Mutel C, Nemecek T, Reinhard J, et al. The ecoinvent database: Overview and methodology, Data quality guideline for the ecoinvent database version 3 2013. www.ecoinvent.org.

[46] Hauschild M, Goedkoop M, Guinee J, Heijungs R, Huijbregts M, Jolliet O, et al. Recommendations for Life Cycle Impact Assessment in the European context - based on existing environmental impact assessment models and factors (International Reference Life Cycle Data System - ILCD handbook). 2011. doi:10.2788/33030.

[47] Goedkoop M, Heijungs R, De Schryver A, Struijs J, van Zelm R, Huijbregts M, et

al. ReCiPe 2008. A LCIA method which comprises harmonised category indicators at the midpoint and the endpoint level. Report I: Characterisation 2009:1–133. doi:http://www.lcia-recipe.net.

[48] Azapagic A. Life cycle assessment and its application to process selection, design and optimisation. Chem Eng J 1999;73:1–21. doi:10.1016/S1385-8947(99)00042-X.

[49] Ehrgott M. Multicriteria optimization. Heidelberg: Springer; 2005.

[50] Kennedy J, Eberhart R. Particle swarm optimization. Neural Networks, 1995 Proceedings, IEEE Int Conf 1995;4:1942–8 vol.4. doi:10.1109/ICNN.1995.488968.

[51] Kennedy J, Eberhart RC. A discrete binary version of the particle swarm algorithm. 1997 IEEE Int Conf Syst Man, Cybern Comput Cybern Simul 1997;5:4–8. doi:10.1109/ICSMC.1997.637339.

[52] Hooke R, Jeeves TA. “Direct Search” Solution of Numerical and Statistical Problems. J ACM 1961;8:212–29. doi:10.1145/321062.321069.

[53] Institute for Energy Diversification and Saving - IDAE, IDAE. Análisis del consumo energético del sector residencial en España. INFORME FINAL. 2011.

[54] Guadalfajara M. Evaluación de centrales solares térmicas con acumulación estacional para el sector residencial en España. Trabajo final de máster. 2013.

[55] Arcon Solar. Datasheet ARCON Solar Collector type HT-SA 28/10. n.d.

[56] United Nations Environment Programme. Solar Thermal Energy Technology Fact Sheet 2014.

[57] Colclough S, McGrath T. Net energy analysis of a solar combi system with Seasonal Thermal Energy Store. Appl Energy 2015;147:611–6. doi:10.1016/j.apenergy.2015.02.088.

[58] U.S. Department of Energy. EnergyPlus. Energy Simulation Software: Weather Data n.d. http://apps1.eere.energy.gov/buildings/energyplus/ (accessed March 23, 2018).

[59] Trimble. SketchUp 2017. http://www.sketchup.com.

[60] Turton R, Bailie RC, Whiting WB, Shaeiwitz JA, Bhattacharyya D. Analysis, synthesis, and design of chemical processes. 3rd ed. Prentice Hall; 2008.

[61] Ellehauge K, Pedersen TE. Solar heat storages in district heating networks. Energinet.dk, PREHEAT project no. 2006-2-6750. 2007.

[62] Schmidt T, Mangold D. Status of Solar Thermal Seasonal Storage in Germany. Effstock 2009.

[63] Calise F, Dentice d'Accadia M, Palombo A. Transient analysis and energy optimization of solar heating and cooling systems in various configurations. Sol Energy 2010;84:432–49. doi:10.1016/j.solener.2010.01.001.

[64] Spanish Ministry of Industry Energy and Tourism. Resolución de 26 de diciembre de 2014, de la Dirección General de Política Energética y Minas, por la que se publica la tarifa de último recurso de gas natural. BOE n. 315, 30 de diciembre de 2014 n.d.:106920.

[65] European Commission. Eurostat. Energy database n.d. http://ec.europa.eu/eurostat/data/database (accessed May 10, 2018).

[66] National Statistics Institute. Consumer Price Index n.d. http://www.ine.es/dyngs/INEbase/en/operacion.htm?c=Estadistica_C&cid=1254736176802&menu=ultiDatos&idp=1254735976607 (accessed September 21, 2015).

[67] EUROSTAT. Annual Average Rates of Inflation n.d. http://ec.europa.eu/eurostat/statistics-explained/index.php/Inflation_in_the_euro_area (accessed September 21, 2015).

[68] Braungardt S, Eichhammer W, Elsland R, Fleiter T, Klobasa M, Krail M, et al. Study evaluating the current energy efficiency policy framework in the EU and providing orientation on policy options for realising the cost-effective energy-efficiency/saving potential until 2020 and beyond. Karlsruhe/Vienna/Rome: 2014.

III EUROPEAN CASE STUDIES

Economic and environmental potential for solar assisted central heating plants in the EU residential sector: Roadmap to the 2030 climate and energy EU targets [§]

Victor Tulus [a], **Mohamed Hany Abokersh** [b], **Luisa F. Cabeza** [c], **Manel Vallès** [b], **Laureano Jiménez** [a], **Dieter Boer** [b,*]

[a] Departament d'Enginyeria Química, Universitat Rovira i Virgili, Av. Països Catalans 26, 43007 Tarragona, Spain

[b] Departament d'Enginyeria Mecànica, Universitat Rovira i Virgili, Av. Països Catalans 26, 43007 Tarragona, Spain

[c] GREiA Research Group, INSPIRES Research Centre, Universitat de Lleida, Pere de Cabrera s/n, 25001 Lleida, Spain

** Corresponding author: dieter.boer@urv.cat*

[§] Under peer review (September 2018)

Keywords:
central solar heating plant with seasonal storage
life cycle assessment (LCA)
life cycle cost (LCC)
multi-objective optimization
thermal energy storage
forecasting

1. INTRODUCTION

The global tendency for changing the world energy map is a booming topic, and more efforts should be scaled up to shift the current energy production systems towards the use of cleaner and less carbon-intensive sources. Currently, fossil fuels share about 80% of the primary energy use [1]. The International Energy Outlook [2] forecasts a significant increase in the world energy demand over the next decades. It is projected that the global energy consumption will evolve by 48% in 2040 with a growth in the usage of crude oil and natural gas by 30% and 53.2%, respectively. This outlook trend leads to serious environmental problems such as more greenhouse gas (GHG) emissions and the subsequent impact on the climate [3].

Europe is one of the relevant players in this scenario contributing 21.6% to the overall energy consumption [4]. Additionally, in the European Union (EU) the building stock accounts for about 40% of the total energy demand [5], while the residential sector consumes 63% of this energy [6]. According to estimations of the US Energy Information Administration (EIA) [2], the energy consumption demand for the residential section in the EU increases by an average of 0.9% per year. Along with all of these figures, the residential buildings are the fourth most important source of GHG in the EU and it accounted for about 10% of the total GHG in 2016 [7]. In response to this challenge, the EU has adopted the 2020 climate and energy package [8] which includes a set of requisite legislation to tackle the environmental concerns and support the energy security and independence. The package sets three main targets: (i) reduce by 20% the GHG emissions compared to the 1990 levels, (ii) increase the renewable energy share and (iii) improve its energy efficiency by 20%. In 2013, the EU approved a new ambitious framework for the climate and energy between 2020 and 2030. This strategy plans to cut the GHG emissions by 40%, to achieve a share of at least 27% of renewable energies, and to improve the energy efficiency by at least 27% [9].

Among all of the renewable energy resources, the solar thermal energy obtained a considerable attention since it is a CO_2 neutral and it can be used for both space and water heating [10,11]. Apparently, the solar thermal technologies could satisfy substantially the heat demand in the residential sector in many countries [12]. Furthermore, it has several advantages which include [13] (i) savings in the primary energy consumption at the end user and country planning level, (ii) increase in energy security against the fluctuations in the prices of the conventional energy resources, (iii) decrease the dependency on the electricity from the network, and (iv) contribute to the network stabilization. These solar thermal energy systems continue to increase their market share across whole Europe. More than 1.2 $GW_{thermal}$ was installed within 2015 to raise the total installed capacity to 34.4 $GW_{thermal}$ [14].

However, the solar thermal systems are facing a great challenge of intermittency and predictability, which cause a gap between the supply and the energy demand [15,16]. The thermal energy storage (TES) systems can effectively solve this issue [17]. There are three main categories of the TES. These categories include the sensible TES through a temperature gradient, the latent TES based on the phase change materials, and the thermo-chemical TES through chemical reactions [18]. Currently, sensible storage is the most common system to be used in the residential sector, while latent and chemical systems are promising technologies under development [19].

The specific heat and energy density are the two main characteristics that evaluate the thermal capacity of the sensible TES. Besides thermal capacity characteristics, the TES cost has also a vital role in the selection process. Therefore, water, rock material, and soil/ground are the usually employed storage media in the sensible TES systems. The energy storage in the sensible TES systems can be classified into long-term (seasonal) and short-term (diurnal) [20]. The main difference between these two systems is the solar collector and storage volume sizing where the investment per square meter of collector area is almost doubled in the long-term seasonal storage systems [21]. In addition to that, seasonal storage is always coupled with an auxiliary heater to cover the shortage in supply [22]. On the contrary, short-term storage allows a direct usage in the heating district network.

The sensible seasonal storage coupled with the solar heating system has been subjected to several investigations and it has already been introduced as a feasible alternative. Initially, in the 1950's, Speyer [23] assesses theoretically the potential of the central solar heating plant coupled with seasonal storage (CSHPSS) to benefit from the excess of solar energy in summer during the winter period. The first proof of concept for this system was developed in Sweden in the 1970's to address the energy shortage crisis [24], followed by Denmark and Germany in the 1990's [25]. Since then, the market for the solar heating plants has grown throughout Europe [26], particularly in Northern and Central European countries. During 2016, 37 large heating plants were installed in Europe compared to 21 new installed in 2015. Within these installations, 31 systems were added to the Denmark district heating networks, 4 systems in Germany, 1 system in Sweden and 1 system in France [27]. In the southern European countries, some positive signs of growth of solar thermal energy are noticed from Spain and Greece. These evolution signs are due to the legislation imposed by the governments to scale up the utilization of renewable energy technologies [28].

Regarding this evolution, several review papers tend to discuss the principal methods available for the seasonal storage of the central solar heating system [12,21,22,29,30]. In addition, several studies were conducted to give insight into the technical [31–35], and economic potential of the CSHPSS [36,37] with consideration for the environmental impacts [13,38].

To maximize the benefits from the CSHPSS in the residential sector, the optimal sizing of the system components and their operation should be planned properly. This can turn into a computationally requesting task. Li et al. [39] explored the optimal operation strategy for the CSHPSS based on the orthogonal schedule using real data. Ucar and Inalli [40] and Durâo et al. [41] lean towards optimizing the design parameters of CSHPSS for different locations from an economical point of view using Genetic Algorithms. Buoro et al. [42] formulated a Mixed Integer Linear Programming (MILP) approach for optimizing the CSHPSS plant together with a conventional power unit for a large district heating network. Recently, several studies emphasized on the importance of taking into account the techno-economic and environmental impact simultaneously when expanding the optimization approach for designing a new CSHPSS plant. Tulus et al. [43] proposed a systematic multi-objective optimization (MOO) approach for CSHPSS plants based on a generic optimization tool according to economic and environmental indicators. This becomes especially important as the main impact weight shifts from the fossil fuel consumption to the materials used for the installation. Besides, Pavičević et al. [44] developed and demonstrated a long-term MILP optimization model based on SCIP (Solving Constraint Integer Program) solver for district heating systems. This model can handle the operation strategy and system component sizing in the planning and evaluation process with considerations for the cost and the environmental impacts throughout the project lifetime.

Even though the tendency of the CSHPSS plants is promising, a range of potential barriers (technical, financial and administrative) are still obstructing the wide deployment of CSHPSS in Europe. One of the greatest challenges associated with the CSHPSS is the performance uncertainty. According to several large-scale seasonal energy storage systems, the solar fraction of the plants has a quite wide variation [45] which suggests a high degree of uncertainty in the quantifiable costs and benefits. In German and Spanish CSHPSS projects [31, 36] the combination of a seasonal heat storage with a central solar heating system enables solar fractions of over 50%. While in a CSHPSS project for a residential area in Alberta (Canada) 97% of solar fraction was achieved in the fifth year of operation [46]. A simulation study for district solar heating combined with borehole seasonal storage in Helsinki showed that high solar fraction of 96% is feasible [47]. Besides the performance uncertainty, the high capital costs of this technology represent a challengeable barrier and make it more difficult to obtain the required funding [48]. Also, there are primarily political and legal barriers which include: lack of a clear model of the system which could help the European 2030 climate and energy framework achieve its targets; the sudden change in the renewable energy legal framework in some EU countries such as Spain [49]. All these technical, economic and legal barriers promote high uncertainty in quantifying the CSHPSS benefits over its lifetime and add more difficulties for the EU members to state their own forecast plans for future deployment of the CSHPSS in district heating fields.

Up to our comprehensive literature review of CSHPSS plants in the residential sector, simultaneous optimization of life cycle costing (LCC) for the economic analysis and Life Cycle Assessment (LCA) for the environmental impact burdens considering technical performances of CSHPSS plants in various EU member states has not been addressed so far. Furthermore, we additionally considered short-term heat storage incorporating domestic hot water (DHW) services as an individual process coupled to the CSHPSS, which is not usually included in other works. And finally, we attempt to forecast the tendencies of CSHPSS installation in the EU for the next decade.

Thus, this work aims to develop a systematic MOO framework capable of providing sets of economically and environmentally optimal solutions for CSHPSS plants in different EU member states (with different types of climate) with comparison to a conventional heating system using natural gas as the main heat source. The simulation-optimization methodology framework begins with a detailed simulation of the CSHPSS plant performance using TRNSYS 18 software [50] considering seasonal and short-term storage systems and their respective load profiles based on the explored climates. Then the multi-objective optimization is performed by an external generic optimization toolbox (GenOpt [51]). The proposed methodology can serve as a supportive tool for decision-makers helping them assess the potential of the CSHPSS plants in Europe and subsequently, promote a clear statement towards the possibility of achieving the 2030 European climate and energy framework targets.

The chapter organization is the following: in section 2 a general overview of the CSHPSS system is provided; the mathematical formulation of the simulation-optimization methodology together with the mathematical basis of the CSHPSS market forecasting are provided in section 3; section 4 describes the application of the methodology to four EU climate zones and section 5 offers the necessary results and discussions; finally, the conclusions of the work are presented in section 6.

2. OVERVIEW OF THE CSHPSS SYSTEM

Central solar heating plants with seasonal thermal energy storage are designed to fulfill energy demands for space heating (SH) and DHW in a residential sector (see Fig. III-1). Usually, these systems are designed to supply district heating for more than 100 apartments with a solar fraction of approximately 50% [31]. The main components of the CSHPSS system are the thermal solar collector, the seasonal storage tank (SST), and the DHW storage tank (DHWT). The solar collector transfers the heat gained from the solar radiation to the storage tanks which is then supplied to the customer on demand. The mismatching between the energy supply and demand in the daily and seasonal bases is balanced through the storage tanks. Auxiliary natural gas heaters are installed to back up the required heat demand in case the solar heating system failed to cover it.

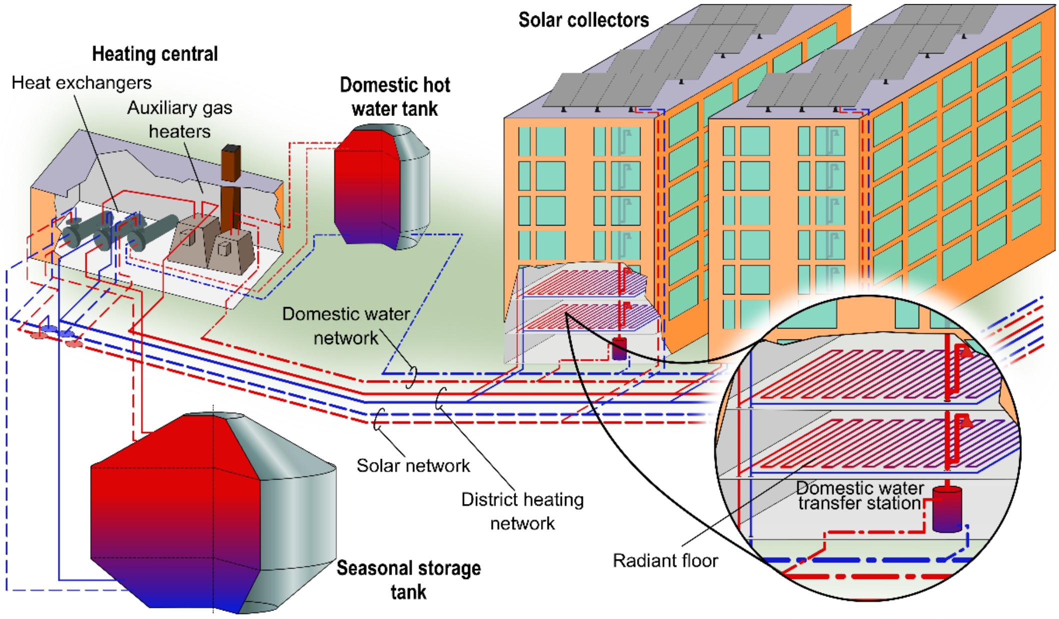

Fig. III-1. Overview of the central solar heating system with a long and short-term storage tanks coupled to a district heating network.

The SST facilitates long-term storage of thermal energy used to cover the SH demand during a winter season with solar energy stored during a summer period. The long-term storage implies relatively large dimensions for the SST which favors slow charging and discharging processes. On the other hand, the DHWT is a short-term independent storage tank which is used to cover the daily DHW service at a temperature of 60ºC.

The proposed CSHPSS system is divided into four circuits, three of them are closed: solar field circuit, seasonal storage circuit, and SH distribution circuit; and the last one, DHW distribution circuit, is open (*i.e.* fed from the water main) as shown in Fig. III-2. The water-glycol mixture is the primary heat transfer fluid in the solar field circuit. The solar energy is collected through the field of solar collectors (COL) and centrifugal pump (P_1) impulses the fluid to reach the heat exchangers (HE_1) and (HE_2). These heat exchangers connect the solar field circuit to the seasonal storage circuit or DHW distribution circuit depending on the selected control mode through Y-type valves. The heat exchangers separate the solar field circuit from the SST and DHWT to protect the solar collectors from damage [52].

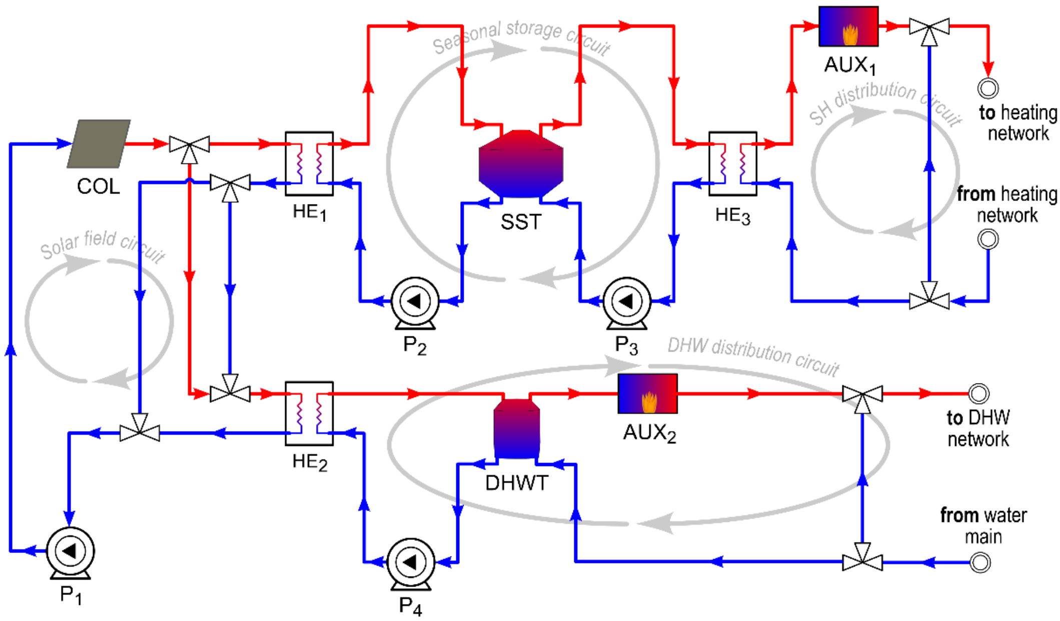

Fig. III-2. Process flow diagram of the CSHPSS plant simulated in TRNSYS 18, where COL is the field of solar collectors, SST is the seasonal storage tank, DHWT is the domestic hot water tank, AUX_i are the auxiliary heaters, HE_i are the heat exchangers, and P_i are the centrifugal pumps.

In the DWH operation mode (priority 1) the monitored variables are the average DHWT temperature and the COL output temperature. Once the mode is triggered, the centrifugal pumps P_1 and P_4 are activated, and the water is sent towards the DHWT through HE_2. A natural gas boiler AUX_2 is installed to cover any occasional shortages in the thermal energy supply to the DHW network. Two Y-type valves regulate the water temperature arriving to the DHW network through mixing of fresh water from the water main with the hot water coming from the AUX_2.

In the SH operation mode (priority 2) the monitored variables are the SST temperatures, the average DHWT temperature and the COL output temperature. Once the average DHWT temperature hits its setpoint and the COL output temperature is higher than the SST bottom temperature, the mode is activated by starting pumps P_1 and P_2 and allowing the heat transfer through HE_1 in order to charge the SST. During the heat demand period, a variable speed pump P_3 impulses the cold water to the bottom of the SST and discharges the hot water to the HE_3 that connects the seasonal storage circuit to the SH distribution circuit. Downstream the HE_3 a natural gas boiler AUX_1 is installed. This boiler operates when the SST cannot reach the setpoint. The combination of two Y-type valves regulates the water temperature arriving to the heating network through back-mixing of the returned water from the network with the hot water coming from the AUX_1.

Beside these two operation modes, the simultaneous SH and DWH mode (priority 3) is also established and regulated based on the controlling system when the conditions of the two previous modes are satisfied.

Additional control loops regulate the operation of the Y-type valves in the SH and DHW distribution circuits in order to maintain the established setpoints at the entrances of the heating and DHW networks.

3. METHODOLOGY FRAMEWORK

Our simulation-optimization approach [53–57] incorporates the evaluation of a CSHPSS plant performance at various EU locations and the definition of a set of optimal configurations of the plant from both techno-economic and environmental aspects simultaneously. Thus, the proposed methodology is a multi-objective optimization problem. The transient performance of the CSHPSS plant is modeled in TRNSYS 18, simulation software which allows to interconnect available standard equipment units to obtain more complex systems. The optimization is performed externally using a generic optimization toolbox, GenOpt. The first subsection of the methodology illustrates the developed TRNSYS model and its input and output data. The second subsection shows the techno-economic and environmental criteria for assessing the proposed CSHPSS. Finally, the third subsection dives deeper into the optimization framework itself and the implemented algorithm.

3.1. TRNSYS simulation model

TRNSYS 18, transient simulation software, is employed to analyze the dynamic behavior of the proposed CSHPSS. The software operates by solving partial differential equations of the mass and energy balances within previously defined boundaries.

The dynamic nature of the program intends to offer a realistic simulation of the CSHPSS plant. On the other hand, to reduce the computational cost, the model is simulated over a typical year of operation and the solution is extrapolated over the plant lifetime assuming same climatic conditions and demand profiles year after year.

The proposed simulation model follows the models previously developed by Guadalfajara et al. [36] and Tulus et al. [43] with modifications to include the DHW distribution circuit and a more sophisticated controlling loop. See the information flow diagram presented in Fig. III-3 for details about the individual components (called Types inside the software) used in TRNSYS. Each type has three main information boxes which include the component-specific parameters, input variables, and output variables.

The main types used in our CSHPSS model are: flat plate solar collectors (Type 1a) with an optical efficiency of 0.817, sensible storage tanks (Type 4c) with heat loss coefficient of 0.06 $W/m^2 \cdot K$ and 0.3125 $W/m^2 \cdot K$ for the SST and DHWT, respectively, counter flow heat exchangers (Type 5b) with overall heat transfer coefficient of 3931 $W/m^2 \cdot K$, and auxiliary heaters (Type 6) with an efficiency of 93%. The secondary model types are: single speed centrifugal pumps (Type 3b), inlet and outlet pipe ducts (Type 709), three-way valves (Type 11h),controlled flow diverters (Type 11f), tempering valves (Type 11b), soil temperature profile for the SST (Type 77), weather data processor (Type 15-3), time-dependent forcing functions for the heating and DHW demand profiles (Type 9c), and controllers (Type 2b).

3.2. Evaluation criteria

Several evaluation criteria were formulated to quantify the CSHPSS performance.

3.2.1. Technical criteria

The technical evaluation of the dynamic behavior of the CSHPSS plant is described through several parameters that include the energy supplied by the SST, DHWT, and auxiliary boilers.

The storage tank has a vital role in the CSHPSS plant performance. Thus, the energy provided by the fully stratified seasonal and DHW storage tanks are described in Eq. III-1 and III-2, respectively [58]:

$$Q_{SST} = \int_0^t \dot{m}_f c_p \Delta T_{SST} \quad \text{(III-1)}$$

$$Q_{DHW} = \int_0^t \dot{m}_{DHW} c_p \Delta T_{DHW} \quad \text{(III-2)}$$

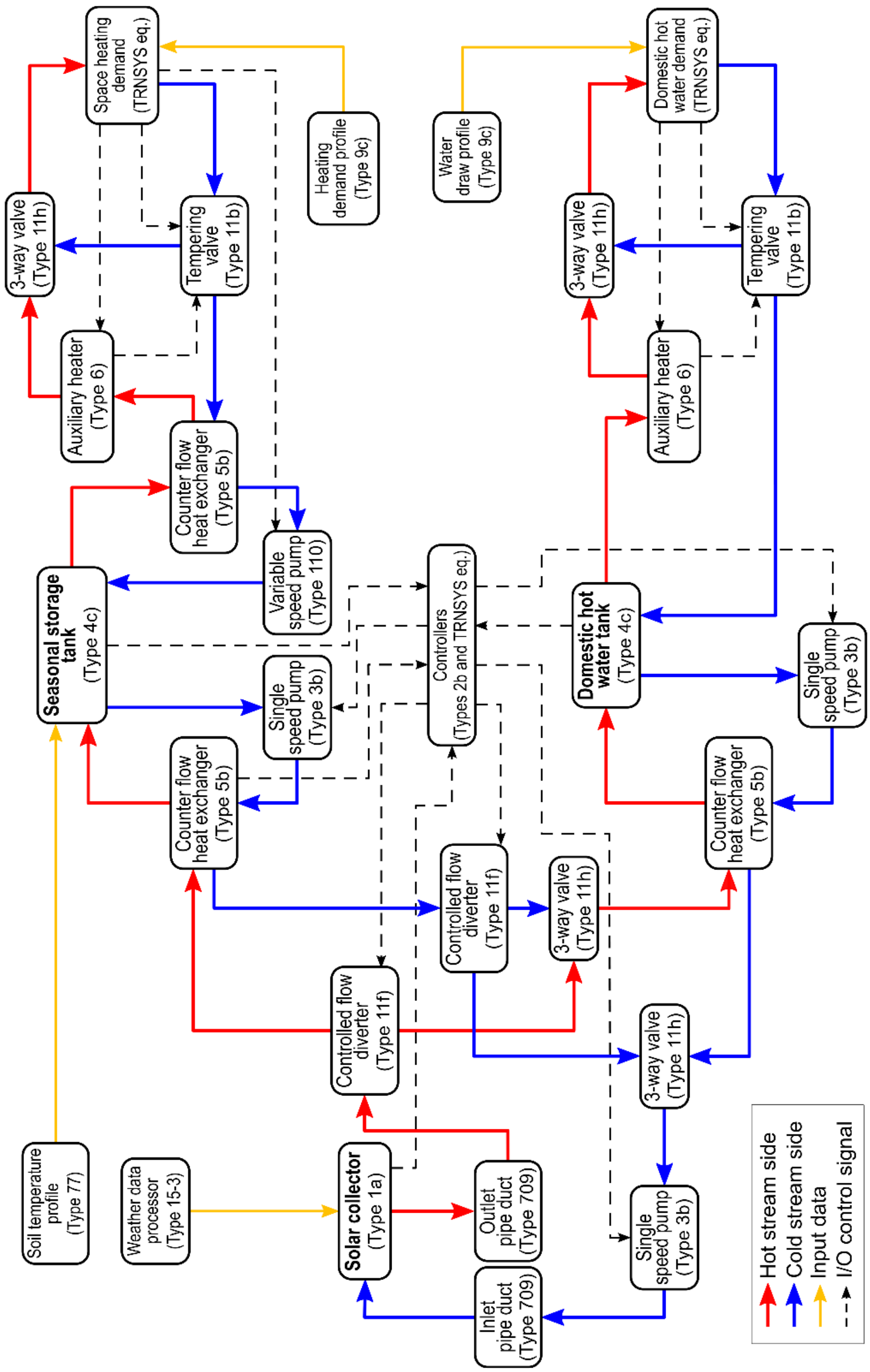

Fig. III-3. Information flow diagram of the CSHPSS system modelled in TRNSYS 18 with the representation of the software components and their interconnections.

where $\dot{m}_f$ and $\dot{m}_{DHW}$ are the mass flow rates of the recirculated water inside the SH and the DHW distribution circuits, respectively, c_p is the specific heat capacity, ΔT_{SST} and ΔT_{DHW} are the temperature differences between the extracted and replaced water at storage tanks to cover the SH and DHW load, respectively.

Auxiliary boilers are utilized to cover the SH demand and the DHW demand when the solar system is unable to reach the set temperature point. The auxiliary energy rate supplied to the SH and DHW networks can be expressed as shown in Eq. III-3 and III-4, respectively [59]:

$$\dot{Q}_{AUX1} = \dot{m}_f c_p \Delta T_L \tag{III-3}$$

$$\dot{Q}_{AUX2} = \dot{m}_{DHW} c_p \Delta T_L \tag{III-4}$$

where ΔT_L is the temperature difference between the distribution circuits and the solar field circuit.

Annual solar fraction [60,61] for the SH and DHW distribution circuits are introduced as technical performance indicators. These indicators can be computed using Eq. III-5 and III-6 as a function of the heating network demand ($Q_{heating\ load}$), and the DHW network demand ($Q_{DHW\ load}$).

$$SF_{SH} = 1 - \frac{\int_0^t \dot{Q}_{AUX1}}{Q_{\text{heating load}}} \tag{III-5}$$

$$SF_{DHW} = 1 - \frac{\int_0^t \dot{Q}_{AUX2}}{Q_{\text{DHW load}}} \tag{III-6}$$

3.2.2. Economic criteria

In the current study, the economic evaluation of the CSHPSS system follows the work of Tulus et al. [43] which is carried out based on the life cycle costing (LCC) methodology [58,62].

The LCC methodology is a valuable monetary approach for assessing the energy system designs in terms of the initial purchase cost and the operational costs throughout the expected lifetime of the system. The LCC perspective in the early stages of design empowers the decision-makers to deeply comprehend the lifetime costs of the system

[44], and subsequently enhance the possibility of an additional reduction in the system operational cost even if more investment cost is required [63].

The main principle of the LCC methodology is the future cost approach. Its feature is to discount the summation of all expenses during the lifetime of the system to its present value where the net present cost (*NPC*) can be estimated by adding the initial capital cost (C_C), the operational cost (C_O) and the total replacement cost of the equipment (C_R):

$$NPC = C_C + C_O + C_R \tag{III-7}$$

3.2.2.1. Initial capital cost

The initial capital cost is the investment cost at the project starting point. It takes into consideration the actual equipment cost, the installation labor and transportation costs along with any possible contingency expenses:

$$C_C = (1+\alpha_{CF})\sum_k (PEC_k \cdot FBM_k) \tag{III-8}$$

where PEC_k is the initial purchase cost of equipment unit *k*, FBM_k denotes the bare module factor, which represents the installation labor and transportation costs, and α_{CF} denotes the contingency fees factor.

The PEC_k is brought to its present worth value from the base year (*year A*) to the year of installation (*year B*) using the Chemical Engineering Plant Cost Index (*CEPCI*) [64] as follows:

$$PEC_k = PEC_k^{yearA} \frac{CEPCI^{yearB}}{CEPCI^{yearA}} \quad \forall k \tag{III-9}$$

The initial purchase cost of equipment unit *k* at year A can be estimated as shown in Eqs. III-10 to III-12:

$$PEC_k^{yearA} = \alpha_k CAP_k^{\beta k} \quad \forall k = COL, SST, DHW, AUX \tag{III-10}$$

$$PEC_k^{yearA} = CAP_k^{\beta k} \cdot 10^{\left\lfloor \alpha_k \left(\log_{10} CAP_k\right)^{\beta_k} \right\rfloor} \quad \forall k = HE_1, HE_2 \tag{III-11}$$

$$PEC_k^{yearA} = \alpha_k \ln\left(\frac{CAP_k}{1000}\right) + \beta_k \quad \forall k = P_1, P_2, P_3, P_4 \tag{III-12}$$

where α_k and β_k are the equipment purchase parameters of unit *k* and CAP_k is the design variable of unit *k*. In the current study, the design variables are the solar collector area (A_{COL}), the volume of the storage tanks (V_{SST}, V_{DHW}), the capacity of the auxiliary heaters (AUX_1, AUX_2), the effective heat transfer area of the heat exchangers (HE_1, HE_2, HE_3) and the mass flow rates of the pumps ($\dot{m}_1$, $\dot{m}_2$, $\dot{m}_3$).

3.2.2.2. Operational cost

The operational cost refers to the sum of all the annual operating costs such as maintenance costs of the different equipment units and facilities, the consumption of electricity by hydraulic equipment and the consumption of natural gas by auxiliary heaters. It can be expressed as follows:

$$C_O = C_M PWF_M + C_P PWF_P + C_{AUX} PWF_{AUX} \tag{III-13}$$

where C_M, C_P and C_{AUX} represent the annual maintenance cost, hydraulic equipment (*i.e.* pumps) and auxiliary consumption costs, respectively. The present worth factor (PWF) counts for the time value of money considering the inflation rate (i), discount rate (d), and lifetime of the proposed system (N_e) as expressed in Eq. III-14:

$$PWF = \begin{cases} \dfrac{1}{d-i}\left[1-\left(\dfrac{1+i}{1-d}\right)^{N_e}\right] & \forall i \neq d \\ \dfrac{N_e}{1+i} & \forall i = d \end{cases} \tag{III-14}$$

3.2.2.3. Replacement cost

Several equipment units in the CSHPSS plant have a high depreciation rate and subsequently need to be replaced during the plant operation. These units are the field of solar collectors, the heat exchangers, and the auxiliary heaters. The replacement cost can be expressed as shown in Eq. III-15 with consideration for the equipment present value:

$$C_R = PVF_n \sum_k (PEC_k \cdot FMB_k) \tag{III-15}$$

where PVF_n is the present value factor of a future cash flow at year n and it can be expressed as follows:

$$PVF_n = \frac{(1+i)^n}{(1+d)^n} \tag{III-16}$$

3.2.3. Environmental criteria

The LCC is purely based on an economic approach not considering the environmental performance of the CSHPSS plant. In this context, the environmental impact is assessed by using the life cycle assessment (LCA) methodology. This methodology enables a comprehensive estimation of the local environmental impacts by analyzing the product lifecycle from a global perspective. Thus, LCA assesses the product based on the “cradle-to-grave” concept [65] taking into account a range of environmental categories. The LCA methodology was standardized through ISO 14040 series [66–68], and it comprises four main phases which trail a specific sequence: goal and scope definition, inventory analysis, impact assessment and interpretation. These phases are depicted in details in the next subsections as mentioned previously by Guillén-Gosálbez et al. [69].

3.2.3.1. Goal and scope definition

This phase comprises three main scopes: the system, its boundaries, and the functional unit. In the system boundary, the entire product life cycle should be analyzed (“cradle-to-grave” concept). However, this study focuses on the CSHPSS plant itself, which is connected to an existing district heating network. Therefore, the system boundary would be drawn based on the “cradle-to-gate” concept with exclusion for the end user distribution networks, that is, from extraction of raw materials for equipment units manufacturing to delivery of hot water to the district heating network. The functional unit in this study is the energy amount demanded by the end user to cover his heating and hot water necessities over the entire time horizon.

3.2.3.2. Inventory analysis

This is the second phase in the LCA sequence, it quantifies the input and output materials and the energy consumption associated with the CSHPSS plant construction and operation. In the current problem, several sources of impact are considered: equipment manufacturing and utility energy consumption (natural gas and electricity) by the system during the whole lifetime (LCI_i^{MP}); material and finished equipment units' transportation to the site (LCI_i^{TR}); plant operation during the entire time horizon (LCI_i^{OP}).

These resources consumption associated with the whole elementary flows during its lifetime has been retrieved from the Ecoinvent 3.0 database [70]. Mathematically, the inventory entries can be expressed as follows:

$$LCI_i^{TOT} = LCI_i^{MP} + LCI_i^{TR} + LCI_i^{OP} \quad \forall i \qquad \text{(III-17)}$$

where LCI_i^{TOT} is the total life cycle inventory associated with the elementary flow *i*. LCI_i^{MP}, LCI_i^{TR}, and LCI_i^{OP} refer to the manufacturing processes, the transportation tasks and the plant operation associated with the elementary flow *i*, respectively.

3.2.3.3. Impact assessment

In this phase, the inventory data are translated into environmental impacts. As mentioned previously, three different damage categories include the human health, the ecosystem, and the resources damages based on the ReCiPe 2008 framework [71]. The characterization of the promoted framework has been carried out based on the endpoints level not considering the midpoints. Mathematically, the impact values associated to each impact category can be expressed as follows:

$$IMP_e = \sum_i \theta_{ei} \cdot LCI_i^{TOT} \quad \forall e \qquad \text{(III-18)}$$

where θ_{ei} denotes the characterization factor which links the elementary flow *i* with endpoint impact category *e*.

Finally, the endpoint impact categories *e* are aggregated into damage categories (DAM_d), which are further normalized and aggregated into a single final indicator *RCP* as stated in Eqs. III-19 and III-20:

$$DAM_d = \sum_{e \in ID_d} IMP_e \quad \forall d \qquad \text{(III-19)}$$

$$RCP = \sum_d \delta_d \varepsilon_d DAM_d \quad \forall d \qquad \text{(III-20)}$$

where ID_d represents a set of endpoint impacts *e* that contribute to the damage category *d*, *RCP* is the ReCiPe 2008 aggregated metric, and δ_d, ε_d are the specific normalization and weighting factors, respectively. The normalization factors are estimated based on the damage calculations for relevant European land uses, emissions and extractions [72], whereas the weighting factors are specified based on recommended values defined in the ReCiPe 2008.

3.2.3.4. Interpretation

This phase provides an analysis of the results in addition to a set of recommendations that assist in improving the system performance. In this context, the environmental impact indicator *RCP* for different design alternatives is coupled with the

LCC methodology which uses *NPC* for evaluating the future cost through a multi-objective optimization algorithm. This framework assists in optimizing the economic and environmental impacts simultaneously obtaining a set of Pareto optimal solutions which give a further insight into different design alternatives, and subsequently promote various solutions for the decision-makers that best fit their legislations.

3.2.4. Future market development criteria

In order to try to anticipate the future development of the CSHPSS technology in monetary terms taking into consideration the actual effect of the technology deployment, we performed a CSHPSS market projection up to 2030 [73–75]. The obtained learning curve by definition [76,77] tends to develop a relation between the cumulative market size and the production cost of the CSHPSS plant (Eq. III-21).

$$C(x_t) = C(x_o) - \left(\frac{x_t}{x_o} \right)^{-b} \qquad \text{(III-21)}$$

Here $C(x_t)$ is the marginal cost of the CSHPSS plant production (x) at a certain time t, $C(x_o)$ is the cost production at the reference point (x_o), and b is the learning parameter which is estimated based on the fractional reduction in the CSHPSS plant cost represented by the learning rate (LR). The values for the LR are estimated based on stated recommendation in the European Energy Scenario [75]. In addition to the market projection for the next decade, several specific annual figures can be assigned so the CSHPSS cost reduction can be anticipated on a chronological index.

3.3. <u>Optimization procedure</u>

The main goal of the optimization procedure is to simultaneously reduce the total cost of the plant (*NPC*) and its environmental impact (*RCP*) while still satisfying the technical requirements. The main decision variables in our model are the area of solar collectors (A_{COL}) and the volume of the seasonal storage tank (V_{SST}), the dimensions of the other equipment units are related to the decision variables through mathematical equations. It is worth noting that our methodology is general enough to incorporate additional decision variables.

The developed TRNSYS model is connected to the GenOpt optimization toolbox, which integrates several predefined optimization algorithms. The general mathematical representation of the simulation-optimization model can be seen below:

$$\begin{aligned} \min_{x} \quad & f_1(x), f_2(x) \\ \text{s.t.} \quad & h(x) = 0 \\ & x^L \leq x \leq x^U \\ & x \in \mathbb{R} \end{aligned} \tag{M III-1}$$

where $f_1(x)$ and $f_2(x)$ are the objective functions, in this case net present cost, $NPC(x)$, and ReCiPe 2008 aggregated impact factor, $RCP(x)$, and x denotes the continuous variables of the simulation model, which can vary between their lower and upper bounds x^L and x^U, respectively. The equality constraints $h(x) = 0$, that model mass and energy balances as well as thermodynamic correlations, are implicitly solved in TRNSYS.

The solution of the multi-objective problem introduced in model M III-1 provides a set of Pareto points, which represent the optimal trade-off between economic and environmental objectives. The extreme points of this Pareto frontier are the so-called anchor points, which correspond to the individual minimum of each objective. The Pareto solutions are calculated here via the weighted-sum method [78], which relies on formulating an auxiliary single-objective model that optimizes a linear weighted-sum (WS) of the original objectives (M III-2). Note that the weighted-sum method cannot generate solutions lying on the nonconvex part of the Pareto set.

$$\begin{aligned} \min_{x} \quad & WS = (1-\lambda)\overline{f}_1(x) + \lambda \overline{f}_2(x) \\ \text{s.t.} \quad & h(x) = 0 \\ & x^L \leq x \leq x^U \\ & 0 \leq \lambda \leq 1 \\ & x \in \mathbb{R}, \lambda \in \mathbb{R} \end{aligned} \tag{M III-2}$$

Here, $\overline{f}_1(x)$ and $\overline{f}_2(x)$ are the normalized objectives, and λ is the non-negative weight given to $\overline{f}_2(x)$, *i.e.* the normalized $RCP(x)$ function. We normalize the objectives as shown below:

$$\overline{f}_c(x) = \frac{f_c(x) - f_c^{UT}}{f_c^{PN} - f_c^{UT}} \quad \forall c = 1,2 \tag{III-22}$$

where f_c^{UT} denotes the c^{th} coordinate of the utopia points and f_c^{PN} denotes the c^{th} coordinate of the pseudo nadir point. These points, f_c^{UT} and f_c^{PN}, are the anchor points.

The solution procedure was integrated via MATLAB routine designed to speed up the optimization process. The routine would launch several GenOpt toolboxes or start TRNSYS simulations whenever required.

The procedure starts with the determination of the anchor points. To obtain the individual minimum of the *RCP*(*x*) function, M III-2 is solved for λ=1. Next, to determine the individual minimum of the *NPC*(*x*) function, M III-2 is solved for λ=0. The two previous cases run simultaneously sharing all the available RAM memory of the computer. Once the anchor points are identified, the WS normalization is performed. Afterwards, M III-2 is solved a finite number of times for different weight values between 0 and 1 (see details in Fig. III-4) to generate desired number of Pareto points (NPP is specified by the user). The MATLAB routine launches simultaneously various optimizations with different λ weights until there is no available memory. Once all the memory slots are occupied, the routine halts until necessary RAM memory is liberated and launches the next points. The procedure terminates after all the optimization runs have stopped displaying the full Pareto frontier.

3.3.1. Optimization algorithm

To perform the separate single-objective optimization steps we used a hybrid metaheuristic optimization algorithm [51], known as the Generalized Pattern Search algorithm with Particle Swarm Optimization with Construction Coefficient and Hooke-Jeeves (GPSPSOCCHJ). This algorithm uses the combined benefits of the Particle Swarm Optimization (PSO) algorithm [79,80] and the Hooke-Jeeves (HJ) algorithm [81]. The details of this hybrid metaheuristic algorithm are discussed in Wetter [51].

The PSO algorithm is in charge of performing a global search over the feasible space of possible solutions. Since PSO is a population-based probabilistic algorithm, it generates several particles uniformly scattered over the feasible space, where each of the particles are potential optimal solutions. This is achieved by performing runs with randomly generated values for the decision variables. On the other hand, the HJ is a local generalized pattern search algorithm, and it explores the feasible space following paths of potential minimization of the objective function. The best particle found by PSO, the potential optimal solution, is used as a starting point for the HJ algorithm, which exhaustively explores its neighborhood in an attempt to improve the solution. To reduce the probability of falling in a local optimum we included multiple starts of the HJ algorithm.

This combined PSO-HJ architecture is used to avoid possible local optimal solutions which may exist due to the nonconvex nature of the problem. Note that our methodology is not limited to be used only with GPSPSOCCHJ algorithm; any other algorithm can be easily implemented.

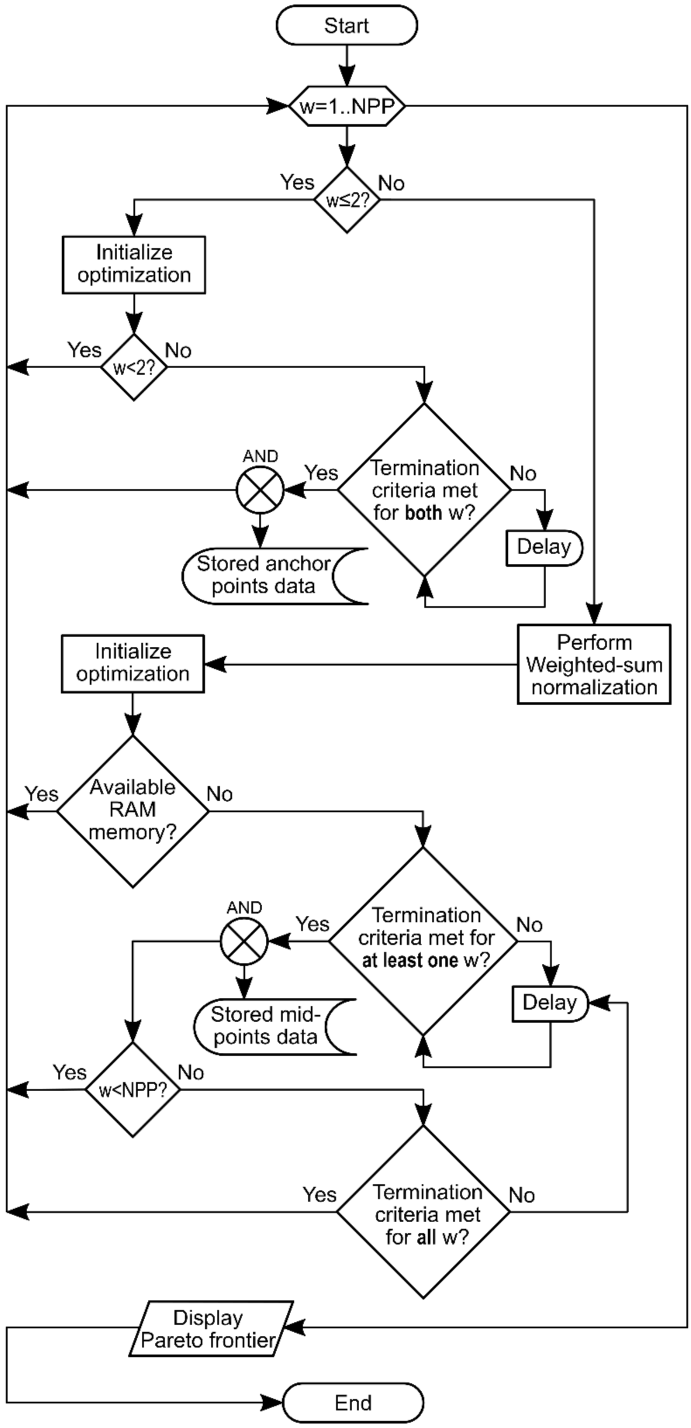

Fig. III-4. Flow chart of the solution procedure performed in MATLAB environment, where NPP is the number of points of the Pareto frontier specified by the user.

4. CASE STUDIES (FOUR EU CLIMATE ZONES)

In this section, the proposed methodology procedure was applied to four climatic zones in Europe. The main objective is to assess the feasibly of the CSHPSS plant in the residential sector of these countries in techno-economic and environmental terms.

The CSHPSS plant is connected to a reference residential neighborhood community of 1120 apartments [43] which is placed in various European countries. Each apartment of this neighborhood community has a useful area of 90 m^2 [82]. The buildings are equipped with a radiant underfloor heating system and a domestic hot water system in order to meet the SH and DHW demand at 50ºC and 60ºC, respectively. The CSHPSS model validation is performed based on the implemented work by Guadalfajara et al. [36].

Besides, a boiler fueled with natural gas is considered as a base case for comparison purposes. This conventional system is designed to satisfy the heating and DHW demand alone independently on the CSHPSS plant.

4.1. Specifications of the simulation model

A field of flat plate solar collectors supplies thermal heat to the CSHPSS model. These collectors are coupled in series and oriented to the south with a specific inclination based on the respective latitude of the cities [83] as shown in Table III-1. The primary working fluid in the solar field circuit is a 67/ $33_{w/w}$ mixture of a water-glycol solution with a flow rate of 20 $kg/h{\cdot}m^2$. Whereas the other three circuits (seasonal storage, SH distribution, DHW distribution circuits) are operated with water.

A partially buried tank with a cylindrical cross-section is used for a seasonable storage purpose. This tank has a fixed height to diameter ratio of 0.6, insulated with 0.5 m of extruded polystyrene and divided into 20 equally stratified levels. On the other hand, the DHW tank is relatively small since it covers only the daily DHW service. The DHWT has a height to diameter ratio of 1.7 with 10 equally stratified levels.

Natural gas boilers with 93% efficiency are utilized as auxiliary heaters in both the SH and DHW distribution circuits. The boilers are designed to satisfy up to 100% of the heat demand when required.

The TRNSYS simulation predicts the transient response of the CSHPSS plant based on a simulation time step of 15 min. The system evaluation was performed over three years of simulation (28,260 hrs.). Then the performance of the third year was extrapolated over the total lifetime of the CSHPSS plant. Due to initial homogeneity assumption of 30ºC inside the storage tanks, the first two years of simulation were performed to eliminate the initial assumption effect. The lifetime of the CSHPSS is 40 years [84]. However, the solar collectors, the DHWT, the heat exchanger, and the auxiliary heaters need to be replaced after 20 years of operation, while the lifespan of the SST is considered to reach 80 years [85].

4.2. Meteorological data

Various climate zones were selected to evaluate the application performance of the CSHPSS plants in the EU. In Europe, the climate can be categorized into three major climate types [86,87]: Mediterranean climate, central European climate, and Nordic climate. Four cities were selected to represent these major climatic types:

- Mediterranean climate: Madrid and Athens represent this climatic type with difference in the daylight hours, the daily ambient temperature and the humidity due to their geographical location. Madrid is considered Continental Mediterranean climate, while Athens is considered Mediterranean climate.
- Central European climate: Berlin is selected as representative for this climate type. In comparison with the Mediterranean climate, a moderate reduction in the ambient temperature and daylight hours is noticed.
- Nordic climate: Helsinki is chosen as an example of this climate type. This type of weather is elected as an opposite to the Mediterranean climate with a drastic reduction in both the ambient temperature and the daylight hours.

The geographic information including the latitude and the solar collector inclination angle for the four cities are illustrated in Table III-1. Whereas the climate conditions of the four cities including the average ambient temperature and the annual incident solar radiation per area are extracted from the EnergyPlus database [88] as shown in Fig. III-5.

Several parameters need to be defined based on the climate conditions of the cities. These parameters include the SH and DHW consumption, the economic [89] and the environmental [90] data which are defined in the following sections.

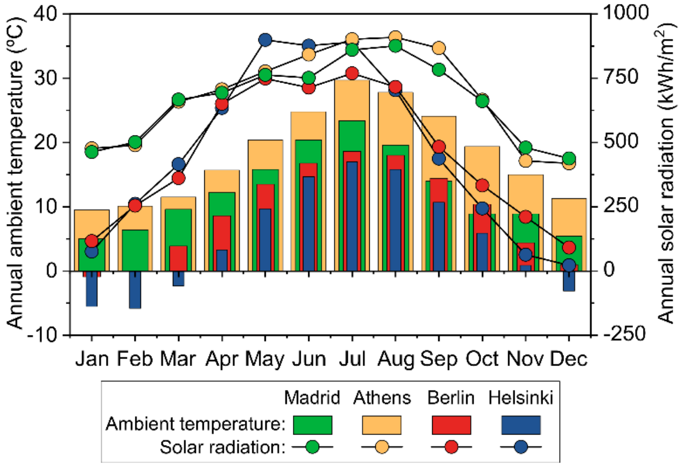

Fig. III-5. Climatic conditions in the four European cities taken as representatives for the different EU climate zones.

Table III-1. Latitudes and relative inclination angles of the solar collectors in the four European cities taken as representatives for the different EU climate zones.

City	Latitude (º)	Inclination angle (º)
Madrid	40	50
Athens	37	50
Berlin	52	60
Helsinki	60	70

4.3. Space heating and DHW profiles

The heating demand for the residential neighborhood community follows Guadalfajara et al. [36] and Tulus et al. [43] studies. A 3-D building model was generated using a graphical tool SketchUp [91] and imported into the TRNSYS model. In TRNSYS, the occupation profiles of the apartments and physical properties of the construction materials were included. A typical hourly heating load over a year of operation depending on the climatic conditions of the city was simulated in this TRNSYS building model. These data were then extrapolated to the whole neighborhood of 40 buildings (see the profiles in Fig. III-6).

The DHW demand for the residential neighborhood community depends on four main factors which comprise:

- The daily water consumption per person: Ahmed et al. [92] indicated that the water consumption is highly dependent on the geographical location. Therefore, the DHW consumption has a high level of diversity from one city to another. The DHW consumption per capita is 28, 30, 35, and 35 liter/capita·day in Madrid, Athens, Berlin, and Helsinki, respectively [93].

- Monthly water temperature from the public distribution network: The water temperature was calculated on the basis of the town and the month of the year using EnergyPlus database [88].
- The number of people living in each household: The DHW consumption is dependent on the people/property value, and it is considered as a constant value (4 people/property) referring to the European average [94,95].

The daily DHW consumption profiles are simulated using a computer software, DHWcalc [96]. This software assists in developing a realistic and detailed hourly DHW consumption profiles with consideration for the main factors controlling the DHW demand (see the profiles in Fig. III-6).

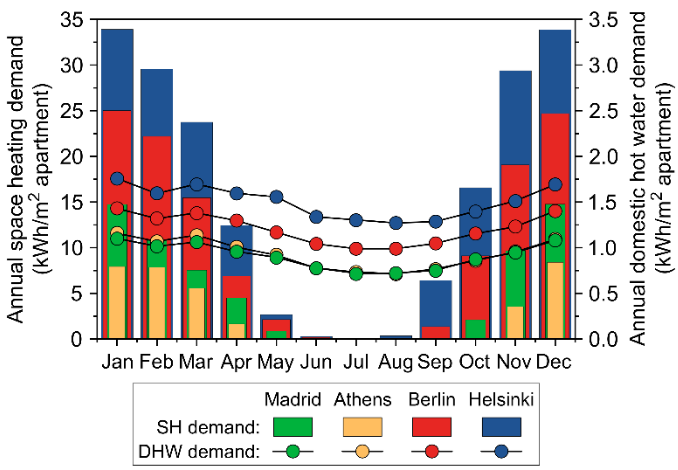

Fig. III-6. Annual space heating and DHW demand profiles in the four European cities taken as representatives for the different EU climate zones.

4.4. <u>Economic and environmental data</u>

The parameters for the initial purchase cost estimation of the main equipment units of the CSHPSS are summarized in Table III-2 following Tulus et al. [43]. While the operational cost is estimated as 1.5% of the initial purchase cost based on Kalogirou [62] recommendation. The cost for both the electricity and natural gas are dependent on the country policies. Therefore, the electricity and natural gas costs were extracted from the EUROSTAT database [89] and summarized in Table III-4. Furthermore, the inflation rate associated with the price of these power resources is set to 5%, and 5.9% for the electricity and natural gas, respectively [43]. In addition, the inflation rate associated with the proposed system during its life cycle is set to 2.3% [97], while the annual discount rate is set to 3.5% [98].

Table III-2. Parameters of initial equipment purchase cost [43].

Unit	α_k	β_k	CAP_k	Range	Base year	FBM_k
Solar collector	974.2	0.8330	Aperture area (m^2)	4000-150,00 m^2	2007	1.00
Storage tank	3955	0.6500	Volume (m^3)	1-100,000 m^3	2007	1.00
Auxiliary heater	225.0	0.7460	Duty (kW)	600-100,00 kW	2001	2.10
Heat exchanger	3.133	-0.3310	Exchange area (m^2)	10-1000 m^2	2001	3.29
Pump (P_1, P_2)	389.0	-283.2	Mass flow rate (kg/h)	15000-100,000 kg/h	2009	3.24
Pump (P_3, P_4)	389.0	717.0	Mass flow rate (kg/h)	15000-100,000 kg/h	2009	3.24

The LCA data are retrieved from the Ecoinvent database [90]. These data include the impact of various CSHPSS equipment units (Table III-3) and utilities (Table III-4) based on the ReCiPe 2008 methodology.

Table III-3. ReCiPe 2008 aggregated impact factor for the CSHPSS equipment units, in ReCiPe points (Pt) per characteristic dimension.

Unit	Impact factor (ReCiPe 2008)
Solar collector	17.0 Pt/m^2
Storage tank	117 Pt/m^2
Auxiliary boiler	$1.57 \cdot 10^3$ Pt/unit
Heat exchanger	9.00 Pt/m^2
Pump	82.0 Pt/unit

The pollution associated with the extraction of natural gas from the underground reserves should be limited in the proposed system. On the other hand, the pollution associated with the electricity generation is highly dependent on the electricity mix of the specific country. Therefore, the natural gas environmental impact is considered the same for the selected cities, while the electricity impacts are variable, as indicated in Table III-4.

Table III-4. Specific costs and ReCiPe 2008 aggregated impact factors for the utilities in the four European cities taken as representatives for the different EU climate zones.

City	Electricity		Natural gas	
	Cost (€/kWh)	***Impact* (*Pt*/kWh)**	**Cost (€/kWh)**	***Impact* (*Pt*/kWh)**
Madrid	0.101	0.0357	0.0294	0.0230
Athens	0.0862	0.0193	0.0242	0.0230
Berlin	0.0761	0.0529	0.0277	0.0230
Helsinki	0.0596	0.0261	0.0296	0.0230

4.5. Future market development data

By the end of 2016, the cumulative capacity of the installed solar heating systems in Europe increased by 2.6% compared to previous year to achieve a total installed capacity of 34.5 GW_{th}. Germany has the lead in the solar heating systems installation in Europe where a 0.52 GW_{th} within 2016 was added to a total capacity of 13.14 GW_{th}. Elsewhere in Europe, Spain added a 0.146 GW_{th} to achieve a total capacity of 2.4 GW_{th}, whereas Greece and Finland added 0.19 GW_{th} and 0.0028 GW_{th} [14].

The future market of the CSHPSS based on a deep analysis of solar heating energy systems from the technical, social and political perspectives, shows diverse expansion scenarios for this technology in Europe. Greenpeace international [99] proposed the EU 27 energy scenario for the CSHPSS expansion up to year 2030 as shown in Table III-5.

Besides, the natural gas price trends are assumed to increase in a moderated manner based on the recommendations of the Federal Ministry of Environment of Germany [100] (see Table III-5). This is due to the shortage in the CO_2 allowance [101].

Table III-5. Estimated growth of CSHPSS installed capacity according to Greenpeace international and projected increase of the natural gas price up to 2030.

Parameter	2017	2020	2025	2030
Total installed capacity (GW_{th})	34.50	40.66	52.77	67.16
Average EU natural gas price (Euro/kWh)	0.02700	0.03200	0.03415	0.03630

The forecast cost for the CSHPSS technology can be generated based on the observed historical learning rate of solar thermal collector systems over the forecasted period between 2020 and 2030. The learning rate of such systems is 0.90 according to Greenpeace international [75].

5. RESULTS AND DISCUSSIONS

In this study, the results are presented in four main parts. The first part depicts the behavior of CSHPSS in one of the proposed EU climate zones. Then, in the second part, the discussion is extended to the other three cities. These two parts provide a detailed analysis of techno-economic and environmental characteristics based on a set of Pareto optimal solutions in comparison to a conventional heating system fueled by natural gas (base case). Next, the main results are expressed along with an appropriate sensitivity analysis for the proposed optimal solutions of the system. Finally, the market projection forecast for the CSHPSS is portrayed using historical learning rates.

5.1. Application analysis (Madrid case study)

The capabilities of the formulated multi-objective optimization model are illustrated through Madrid case study that addresses the design of CSHPSS in the Mediterranean EU climate zone. A set of optimal solutions that define the Pareto frontier are obtained as a result of the optimization process (see Fig. III-7). Each point of the Pareto front comprises a defined configuration of the CSHPSS plant under a set of operational conditions. The average computation time for the anchor points was 15,700 CPU seconds (8 execution units of 2.0 GB RAM each for every anchor point, optimizing both simultaneously) and 47,000 CPU seconds for the intermediate Pareto solutions (2 execution units of 2.0 GB RAM each for every intermediate point, optimizing all of them simultaneously) using an Intel® Xeon® E5-2620 v4 2.10 GHz processor with 32.0 GB RAM.

As observed in Fig. III-7, there is a clear trade-off between the proposed objective functions since the reduction in the environmental impact can be only achieved through an increment in the expenses of the CSHPSS plant. The projected optimal solutions, following our methodology framework, clearly improve the environmental impact in comparison to the base case. Point A and B are the optimal design Pareto points with minimum cost and impact, respectively. Note that these points consider the integration of the solar thermal energy storage. Replacing the base case with a CSHPSS plant following point A configuration can reduce the environmental impact by 81.1%, whereas point B reduces it even more, by 86.5%. On the other hand, the Pareto optimal systems could not provide a marginal economic reduction compared to the base case. The installation of a CSHPSS in these cases corresponds to an increase in the cost of approximately 1% and 6.1% in A and B cases, respectively with respect to the base case.

In the optimal minimum cost solution (point A), the *NPC* is equal to 52.6 €/MWh which is smaller than solution B by 4.7%, whereas in the minimum impact solution (point B), the *RCP* is 3.34 Pt/MWh which is smaller than solution A by 28.6%. Besides, point C embodies one possible intermediate Pareto optimal solution where the *NPC* is equal to 53.3 €/MWh and the *RCP* reaches 3.6 Pt/MWh, this intermediate point increases the economic cost by 1.25% with respect to the point A, but simultaneously reduces the environmental impact by 23.1%. It is worth noting that point C is selected as an example solution for comparison purposes, likewise any intermediate solution could be selected since all of them are Pareto optimal.

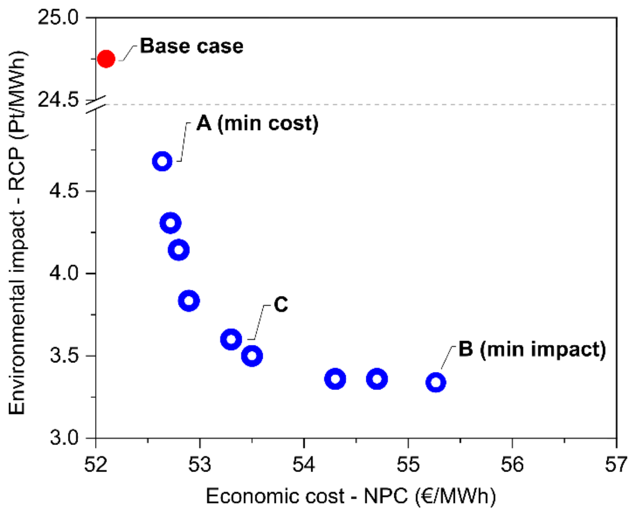

Fig. III-7. Pareto set of optimal solutions for the CSHPSS in Madrid which covers 7654 MWh/year of combined SH and DHW demand during its lifetime. Anchor point A is the minimum cost solution, anchor point B is the minimum impact solution, and intermediate point C is one of the trade-off solutions with λ = 0.44 (weight) given to the normalized environmental impact objective function, the *RCP*(*x*); the base case represents a natural gas heating system.

Following that, each point in the Pareto set represents a different configuration of the CSHPSS plant. The proposed methodology offers the possibility to perform a detailed analysis on any Pareto optimal solution. Here we analyzed the anchor points (point A and B) from the economic and environmental perspectives comparing them to the base case.

5.1.1. Economic cost analysis

To facilitate the detailed economic analysis, Fig. III-8 provides a comprehensive breakdown for the cost contribution of each parameter in the Pareto optimal solutions A and B during its lifetime together with the base case solution. In this figure, the initial capital cost, associated with both A and B solutions, has a significant contribution compared to the base case. This contribution is 49.06% and 52.4 % in solution A and B, respectively, whereas in the base case, it is only 2.73%. This marginal capital cost contribution is commonly arisen in the CSHPSS plants due to the deployment of the solar energy in a district heating field which requires a high investment cost [22]. To be more specific, the solar collectors and SST represent 28.24% and 30.52% of the capital cost for the Pareto optimal solution A and B, respectively. The minimum cost solution (A) has solar collector field of 6888 m^2 and SST of 65784 m^3, whereas the minimum impact solution (B) has solar collector field 8802 m^2 and SST of 74322 m^3. Since the DHWT is used only for the daily services without seasonal storage, it represents almost about 2.2% of the initial capital cost in both the Pareto optimal solution A and B with a tank size of 109.6 m^3.

The same behavior was noticed for replacement cost which represents 19.4% and 21.3% in solution A and B compared to only 1.88% in the base case. On the contrary, the operational cost has a predominant contribution of 95.4% in the base case compared to 31.5% and 26.3% in the optimal solutions A and B, respectively. This is due to the dependency of the base case on natural gas cost. In general, solution A and B have a similar distribution for the *NPC* components. However, the minimum cost solution (A) has a slightly higher contribution of 6.9% for the natural gas compared to the minimum impact solution with only 0.27% which will be reflected in the environmental impact analysis.

5.1.2. Environmental impact analysis

As shown in Fig. III-9, solution A and B success in declining the environmental impact up to 7 times compared to the base case due to the deployment of the solar water heating systems and the saving of non-renewable energy systems (i.e., natural gas and electricity). In the base case, the natural gas represents almost 100% of the environmental damage ($1.88 \cdot 10^5$ Pt). While this contribution is reduced to 38.8% ($1.39 \cdot 10^4$ Pt) in the minimum cost solution (A) and it becomes almost negligible in the minimum impact solution (B) where it counts only for 2.20% ($5.60 \cdot 10^4$ Pt).

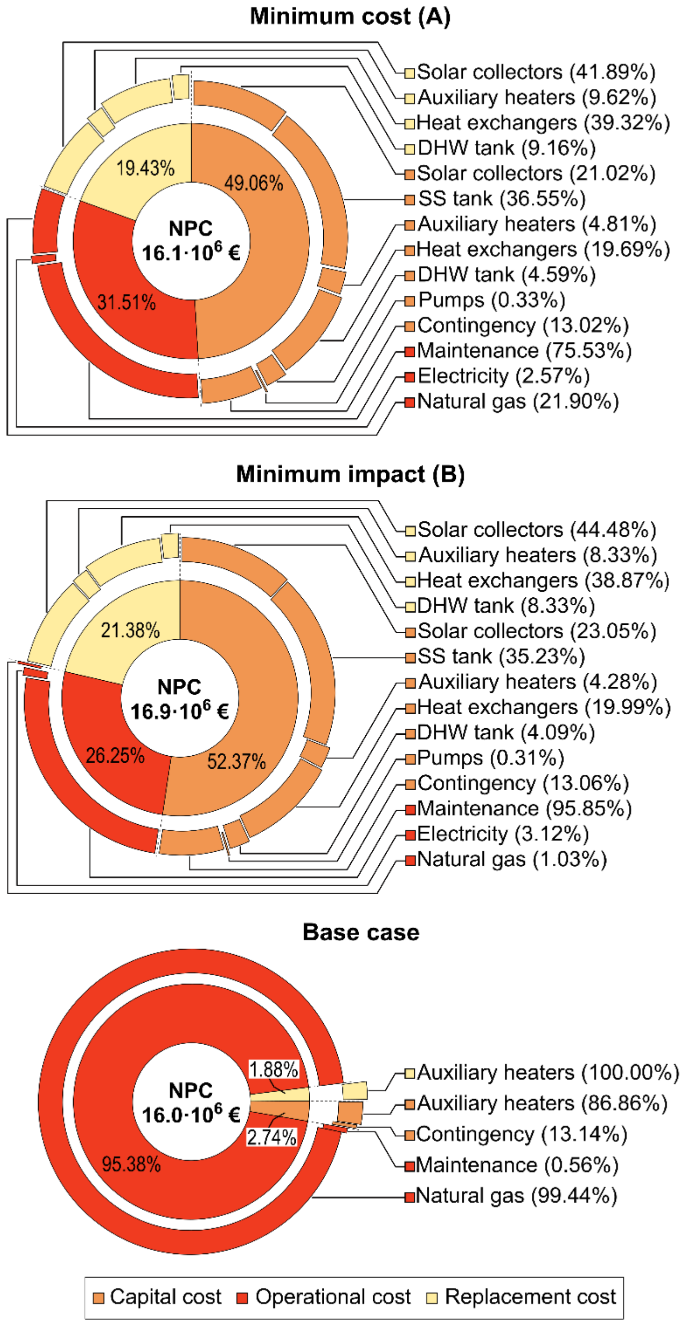

Fig. III-8. Distribution of the net present costs of two Pareto optimal solutions (point A and B in Fig. III-7) for the CSHPSS in Madrid which covers 7654 MWh/year of combined SH and DHW demand during its lifetime and the base case, which represents a natural gas heating system.

Following the economic analysis of the anchor points (A and B), the solar collector and the SST share most of the contribution to the total environmental impact [59]. In solution A, the solar collector counts for 16.7% of the total damage to the environment, whereas this fraction increases up to 30% in the solution B due to the limitation of using natural gas as the main fuel. On the other hand, the impact fraction of the SST represents 37.9 % in solution A and it increases to 57.7% in solution B.

As the latest highlight, the impact of the heat exchangers increased by 40.1% from solution A to B. This is due to the further deployment of the solar collectors in the minimum impact solution (B) and subsequently extra supplement of heat exchange is required to cover the additional solar energy.

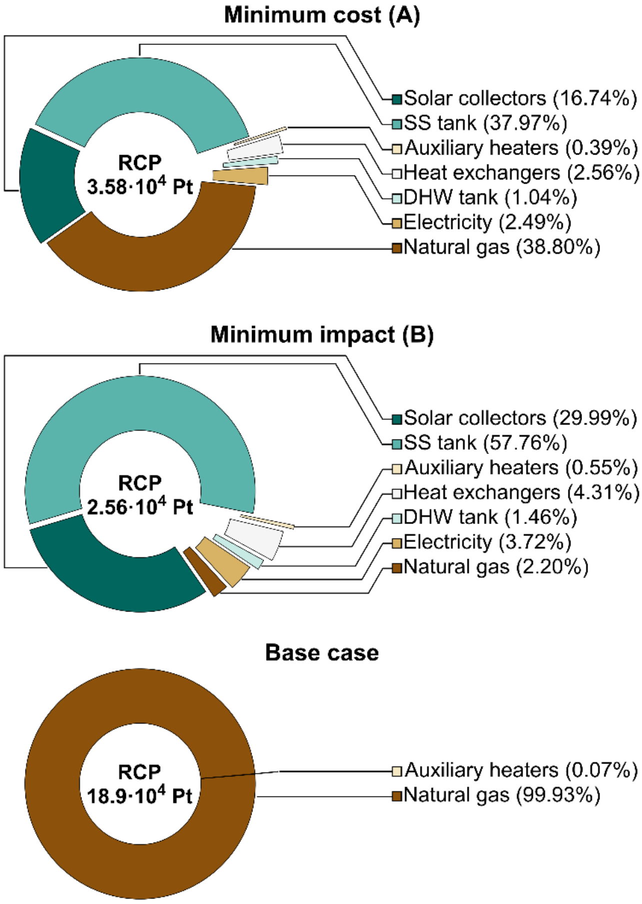

Fig. III-9. Distribution of the environmental impact into its single impact categories of two Pareto optimal solutions (point A and B in Fig. III-7) for the CSHPSS in Madrid which covers 7654 MWh/year of combined SH and DHW demand during its lifetime and the base case, which represents a natural gas heating system.

5.1.3. Energy analysis of an intermediate Pareto optimal solution (C)

The thermal performance characteristics of the optimized CSHPSS plant configuration based on the proposed methodology framework is presented through an intermediate Pareto optimal solution (point C in Fig. III-7). This solution is designed to fulfill a total SH and DHW demand of approximately 6555 MWh/year and 1099 MWh/year, respectively. Note that any other intermediate point in the proposed Pareto set would be similarly comparable in this analysis.

As shown in Fig. III-10, the monthly value of SH and DHW demands are covered by the supplied solar collectors and a combination of the thermal energy stored in the SST and the DHWT. Where the energy provided by the CSHPSS plant is represented as a positive input, whereas the energy stored in the SST is depicted as a negative input.

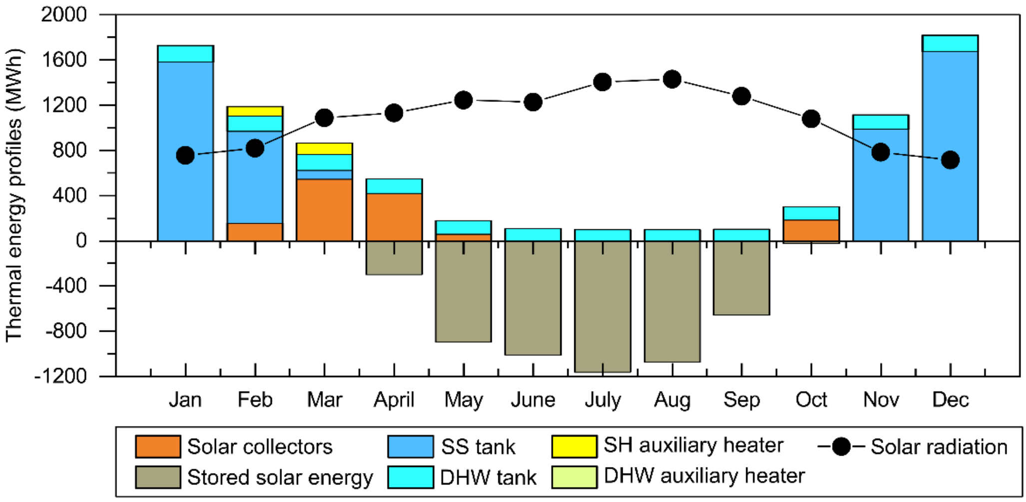

Fig. III-10. Monthly thermal energy profiles of an intermediate Pareto optimal solution (point C in Fig. III-7) for the CSHPSS in Madrid which covers 7654 MWh/year of combined SH and DHW demand during its lifetime.

In summer and autumn seasons (i.e. April to October) where the solar radiation is relatively high, and the SH demand is small, most of the provided energy from the solar collectors are directly stored into the SST, and the remaining is utilized to cover the heating demand. On the contrary, the solar radiation decreases, and the heating load significantly increases during the winter season (i.e. November to January), therefore the total heating demand is covered through a combination between the daily energy supplied by the DHWT and the stored energy in the SST. Moreover, in extreme cases when the proposed solar system failed in fulfilling the required heating demand, the auxiliary heaters using natural gas deliver the necessary energy. These cases happen during February and March where most of the stored energy in the SST is already discharged during the coldest months. This can be reflected in the solar fraction of the distribution circuits during these months. In February, the solar fraction declines by 8% and 4.8% for the SH and DHW circuits, respectively. While in March, this value improved a bit for the DHW distribution circuit and the solar fraction declines by only 1.2% due to the increment in the solar radiation. On the other hand, the solar fraction for the SH circuit keep deteriorating and it drops by 13.9% due to the absence of the seasonal storage and the limited direct energy provided by the solar collectors.

5.2. Application analysis on the selected climate zones in the EU

Following Madrid case analysis combined with the main objective of assessing the CSHPSS plant feasibility in the residential sector at various climate zones in the EU, the proposed methodology framework correspondingly based on the multi-objective approach is applied to optimize the cost against an aggregated environmental metric in Athens, Berlin and Helsinki as a representative for the Mediterranean, central European, and Nordic climates, respectively. The problem is formulated to cover an annual SH and DHW demand of 4661 MWh, 14180 MWh, and 20896 MWh for Athens, Berlin, and Helsinki, respectively.

As shown in Fig. III-11, a clear trend is observed for the deployment of the CSHPSS which causes a rise in the economic cost under various EU climate zones compared to the base cases. The optimal economic solutions in the nominated locations depend on several factors including the climate condition, the heating demand, and the natural gas and electricity prices. In Athens, the NPC in the minimum cost and impact optimal points have been raised by 18.3% and 50.8%, respectively compared to their base case. This high growth is due to the low cost of non-renewable energy resources in Athens compared to Madrid. Following the observed tendency in Athens, the NPC in Berlin case raised by 17.1% and 25.4% compared to their base case. On the other hand, the NPC increase only by 3.12% and 8.11% in Helsinki due to several factors including, the high price of natural gas and electricity, and the high heating demand.

Fig. III-12 shows the optimal environmental solutions for the four locations. For all of these locations, the minimum impact solution follows the Madrid case and it improves the RCP by 84.7%, 82.1%, and 82.9% for Athens, Berlin, and Helsinki cases, respectively. The same tendency was found for Berlin and Helsinki at the minimum cost solution since the RCP improved by 75.3% and 77.9% for Berlin and Helsinki. On the other hand, the low natural gas and electricity prices in Athens restrict substantial improvement in the RCP, and it is improved only by 14.7%. This marginal improvement in the minimum cost optimal solution of Athens case will be mirrored in its breakdown for the NPC and RCP.

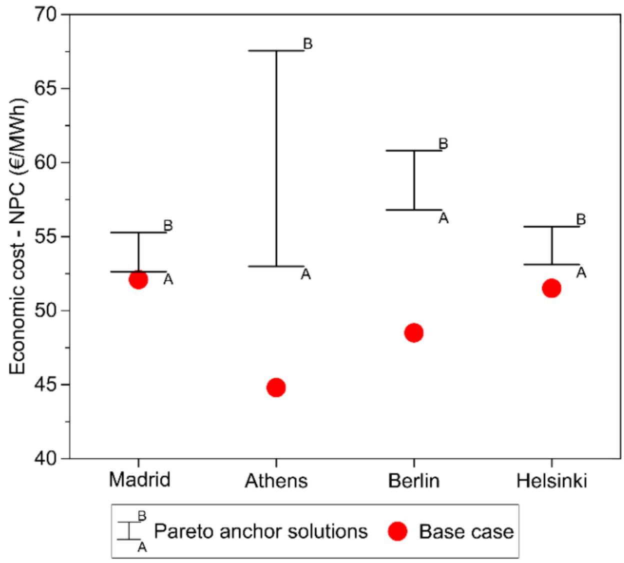

Fig. III-11. Each column depicts a range of cost for the optimal solutions using the CSHPSS plant compared to its base case under various EU climate zones.

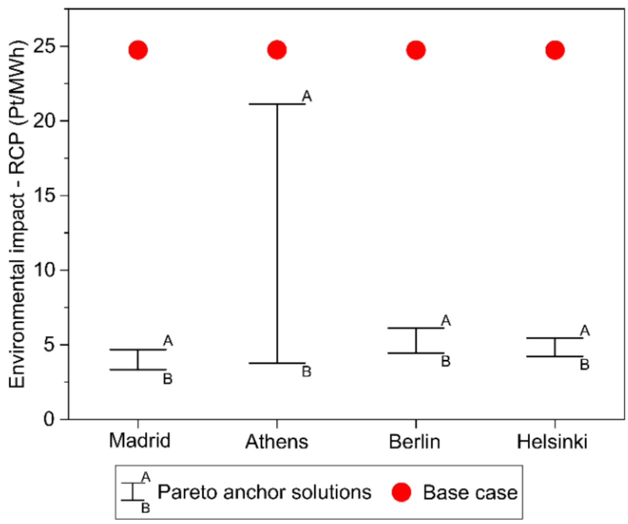

Fig. III-12. Each column depicted a range of environmental impact for the optimal solutions using the CSHPSS plant compared to its base case under various EU climate zones.

5.2.1. Economic cost analysis for the EU climate zones

Fig. III-13 shows a comprehensive breakdown for the NPC of the CSHPSS plant during its lifetime cycle under different EU climate zones. It remarks almost the same contribution for each component in the NPC of Madrid, Berlin and Helsinki cases. Furthermore, the results show that the capital and replacement costs in the minimum cost and minimum impact optimal solutions of Berlin and Helsinki are quite large in comparison to their base cases as mentioned in Madrid case study. Moreover, the results confirm the dependency of the CSHPSS plant configuration on the heating demand where the capital and replacement costs ascending increases with the heating demand based on the climate zone [47] as shown in Madrid, Berlin, and Helsinki, respectively (Table III-6).

Table III-6. Optimal renewable energy equipment sizing in various EU climate zones.

City	Optimal solution	Solar collectors (10^3 m^2)	Seasonal storage tank (10^3 m^3)	Domestic hot water tank (m^3)
Madrid	A	6.888	65.78	109.7
	B	8.802	74.32	109.7
Athens	A	0.5686	0.007392	117.6
	B	5.593	44.39	117.6
Berlin	A	21.00	149.2	137.2
	B	25.50	198.0	137.0
Helsinki	A	32.91	230.4	168.5
	B	38.13	287.9	168.5

On the contrary, the low heating demand combined with the cheap prices for the natural gas and electricity in Athens contribute to dramatically change the distribution for the NPC of the minimum cost optimal solution in this Mediterranean zone. The operational cost has a significant contribution of 68% compared to only 18.8% of the initial capital cost and 12.7% of the replacement cost. This is due to the dependency of the system on natural gas which almost represents 94.4% of the operational cost and the limited involvement for the solar water heating system. More precisely, the solar collectors and SST represent only 11.6% and of the initial capital and 13% of the replacement costs. In term of the renewable energy equipment sizing at the proposed climate zones, Table III-6 shows a summary for the proposed sizing the renewable energy equipment based on the Pareto optimal solution in various EU climate zones. It is noticed that for all the minimum impact optimum solutions under different EU climate zones, the ratio between the SST volume and the solar collector field area is around 8 ± 0.5 m^3/m^2 based on the climate zone. While this ratio completely changes for the Athens climate zone at the minimum cost optimal solution due to the restriction toward the deployment of the solar energy and it becomes only 0.013 m^3/m^2.

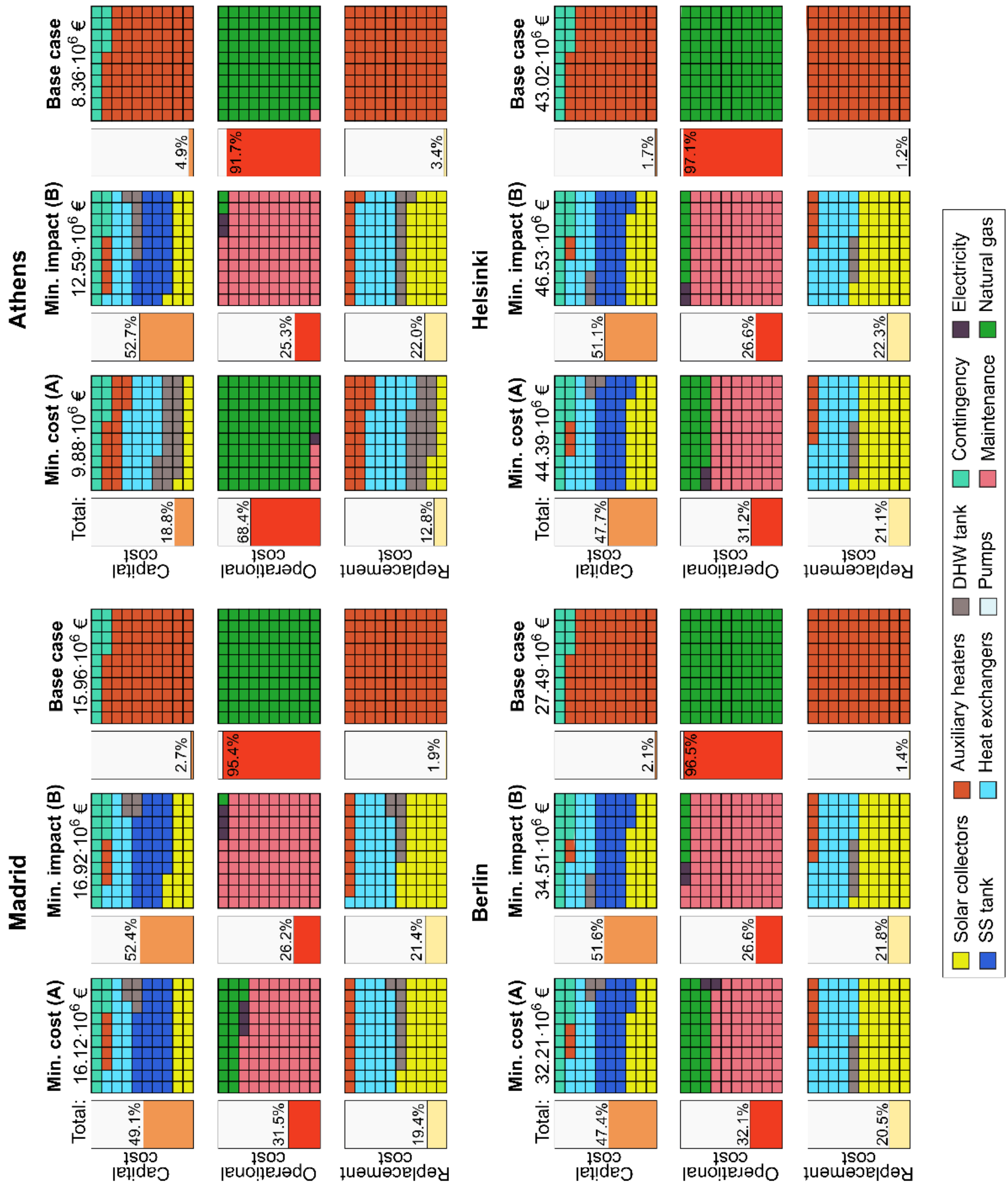

Fig. III-13. Breakdown of the net present costs including; initial capital cost, operational cost, and replacement cost for the minimum cost and impact of Pareto optimal solutions for CSHPSS plant under different climate zones in comparison with its base case.

5.2.2. Environmental impact analysis for the EU climate zones

Fig. III-14 shows a breakdown for the environmental impact into its categories for the minimum cost and impact Pareto optimal solutions of a CSHPSS plant under different climate zones in comparison with its base case. The results follow the environmental impact breakdown of Madrid where the optimal solutions can reduce the environmental impact up to 5.5 and 5.8 times for Berlin and Helsinki cases, respectively. In Athens case, the minimum cost optimal solution decreases the environmental impact only by 1.1 times. This is due to the significant contribution of the natural gas ($9.6 \cdot 10^4$ Pt) which represents almost 98.4% of the total environmental impact.

Following the environmental impact in Madrid case, the solar collector and SST are the main contributor to the total environmental impact in the minimum cost optimal solution with a contribution of 48.2%, and 52.7% in Berlin and Helsinki, respectively. This contribution increases significantly for the minimum impact optimum solutions, where they share 87.7%, 80.2%, and 78.9% in Athens, Berlin and Helsinki solutions, respectively.

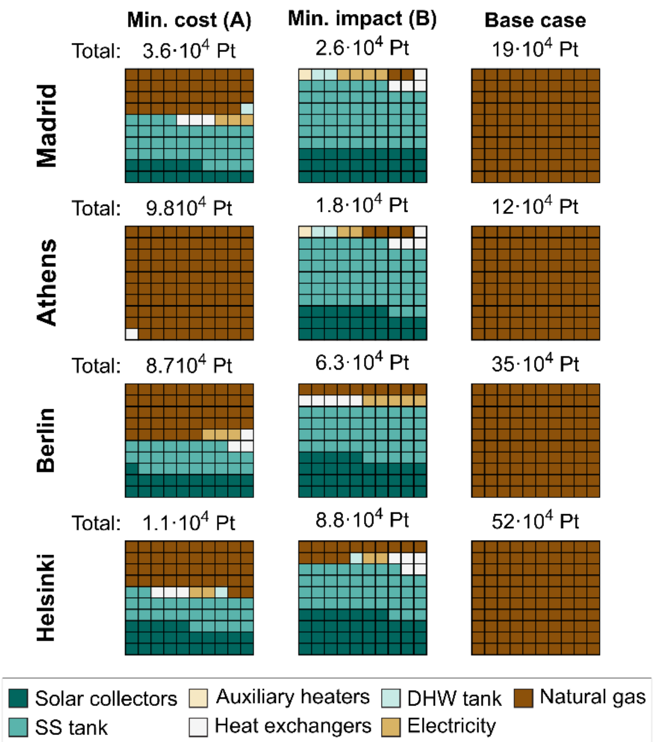

Fig. III-14. Breakdown for the environmental impact of Pareto optimal solutions (Minimum cost and Minimum impact) of a CSHPSS plant under different climate zones in comparison with its base case.

5.2.3. Energy analysis for the EU climate zones

Following the energy analysis in Madrid case study, an intermediate Pareto optimal solution (c) is presented to evaluate the thermal performance of the CSHPSS plant in different EU climate zones as shown in Fig. III-15.

Based on the limitation of the solar heating system in covering the heating demand during several months in Berlin and Helsinki, the AUX_1 operated from February until April due to the full discharging of the SST during the winter period. Furthermore, the AUX_2 almost operates throughout the year except the summer months (June to August) for these climates since the DHW tank is designed to cover only the daily services. In Athens, a limited seasonal storage is projected between April and October where a high solar radiation and low heating demand are observed due to the Mediterranean weather conditions, which were mentioned in Fig. III-5 and Fig. III-6. This limited heating demand reduces the auxiliary heaters usage throughout the whole year.

Based on normalizing the technical performance of the CSHPSS plant, the solar fraction was presented, and its minimum value was noticed during January and March for the DHW and SH circuits, respectively. In the DHW distribution circuit, the solar fraction is 48.2% and 29.6% for Berlin and Helsinki, respectively. While the solar fraction for the SH distribution circuit becomes 66.2% and 78.9% in Berlin and Helsinki, respectively. On the other hand, due to the low price of natural gas in Athens in comparison to the other EU countries, an extensive usage for the auxiliary heaters in March is shown where the solar fraction has reduced to 59.9% for the SH circuit and sustain around 98.1% for DHW circuit due to low DHW heating demand. Even though the uncertainty associated with the monthly performance of the CSHPSS plants under different climate zones, the proposed methodology framework successes in eliminating the yearly system uncertainty when introduced in various climate zone as shown in Table III-7. In the SH distribution circuit, which has a substantial contribution to the life cycle of the CSHPSS plant, the solar fraction never goes below than 92.5% for different EU climate zones. While due to the DHW distribution circuit functionally in covering only the daily services, the solar fraction diminishes up to 66.1% in Helsinki due the high demand in winter period.

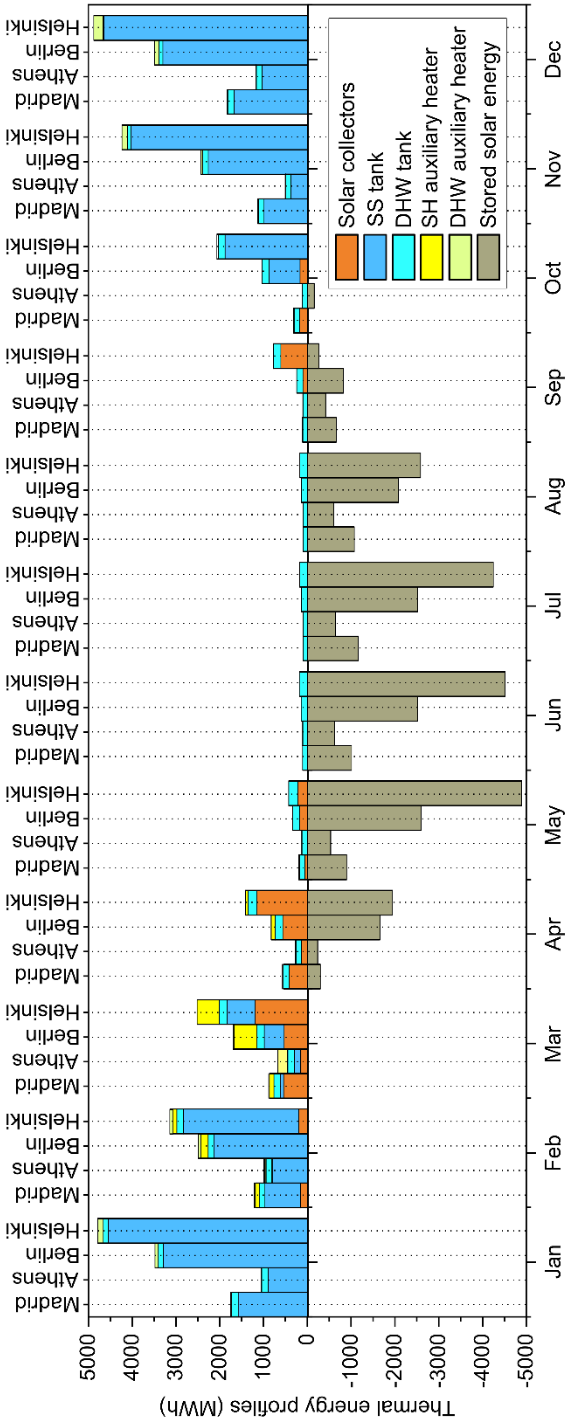

Fig. III-15. Monthly thermal energy profile of an intermediate Pareto optimal solution (C) under various EU climate zones.

Table III-7. The yearly solar fraction of the intermediate Pareto optimal solution (C) under various EU climate zones.

City	SF_{SH} (%)	SF_{DHW} (%)
Madrid	97.1	98.6
Athens	92.5	96.9
Berlin	93.8	79.8
Helsinki	96.6	66.1

Remarking that the proposed optimal solutions for the CSHPSS plants in different EU climate zones are high sensitivity for their geographical locations and economic parameters comprise natural gas and electricity prices. Therefore, the influence of the most relevant economic parameters should be assessed in a sensitivity analysis to give an estimate for the uncertainty associated with the results.

5.3. Sensitivity analysis for the methodology framework

A sensitivity analysis for the most important economic parameters is implemented to understand their influence on both the NPC and RCP objective functions. This analysis is carried out based on One-factor-at-a-time (OFAT) approach [102] in which each economic parameter is varied by up to 20% after another in comparison to a reference case. The Pareto optimal solution (A) of Madrid case study is selected as the reference case. The assessment includes the influence of the natural gas price, electricity price, discount rate, inflation rate, investment cost, operational cost, and replacement cost. The sensitivity analysis not only comprises the influence of the selected parameters on the NPC and RCP, but it also proposes a detailed breakdown for the economic cost and the environmental impact for the influence of each of these parameters.

As shown in Fig. III-16, the sensitivity analysis for a CSHPSS plant configured based on the optimal solution A (minimum cost) under Madrid climate zone demonstrates a high dependency for the NPC on the natural gas price, the investment cost and the operational cost in which it declines by 10%.

This reduction can be explained through the change in the system configuration where the reduction in the natural gas price and the operational cost aggravate more dependency on using the natural gas and subsequently decrease the NPC. Furthermore, a non-linear effect for both the natural gas price and the operational cost is noticed where the NPC increases only by 5% and 6%, respectively. The discount rate and inflation rate have a limited contribution to the NPC since it changes only 6% and 4% for the discount rate and inflation rate, respectively. The electricity price has a minor influence on the NPC since it has a marginal share of the total cost in the reference case.

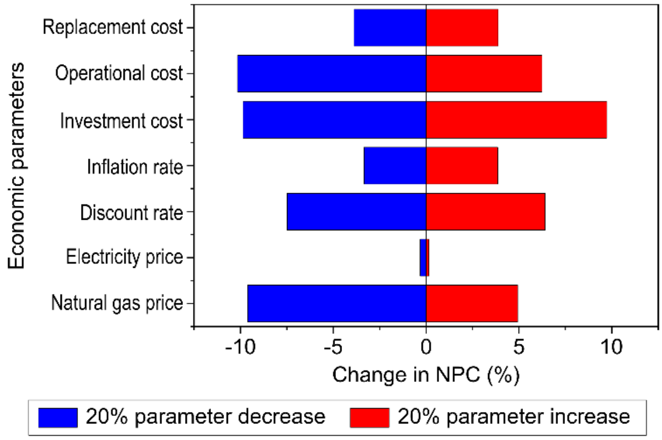

Fig. III-16. A sensitivity analysis for the economic cost objective of Pareto optimal solutions A (Minimum cost) under Madrid climate zone.

Fig. III-17 comprises the effect on the net present cost of the installation exercised by the 7 economic parameters after unilateral their 20% reduction or increment comparing to the reference case.

Fig. III-17 (to the left of the reference case) shows a breakdown for reducing the economic parameters of the optimal solution A by 20% where each layer comprises the share percentage of a certain cost parameter in the NPC breakdown. The NPC breakdown confirms the high dependency on the natural gas price and the operational cost. This reduction intends to propose the natural gas usage as a visible solution instead of the solar water heating system in covering the heating demand. Therefore, a large share of 74.6% and 78.6% is observed when the natural gas price and the operational cost decrease 20%, respectively. On the contrary, the natural gas in the reference case shares only 6.89%. Furthermore, the large share of natural gas reduces the use of solar collectors to only 1.57% and the SST to 5.8%, whereas the reference case shares up to 10.3% and 17.9% of the total shared solar collectors and SST, respectively.

For the breakdown of increasing the economic parameters of the optimal solution A by 20% shown in Fig. III-17 (to the right of the reference case), almost the same pattern is observed for changing each economic parameter with a slight change in the natural gas share when the natural gas price, the operational cost, and the investment cost increased up to 20%.

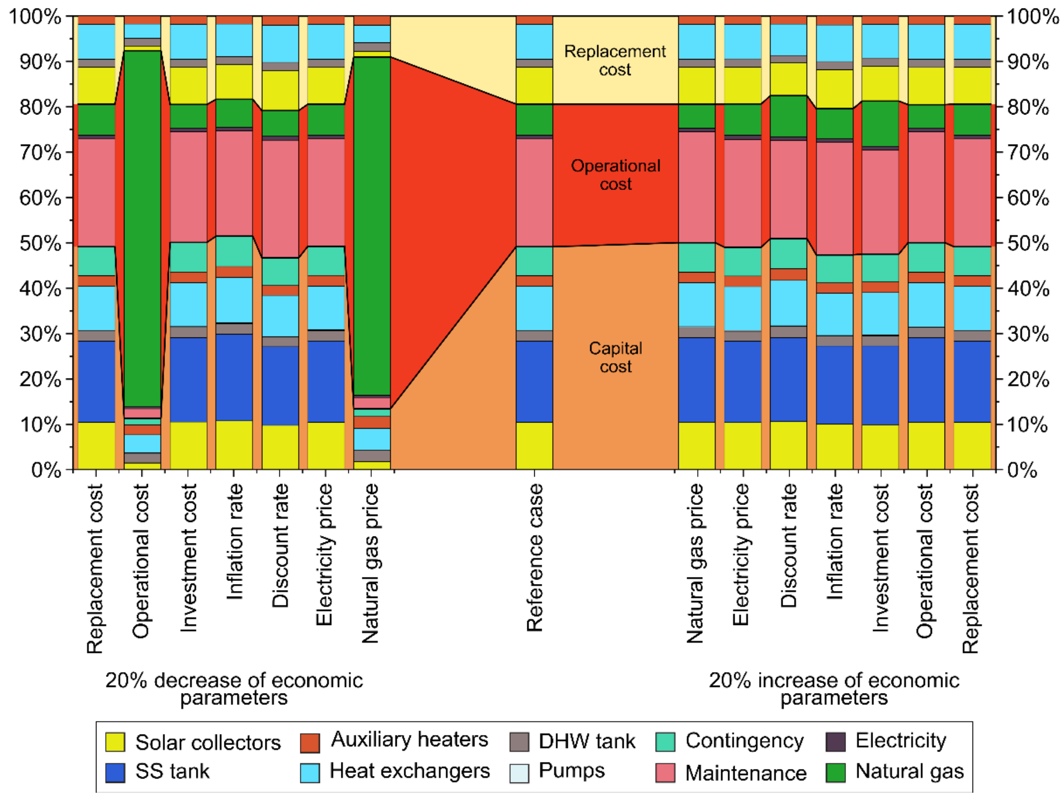

Fig. III-17. Breakdown for the NPC where to the left of the reference case is depicted the breakdown when each economic parameter decreases 20%, whereas to the right of the reference case is depicted the breakdown when each economic parameter increases 20%.

Following the sensitivity analysis for the NPC objective function, Fig. III-18 shows the sensitivity analysis for the RCP when the economic parameters vary by 20%. Recalling the sharp influence for the natural gas price and operational cost in presenting the natural gas usage as a valid solution with a marginal share for the solar collectors and STT, the RCP increases 380% for reducing the natural gas price and the operational cost. Furthermore, when these parameters increase 20% and due to the non-linear noticed effect, the RCP decreases 29% and 8% for natural gas price and operational cost, respectively. On the other hand, decreasing the investment cost, discount rate and the inflation rate 20% has a slight effect of 8%, 4%, and 8%, respectively on increasing the RCP, whereas the RCP decreased 15%, 1%, and 15% when the investment cost, discount rate, and the inflation rate increased 20%.

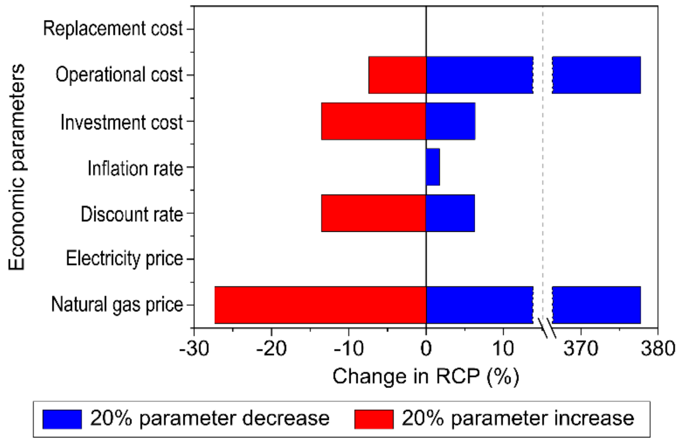

Fig. III-18. A sensitivity analysis for the environmental impact objective of Pareto optimal solutions A (Minimum cost) under Madrid climate zone.

The dramatic increase in the RCP for the reducing the natural gas price and the operational cost can be observed in the RCP breakdown which is shown in Fig. III-19 (to the left of the reference case). A high dependency is noticed when using natural gas instead of the solar water heating system where the natural gas shares 98.8% for varying the natural gas price and the operational cost down 20%, whereas the natural gas shares only 38.8% in the reference case. On the other hand, increasing the economic parameters 20% keeps almost the share for each parameter as the reference case with a marginal change in the natural gas share when the operational cost increases 20%, as shown in the RCP breakdown Fig. III-19 (to the right of the reference case).

5.4. Discussion and future market development

The future potential of CSHPSS plants in different EU climate zones is assessed through various Pareto optimal solutions offered by the proposed methodology framework in which both the techno-economic and environmental impact is considered. Generally, the CSHPSS system succeeded in decreasing the environmental impact in the investigated climate zones. However, the high investment cost of the CSHPSS plants compared to the conventional heating systems that use the natural gas as the main fuel limit the extensive benefit of wide spreading the CSHPSS plants in different EU climate zones.

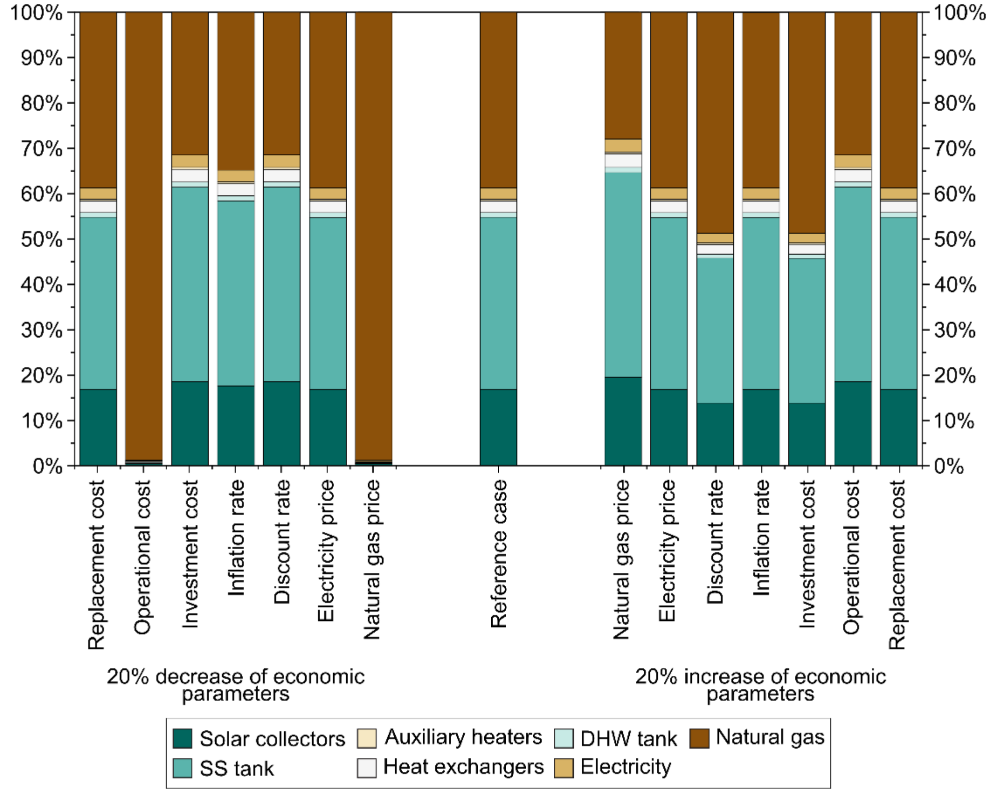

Fig. III-19. Breakdown for the RCP where to the left of the reference case is depicted the breakdown when each economic parameter decreases by 20%, whereas to the right of the reference case is depicted the breakdown when each economic parameter increases by 20%.

This limitation becomes more substantial in Athens (Mediterranean climate zone) where heating demand is low due to the high solar radiation throughout the year and the prices of the non-renewable energy resources are low. However, the growing forecast for the natural gas price in the EU [100] would support more economic feasibility of the CSHPSS plants in different EU climate zones. Therefore, as a part of the methodology framework, the future development in the plant cost with consideration for the actual effect of the technology deployment is evaluated for the proposed EU climate zones based on the historically observed learning curves.

As shown in Fig. III-20, a clear trade-off for the increment in the conventional systems price is observed, this price raise associates with a progressive declination in the CSHPSS plants prices. In the long term, the CSHPSS plants in various EU climate zones can significantly underprice the NPC in comparison to the conventional system using natural gas by 2030. This development can significantly assist in improving the competitiveness of the CSHPSS plant as a sustainable alternative solution in comparison to the conventional systems.

Currently in Madrid, the CSHPSS plants can cover the heating demand for less than 52.6 €/MWh, whereas its base case covers it at 52.1 €/MWh. With this minor difference, the feasibility of the CSHPSS plant under Madrid climate conditions can be proved. In 2030, the NPC will range from 46.3 to 49.9 €/MWh for the CSHPSS while its base case 63.7 €/MWh.

In Athens where the CSHPSS plant can cover the heating demand at high price ranged between 44.8 and 65.2 €/MWh. Beyond 2022, the CSHPSS plants will be able to cover the heating demand at a lower cost than the conventional system, at which the heating demand is covered at a price of 50.3 to 64.5 €/MWh. The CSHPSS plant in Athens will continue decreasing to less than 47 €/MWh by 2030, whereas the base case will increase to 65.2 €/MWh.

In Berlin, a slight cost reduction would be available in the CSHPSS plants by 2020 where the NPC will range from 55 to 59.3 €/MWh. By 2030, the CSHPSS plant NPC drops to 54.9 €/MWh compared to a rise in the NPC of the base case to 62.9 €/MWh.

In Helsinki, the NPC ranges between 53.1 and 55.7 €/MWh, while its base case covers the heating demand at 51.5 €/MWh. These prices embody the CSHPSS plant in Helsinki as a competitive solution due to the high heating demand and high the non-renewable energy resources prices. By 2030, the NPC is expected to decrease below 47 €/MWh, while its base case continues to increase up to 62.7 €/MWh.

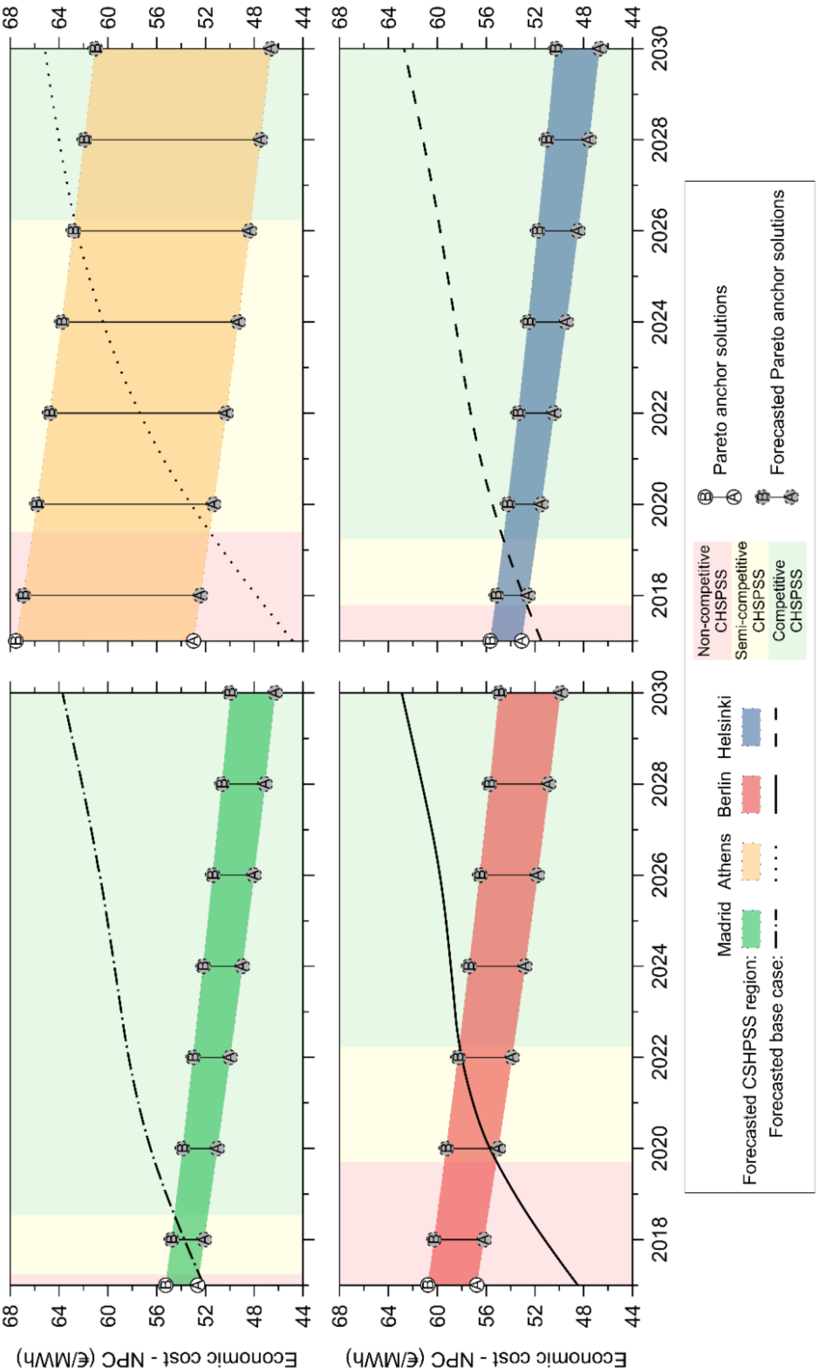

Fig. III-20. Forecast for the development of NPC of the CSHPSS plant in different EU climate zones along with their base cases by 2030.

6. CONCLUSIONS

The EU ambitious plan to cut the GHG up to 40% simultaneously with increasing the share of the renewable energy resource at least 27% by 2030 encourages the prevalent methodology to quantify the renewable energy systems performance including its economic and environmental aspects. This work tends to explore the prospects for wide-scale deployment of the CSHPSS plants in the residential sector under various EU climate zones to solve its challenges. The proposed methodology framework correspondingly based on a multi-objective approach which is applied to optimize the cost against an aggregated environmental metric throughout the life cycle of the proposed system in comparison to their relative conventional heating systems. In this context, the proposed methodology is applied to diverse EU climates comprising Madrid, Athens, Berlin and Helsinki as a representative for the Mediterranean, central European, and Nordic climates, respectively with consideration for the seasonal and short-term storage systems and their relatively load profiles based on the explored climate zones.

Based on the life cycle assessment, the calculated optimal solutions demonstrate an environmental advancement for the CSHPSS plants at various EU climate zones in comparison to the conventional systems using natural gas as the main fuel. The minimum impact solutions improve the RCP by 86.5%, 84.7%, 82.1%, and 82.9% for Madrid, Athens, Berlin, and Helsinki cases, respectively. While this improvement becomes only 14.7% for the Athens climate zone at the minimum cost optimal solution due to the dependency on using natural gas as a competitive solution in comparison to the deployment of the solar energy equipment. On the other hand, the life cycle costing analysis shows a clear tendency for increasing the NPC under various EU climate zones compared to their base cases due to the high initial capital cost of CSHPSS plants. In the minimum cost solutions, the NPC raised by 1%, 18.3%, 17.1% and 3.12% for Madrid, Athens, Berlin, and Helsinki cases, respectively. This increment proofs dependency for the CSHPSS plants on the climate zone condition, the heating demand, and the natural gas and electricity prices. Furthermore, this raise relatively increases in the minimum impact solution and it becomes more substantial in Athens, and Berlin since the NPC increases by 50.8%, and 25.4% for these cities respectively due to the low price of non-renewable energy resources .Recalling the optimal solutions dependency on the design parameters, a detailed sensitivity analysis for the most relative economic parameters in

Madrid case study is presented. The sensitivity results aggravate a high dependency for the CSHPSS plant NPC objective on the natural gas price, the investment cost and the operational cost, where decreasing these parameters by 20% contribute to a significant change in the NPC by 10%. While in terms of the environmental impact, the RCP increases by 380% due to the reduction of the natural gas price and the operational cost by 20%.

Following the challenges facing the CSHPSS in EU member states include high investment costs and the uncertain technical benefits. The proposed methodology framework successes in eliminating the yearly system uncertainty when introduced in various EU climate zone. Thus, the yearly solar fraction never goes below than 92.5% in the investigated climate zones where the SST volume to solar collector field area is around 8 ± 0.5 m^3/ m^2. From the economic point of view, the future development of the CSHPSS plant cost based on the historically observed learning curves combined with the clear tendency for the increment in the natural gas prices at various EU member states proposes a significant economic improvement in the competitiveness of the CSHPSS plant in comparison to the conventional system by 2020. However, the low heating demand and low prices of the natural gas and electricity in Athens (Mediterranean climate zone) provokes a limited improvement in the CSHPSS plant competitiveness till 2022.

Overall this study provides an effective tool for the techno-economic and environmental assessment of the CSHPSS at the residential sector which can be applied to plan its integration into the existing district heating fields. Furthermore, our study highlights the wide applicability of using CSHPSS in different EU climate as a sustainable alternative solution to the conventional systems based on natural gas. Even though this competitiveness cannot be approved without clear and effective policies based on a longer-term view for the deployment of renewable energy systems in the EU with a goal of establishing a more sustainable energy infrastructure.

ACKNOWLEDGEMENTS

The authors would like to acknowledge financial support from Martí i Franquès COFUND Fellowship program. This project has received funding from the European

Union's Horizon 2020 research and innovation programme under the Marie Skłodowska-Curie grant agreement No. 713679 and the Spanish Ministry of Education and Competiveness (CTQ2016-77968, MINECO/FEDER). In addition, this work was partially funded by the Ministerio de Economía y Competitividad de España (ENE2015-64117-C5-1-R (MINECO/FEDER) and ENE2015-64117-C5-3-R (MINECO/FEDER)). The authors at the University of Lleida would like to thank the Catalan Government for the quality accreditation given to their research group (2017 SGR 1537). GREA is certified agent TECNIO in the category of technology developers from the Government of Catalonia.

NOMENCLATURE

A_{COL}	total aperture area of the solar collectors (m^2)
C_{AUX}	annual operational cost of the auxiliary heaters (€)
CAP_k	design variable of equipment unit k
$CEPCI^{year\ A}$	chemical Engineering Plant Cost Index in the base year
$CEPCI^{year\ B}$	chemical Engineering Plant Cost Index in the installation year
C_C	total initial capital cost (€)
C_O	total discounted operational cost (€)
C_R	total discounted replacement cost (€)
C_M	annual cost of equipment unit k (€)
C_p	annual operational cost of pump (€)
c_p	specific heat capacity (kJ/kg. k)
$C(x_t)$	marginal cost of the CSHPSS plant at a certain time (€/MWh)
$C(x_o)$	cost production of a reference point (€/MWh)
DAM_d	indicator result for damage category d
d	annual discount rate (%)
i	annual inflation rate (%)
IMP_e	indicator result for endpoint impact category e
LCI_i^{MP}	life cycle inventory of the elementary flow i related to manufacturing process
LCI_i^{OP}	life cycle inventory of the elementary flow i related to operation activities
LCI_i^{TOT}	total life cycle inventory of the elementary flow i

LCI_i^{TR}	life cycle inventory of the elementary flow i related to transportation
LR	learning rate
FBM_k	bare module factor of equipment unit k
$f_c(x)$	original objective function [*NPC*(*x*) or *RCP*(*x*)]
$\bar{f}_c(x)$	normalized objective function [*NPC*(*x*) or *RCP*(*x*)]
f_m	maintenance factor
$f^{PN}(x)$	pseudo nadir point
$f^{UT}(x)$	utopia point
PEC_k	purchase cost of equipment unit k
PWF_n	present worth factor of periodic future cash flows
PVF_n	present value factor of a single future cash flow at the beginning of n^{th} time period
$\dot{m}$	mass flowrate of the recirculate water pumps (kg/s)
$\dot{Q}_{Aux}$	natural gas boiler duty rate (MW)
Q_{DHW}	total energy supplied by domestic hot water tank (MWh)
$Q_{DHW\ load}$	total domestic hot water heating demand (MWh)
$Q_{SH\ load}$	total space heating demand (MWh)
Q_{SST}	total energy supplied by Seasonal storage tank (MWh)
RCP	ReCiPe 2008 aggregated impact factor (Pt)
SF	solar fraction (%)
V_{DHW}	volume of the domestic hot water tank (m^3)
V_{SST}	volume of the seasonal storage tank (m^3)
$WS(x)$	weighted-sum objective function
x	continuous variables of the simulation model
x^L	lower bounds of the continuous variables of the simulation model
x^U	upper bounds of the continuous variables of the simulation model
x_o	capacity at the reference point (MW)
x_t	capacity at a certain time (MW)

***Greek* symbols**

α_{CF}	factor of contingency charges and fees
α_k	purchase cost coefficient of equipment unit k
β_k	purchase cost exponent of equipment unit k
δ_d	normalization factor for damage category d
θ_{ei}	characterization factor that connects the elementary flow i with endpoint impact category e

ε_d	weighting factor for damage category d
λ	non-negative weight for the weighted-sum method
ΔT_{DHW}	temperature difference between the extracted and replaced water inside the domestic hot water circuit (ºC)
ΔT_L	temperature difference between the demand (ºC)
ΔT_{SST}	temperature difference between the extracted and replaced water inside the space heating circuit (ºC)

Abbreviations

AUX	natural gas boiler
COL	field of solar collectors
CSHPSS	central solar heating plant coupled with seasonal storage
DHW	domestic hot water
DHWT	domestic hot water storage tank
GHG	greenhouse gas
GenOpt	generic optimization program
GPSPSOCCHJ	generalized pattern search algorithm with particle swarm optimization with construction coefficient and Hooke-Jeeves algorithm
HE	heat exchanger
HJ	Hooke-Jeeves algorithm
LCA	life cycle assessment
LCC	life cycle costing
P_i	centrifugal pump
PSO	particle swarm optimization algorithm
SH	space heating
SST	seasonal storage tank
TES	thermal energy storage
TRNSYS	transient system simulation program

Indices

d	damage category
e	endpoint impact category
i	elementary factor
k	equipment unit

Sets

ID_d	set of endpoint impact categories e that contribute to damage d

REFERENCES

[1] Renewable Energy Policy Network for 21st Century (REN21). Renewables 2016-Global Status Report. 2016.

[2] U.S. Energy Information Administration. International Energy Outlook 2016. 2016. doi:www.eia.gov/forecasts/ieo/pdf/0484(2016).pdf.

[3] Rezaie B, Rosen MA. District heating and cooling: Review of technology and potential enhancements. Appl Energy 2012;93:2–10. doi:10.1016/j.apenergy.2011.04.020.

[4] British Petroleum. BP Statistical Review of World Energy 2017. 2017. doi:http://www.bp.com/content/dam/bp/en/corporate/pdf/energy-economics/statistical-review-2017/bp-statistical-review-of-world-energy-2017-full-report.pdf.

[5] European Energy Agency. Final energy consumption by sector and fuel. Denmark: 2017. doi:CSI 027/ENER 016.

[6] Balaras CA, Gaglia AG, Georgopoulou E, Mirasgedis S, Sarafidis Y, Lalas DP. European residential buildings and empirical assessment of the Hellenic building stock, energy consumption, emissions and potential energy savings. Build Environ 2007;42:1298–314. doi:10.1016/j.buildenv.2005.11.001.

[7] European Environment Agency. Annual European Union greenhouse gasinventory 1990–2016 and inventory report 2018. Copenhagen: 2018.

[8] European Commision. Memo on the Renewable Energy and Climate Change Package. Brussels: 2008.

[9] European Commision. Communication from the commission to the European parliament, the council, the European economic and social committee and the committee of the regions - a policy framework for climate and energy in the period from 2020 to 2030. Brussels: 2014.

[10] Olsthoorn D, Haghighat F, Mirzaei PA. Integration of storage and renewable energy into district heating systems: A review of modelling and optimization. Sol Energy 2016;136:49–64. doi:10.1016/j.solener.2016.06.054.

[11] Jamar A, Majid ZAA, Azmi WH, Norhafana M, Razak AA. A review of water heating system for solar energy applications. Int Commun Heat Mass Transf 2016;76:178–87. doi:10.1016/j.icheatmasstransfer.2016.05.028.

[12] Pinel P, Cruickshank CA, Beausoleil-Morrison I, Wills A. A review of available methods for seasonal storage of solar thermal energy in residential applications. Renew Sustain Energy Rev 2011;15:3341–59. doi:10.1016/j.rser.2011.04.013.

[13] Raluy R, Serra L, Guadalfajara M, Lozano M. Life Cycle Assessment of Central Solar Heating Plants with Seasonal Storage. Energy Procedia 2014;48:966–76. doi:10.1016/j.egypro.2014.02.110.

[14] European Solar Thermal Industry Federation (ESTIF). Solar heat markets in Europe: Trends and Market Statistics 2016. Brussels: 2016.

[15] Carrilho da Graça G, Augusto A, Lerer MM. Solar powered net zero energy houses for southern Europe: Feasibility study. Sol Energy 2012;86:634–46. doi:10.1016/j.solener.2011.11.008.

[16] Abokersh M, Osman M, El-Baz O, El-Morsi M, Sharaf O. Review on the Use of Phase Change Material in Domestic Solar Water Heating Systems. Int J Energy Res 2018;42:329–57. doi:10.1002/er.3765.

[17] McDaniel B, Kosanovic D. Modeling of combined heat and power plant performance with seasonal thermal energy storage. J Energy Storage 2016;7:13–23. doi:10.1016/j.est.2016.04.006.

[18] Ibrahim NI, Al-Sulaiman FA, Rahman S, Yilbas BS, Sahin AZ. Heat transfer enhancement of phase change materials for thermal energy storage applications: A critical review. Renew Sustain Energy Rev 2017;74:26–50. doi:10.1016/j.rser.2017.01.169.

[19] Antoniadis CN, Martinopoulos G. Simulation of Solar Thermal Systems with Seasonal Storage Operation for Residential Scale Applications. Procedia Environ Sci 2017;38:405–12. doi:10.1016/j.proenv.2017.03.124.

[20] Dincer I. On thermal energy storage systems and applications in buildings. Energy

Build 2002;34:377–88. doi:10.1016/S0378-7788(01)00126-8.

[21] Fisch MN, Guigas M, Dalenbäck JO. A review of large-scale solar heating systems in Europe. Sol Energy 1998;63:355–66. doi:10.1016/S0038-092X(98)00103-0.

[22] Hesaraki A, Holmberg S, Haghighat F. Seasonal thermal energy storage with heat pumps and low temperatures in building projects - A comparative review. Renew Sustain Energy Rev 2015;43:1199–213. doi:10.1016/j.rser.2014.12.002.

[23] Speyer E. Optimum storage of heat with a solar house. Sol Energy 1959;3:24–48. doi:10.1016/0038-092X(59)90004-0.

[24] Ochs F, Heidemann W, M. ller-Steinhagen H. Performance of Large-Scale Seasonal Thermal Energy Stores. J Sol Energy Eng 2009;131:041005. doi:10.1115/1.3197842.

[25] Bankston CA. The status and potential of central solar heating plants with seasonal storage: An international Report. Adances Sol. Energy, New York: Plenum Press; 1988, p. 352–444.

[26] Tian Z, Perers B, Furbo S, Fan J. Annual measured and simulated thermal performance analysis of a hybrid solar district heating plant with flat plate collectors and parabolic trough collectors in series. Appl Energy 2017;205:417–27. doi:10.1016/j.apenergy.2017.07.139.

[27] Weiss W, Spörk-Dür M, Mauthner F. Solar Heat Worldwide: Global Market Development and Trends in 2016. Gleisdorf, Austria: 2017.

[28] European Solar Thermal Industry Federation. Solar Thermal Markets in Europe. Trends and Market Statistics 2014. Brussel - Belgium: 2015.

[29] Koohi-Fayegh S, Rosen MA. Optimization of seasonal storage for community-level energy systems: status and needs. Energy, Ecol Environ 2017. doi:10.1007/s40974-017-0051-1.

[30] Novo A V., Bayon JR, Castro-Fresno D, Rodriguez-Hernandez J. Review of seasonal heat storage in large basins: Water tanks and gravel–water pits. Appl Energy 2010;87:390–7. doi:10.1016/j.apenergy.2009.06.033.

[31] Bauer D, Marx R, Nußbicker-Lux J. German central solar heating plants with seasonal heat storage. Sol Energy 2010;84:612–23.

doi:10.1016/j.solener.2009.05.013.

[32] Guadalfajara M, Lozano MA, Serra LM. Comparison of simple methods for the design of central solar heating plants with seasonal storage. Energy Procedia 2014;48:1110–7. doi:10.1016/j.egypro.2014.02.125.

[33] Guadalfajara M, Lozano M a. A, Serra LMM. Simple calculation tool for central solar heating plants with seasonal storage. Sol Energy 2015;120:72–86. doi:10.1016/j.solener.2015.06.011.

[34] Xu Q, Dubljevic S. Model predictive control of solar thermal system with borehole seasonal storage. Comput Chem Eng 2017;101:59–72. doi:10.1016/j.compchemeng.2017.02.023.

[35] Liu L, Zhu N, Zhao J. Thermal equilibrium research of solar seasonal storage system coupling with ground-source heat pump. Energy 2016;99:83–90. doi:10.1016/j.energy.2016.01.053.

[36] Guadalfajara M, Lozano MA, Serra LM. Evaluation of the potential of large solar heating plants in Spain. Energy Procedia 2012;30:839–48. doi:10.1016/j.egypro.2012.11.095.

[37] Ucar A, Inalli M. Thermal and economic comparisons of solar heating systems with seasonal storage used in building heating. Renew Energy 2008;33:2532–9. doi:10.1016/j.renene.2008.02.019.

[38] Paiho S, Hoang H, Hukkalainen M. Energy and emission analyses of solar assisted local energy solutions with seasonal heat storage in a Finnish case district. Renew Energy 2017;107:147–55. doi:10.1016/j.renene.2017.02.003.

[39] Li X, Liu M, Duanmu L, Ji Y. The Optimization of Solar Heating System with Seasonal Storage Based on a Real Project. Procedia Eng 2015;121:1341–8. doi:10.1016/j.proeng.2015.09.017.

[40] Ucar A, Inalli M. A thermo-economical optimization of a domestic solar heating plant with seasonal storage. Appl Therm Eng 2007;27:450–6. doi:10.1016/j.applthermaleng.2006.06.010.

[41] Durão B, Joyce A, Mendes JF. Optimization of a seasonal storage solar system using Genetic Algorithms. Sol Energy 2014;101:160–6. doi:10.1016/j.solener.2013.12.031.

[42] Buoro D, Pinamonti P, Reini M. Optimization of a Distributed Cogeneration System with solar district heating. Appl Energy 2014;124:298–308. doi:10.1016/j.apenergy.2014.02.062.

[43] Tulus V, Boer D, Cabeza LF, Jiménez L, Guillén-Gosálbez G. Enhanced thermal energy supply via central solar heating plants with seasonal storage: A multi-objective optimization approach. Appl Energy 2016;181:549–61. doi:10.1016/j.apenergy.2016.08.037.

[44] Pavičević M, Novosel T, Pukšec T, Duić N. Hourly optimization and sizing of district heating systems considering building refurbishment – Case study for the city of Zagreb. Energy 2017;137:1264–76. doi:10.1016/j.energy.2017.06.105.

[45] Xu J, Wang RZ, Li Y. A review of available technologies for seasonal thermal energy storage. Sol Energy 2014;103:610–38. doi:10.1016/j.solener.2013.06.006.

[46] Sibbitt B, McClenahan D, Djebbar R, Thornton J, Wong B, Carriere J, et al. The performance of a high solar fraction seasonal storage district heating system - Five years of operation. Energy Procedia 2012;30:856–65. doi:10.1016/j.egypro.2012.11.097.

[47] Flynn C, Sirén K. Influence of location and design on the performance of a solar district heating system equipped with borehole seasonal storage. Renew Energy 2015;81:377–88. doi:10.1016/j.renene.2015.03.036.

[48] Edenhofer O, Pichs-Madruga R, Sokona Y, Seyboth K, Eickemeier P, Matschoss P, et al. Renewable Energy Sources and Climate Change Mitigation: Summary for Policymakers and Technical Summary. 2011. doi:10.5860/CHOICE.49-6309.

[49] Teske S, Janis L, Luis C, Marcel B, Elena D, Christoph R, et al. Solar Thermal Electricity Global Outlook 2016. Amsterdam: 2016.

[50] Klein SA et al. TRNSYS Version. 18, Solar Energy Laboratory, University of Wisconsin-Madison, Website: <http://sel.me.wisc.edu/ trnsys> 2004.

[51] Wetter M. GenOpt. Generic Optimization Program. User Manual. Berkeley Lab 2011:1–108.

[52] Raab S, Mangold D, Müller-Steinhagen H. Validation of a computer model for solar assisted district heating systems with seasonal hot water heat store. Sol Energy 2005;79:531–43. doi:10.1016/j.solener.2004.10.014.

[53] Gebreslassie HB, Gosálbez GG, Jiménez L, Boer D. Design of environmentally conscious absorption cooling systems via multi-objective optimization and life cycle assessment. Appl Energy 2009;86:1712–22. doi:10.1016/j.apenergy.2008.11.019.

[54] Carreras J, Boer D, Guillén-Gosálbez G, Cabeza LF, Medrano M, Jiménez L. Multi-objective optimization of thermal modelled cubicles considering the total cost and life cycle environmental impact. Energy Build 2015;88:335–46. doi:10.1016/j.enbuild.2014.12.007.

[55] Sameti M, Haghighat F. A two-level multi-objective optimization for simultaneous design and scheduling of a district energy system. Appl Energy 2017;208:1053–70. doi:10.1016/j.apenergy.2017.09.046.

[56] Di Somma M, Yan B, Bianco N, Graditi G, Luh PB, Mongibello L, et al. Multi-objective design optimization of distributed energy systems through cost and exergy assessments. Appl Energy 2017;204:1299–316. doi:10.1016/j.apenergy.2017.03.105.

[57] Zheng X, Wu G, Qiu Y, Zhan X, Shah N, Li N, et al. A MINLP multi-objective optimization model for operational planning of a case study CCHP system in urban China. Appl Energy 2018;210:1126–40. doi:10.1016/j.apenergy.2017.06.038.

[58] Duffie, J.A., Beckman WA. Solar Engineering of Thermal Processes. 3rd ed. John Wiley & Sons, Inc; 2006.

[59] Allouhi A, Agrouaz Y, Benzakour Amine M, Rehman S, Buker MS, Kousksou T, et al. Design optimization of a multi-temperature solar thermal heating system for an industrial process. Appl Energy 2017;206:382–92. doi:10.1016/j.apenergy.2017.08.196.

[60] Hobbi A, Siddiqui K. Optimal design of a forced circulation solar water heating system for a residential unit in cold climate using TRNSYS. Sol Energy 2009;83:700–14. doi:10.1016/j.solener.2008.10.018.

[61] Hang Y, Qu M, Ukkusuri S. Optimizing the design of a solar cooling system using central composite design techniques. Energy Build 2011;43:988–94. doi:10.1016/j.enbuild.2010.12.024.

[62] Kalogirou SA. Solar energy engineering: processes and systems. 1st Ed. Academic Press; 2009. doi:10.1016/B978-0-12-374501-9.00014-5.

[63] Gluch P, Baumann H. The life cycle costing (LCC) approach: A conceptual discussion of its usefulness for environmental decision-making. Build Environ 2004;39:571–80. doi:10.1016/j.buildenv.2003.10.008.

[64] Chemical Engineering Plant Cost Index (CEPCI): Economic Indicator. Chem Eng J 2015. http://www.chemengonline.com/pci-home (accessed July 13, 2015).

[65] Nemerow NL, Agardy FJ, Sullivan P, Salvato JA. ENVIRONMENTAL ENGINEERING: Environmental Health and Safety for Municipal Infrastructure, Land Use and Planning, and Industry. 6th ed. John Wiley & Sons, Inc; 2009.

[66] ISO/TC 207/SC 5, International Organization for Standardization (ISO). ISO 14040:2006 Environmental management — Life cycle assessment — Principles and framework. Geneva: 2006. doi:10.1002/jtr.

[67] International Organization for Standardization (ISO). ISO 14041: Environmental Management - Life Cycle Assessment: Goal and Scope Definition and Inventory Analysis. 1997.

[68] International Organization for Standardization (ISO). ISO 14042:Environmental management - Life cycle assessment - Life cycle impact. 2000.

[69] Guillén-Gosálbez G, Caballero JA, Jiménez L. Application of Life Cycle Assessment to the Structural Optimization of Process Flowsheets. Ind Eng Chem Res 2008;47:777–89. doi:10.1016/S1570-7946(07)80218-5.

[70] Weidema BP, Bauer C, Hischier R, Mutel C, Nemecek T, Reinhard J, et al. Data quality guideline for the ecoinvent database version 3. vol. 3. 2013.

[71] Goedkoop M, Heijungs R, De Schryver A, Struijs J, van Zelm R, Huijbregts M, et al. ReCiPe 2008. A LCIA method which comprises harmonised category indicators at the midpoint and the endpoint level. Report I: Characterisation 2009:1–133. doi:http://www.lcia-recipe.net.

[72] JRC European commission (JRC-IES). ILCD Handbook: Recommendations for Life Cycle Impact Assessment in the European context. 1st editio. Luxemburg: Office of the European Union; 2011. doi:10.278/33030.

[73] Weiss W, Biermayr P. Potential of Solar Thermal in Europe. 2010.

[74] Hutchens P, Paul Hutchens. Solar Heating Roadmap: Strategy and Measures of the Solar Heating Industry for Accelerated Market Growth to 2030. Berlin: 2012.

[75] Greenpeace international. Energy Revolution: A sustainable pathway to a clean energy future for europe. 2005.

[76] Rout UK, Blesl M, Fahl U, Remme U, Voß A. Uncertainty in the learning rates of energy technologies: An experiment in a global multi-regional energy system model. Energy Policy 2009;37:4927–42. doi:10.1016/j.enpol.2009.06.056.

[77] Rubin ES, Azevedo IML, Jaramillo P, Yeh S. A review of learning rates for electricity supply technologies. Energy Policy 2015;86:198–218. doi:10.1016/j.enpol.2015.06.011.

[78] Ehrgott M. Multicriteria optimization. Heidelberg: Springer; 2005.

[79] Kennedy J, Eberhart R. Particle swarm optimization. Neural Networks, 1995 Proceedings, IEEE Int Conf 1995;4:1942–8 vol.4. doi:10.1109/ICNN.1995.488968.

[80] Kennedy J, Eberhart RC. A discrete binary version of the particle swarm algorithm. 1997 IEEE Int Conf Syst Man, Cybern Comput Cybern Simul 1997;5:4–8. doi:10.1109/ICSMC.1997.637339.

[81] Hooke R, Jeeves TA. “Direct Search” Solution of Numerical and Statistical Problems. J ACM 1961;8:212–29. doi:10.1145/321062.321069.

[82] Institute for Energy Diversification and Saving - IDAE, IDAE. Análisis del consumo energético del sector residencial en España. INFORME FINAL. 2011.

[83] Shariah A, Al-Akhras MA, Al-Omari I a. Optimizing the tilt angle of solar collectors. Renew Energy 2002;26:587–98. doi:10.1016/S0960-1481(01)00106-9.

[84] United Nations Environment Programme, Solar Thermal Energy Technology Fact Sheet. 2014.

[85] Colclough S, McGrath T. Net energy analysis of a solar combi system with Seasonal Thermal Energy Store. Appl Energy 2015;147:611–6. doi:10.1016/j.apenergy.2015.02.088.

[86] Kottek M, Grieser J, Beck C, Rudolf B, Rubel F. World map of the Köppen-Geiger climate classification updated. Meteorol Zeitschrift 2006;15:259–63. doi:10.1127/0941-2948/2006/0130.

[87] Rubel F, Kottek M. Observed and projected climate shifts 1901-2100 depicted by world maps of the Köppen-Geiger climate classification. Meteorol Zeitschrift 2010;19:135–41. doi:10.1127/0941-2948/2010/0430.

[88] U.S. Department of Energy. EnergyPlus. Energy Simulation Software: Weather Data n.d. http://apps1.eere.energy.gov/buildings/energyplus/ (accessed March 23, 2018).

[89] European Commission. Eurostat. Energy database n.d. http://ec.europa.eu/eurostat/data/database (accessed May 10, 2018).

[90] Weidema BP, Bauer C, Hischier R, Mutel C, Nemecek T, Reinhard J, et al. The ecoinvent database: Overview and methodology, Data quality guideline for the ecoinvent database version 3 2013. www.ecoinvent.org.

[91] Trimble. SketchUp 2017. http://www.sketchup.com.

[92] Ahmed K, Pylsy P, Kurnitski J. Hourly consumption profiles of domestic hot water for different occupant groups in dwellings. Sol Energy 2016;137:516–30. doi:10.1016/j.solener.2016.08.033.

[93] Instituto de Estadística. Trends in households in the European Union: 1995-2025 2003.

[94] Parakosta K, Papageorgiou N, Sotiropoulos B. Residential hot water use pattern in Greece. Sol Energy 1995;54:369–74.

[95] Ahmed K, Pylsy P, Kurnitski J. Monthly domestic hot water profiles for energy calculation in Finnish apartment buildings. Energy Build 2015;97:77–85. doi:10.1016/j.enbuild.2015.03.051.

[96] Jordan U, Vajen K. DHWcalc: program to generate domestic hot water profiles with statistical means for user defined conditions. Proc. ISES Sol. World Congr., Orlando (US): n.d., p. 8–12.

[97] Eurostat. Inflation in the euro area 2018. https://ec.europa.eu/eurostat/.../Inflation_in_the_euro_area (accessed March 12, 2018).

[98] Braungardt S, Eichhammer W, Elsland R, Fleiter T, Klobasa M, Krail M, et al. Study evaluating the current energy efficiency policy framework in the EU and providing orientation on policy options for realising the cost-effective energy-

efficiency/saving potential until 2020 and beyond. Karlsruhe/Vienna/Rome: 2014.

[99] Greenpeace international. Energy [R]evolution - A sustainable EU 27 energy outlook. 2012.

[100] Joachim Nitsch, Thomas Pregger, Scholz Y, Naegler T, Sterner M, Gerhardt N, et al. Langfristszenarien und Strategien für den Ausbau der Erneuerbaren Energien in Deutschland bei Berücksichtigung der Entwicklung in Europa und global. 2012. doi:BMU - FKZ 03MAP146.

[101] Kost C, Mayer JN, Thomsen J, Hartmann N, Senkpiel C, Philipps S, et al. Levelized Cost of Electricity Renewable Energy Technologies. Freiburg, Germany: 2013. doi:10.1613/jair.301.

[102] Montgomery DC. Design and Analysis of Experiments Eighth Edition. John Wiley & Sons, Inc.; 2013. doi:10.1198/tech.2006.s372.

IV CASE STUDY: PASSIVHAUS

Multi-objective optimization of a solar combi-system with seasonal thermal energy storage coupled to a passive house **

Victor Tulus [a], Shane Colclough [b], Philip Griffiths [b], Joshua Clarke [c], James T. McLeskey Jr. [c,d], Laureano Jiménez [a], Dieter Boer [e,*]

[a] Departament d'Enginyeria Química, Universitat Rovira i Virgili, Av. Països Catalans 26, 43007 Tarragona, Spain

[b] Built Environment Research Institute, Ulster University, Shore Rd, BT37 0QB, Newtownabbey, Co. Antrim, Northern Ireland

[c] Virginia Commonwealth University, Richmond, Virginia, USA

[d] Department of Physics, Randolph-Macon College, Ashland, 23005, Virginia, USA

[e] Departament d'Enginyeria Mecànica, Universitat Rovira i Virgili, Av. Països Catalans 26, 43007

** Corresponding author: dieter.boer@urv.cat*

** Ongoing work

Keywords:

seasonal thermal energy storage
solar assisted
multi-objective optimization
life cycle cost (LCC)
life cycle assessment (LCA)
modeling
TRNSYS
buildings

1. INTRODUCTION

Substantial reductions of greenhouse gas emissions are expected among the optimized solutions, which could reduce climate risks [5]. The World energy outlook 2015 proposed in their strategy to implement policy measures to increase energy efficiency in industry, buildings and transport sectors and to increase investment in renewable energies in order to address the climate change issue [6]. Research and implementation of technologies with the potential of a significant reduction of energy consumption and emissions are required.

In the building sector, space and water heating represent a major contribution to energy consumption. Seasonal thermal energy storage (STES) when combined with solar thermal energy [7] has the potential to significantly increase solar fractions for space heating [8,9]. Thus, emissions could be reduced by more than half. An overview on seasonal thermal energy storage technologies can be found in [10,11]. In the past 30 years more than 30 pilot installations were realized. They have shown to be technically feasible and reliable [12]. Most installations are for large applications as buildings or district heating systems. More information on existing plants can be found for different countries: Poland [13], Germany [14,15], Sweden [16] and Canada [17].

Only a few articles were published on existing smaller systems. High initial cost presents a barrier, but the combination with passive house design can make STES more competitive [18]. Critical success factors for passive houses were discussed by Colclough et al. [19]. One representative example for this type of system is a passive house with seasonal store in Ireland [20,21]. Regarding this concept of combining passive house architecture and seasonal storage further analysis was done including energy [22] and financial analysis [23].

Modelling presents a necessary step towards further improving the design and the operation of STES. Models were presented both for buildings and single-family houses. Hugo [24] modelled a residential building in Canada and included a life cycle analysis. Terziotti et al. [25] evaluated a five story student housing complex in USA. Single family houses were considered by Wills [26] for Canada and Sweet & McLeskey Jr. [27] for USA. Optimal ratios between the main system's parameters were determined by Pahud [28]. A simplified model to predict solar fraction was presented by Guadalfajara et al. [29].

Models which were validated by comparison with existing installations were achieved for a district heating systems in Germany [30], 52 detached energy-efficient homes through a district heating network in Canada [17] and a passive house in Ireland [21].

Once these models were established, they present a powerful tool to further optimize STES systems. Buoro et al. [31] minimized the total annual cost of a solar thermal plant and CHP with STES. The MILP model used the sizes of various components as decision variables. The model of Durão et al. [32] aimed to satisfy the total energy required for the greenhouse heating, during the four coldest months of the year. The area of solar collectors and the capacity of the storage tank were the basic sizing parameters in their genetic algorithm. Tulus et al. [33] presented a multi-objective optimization of a complex of residential buildings minimizing simultaneously economic cost and environmental impact with collector area and storage volume as decision variables. Rey and Zmeureanu [34] proposed a bi-objective optimization of a residential solar thermal combisystem reducing the life cycle cost and life cycle energy. Both previously mentioned studies were based on a simulation model.

In addition to the already mentioned economic and energetic aspects, environmental aspects should also be introduced in a thorough analysis of STES. The life cycle assessment (LCA) emerged as a prevalent approach that takes into account the environmental impact during the whole lifecycle of a process, product or activity [4]. Concerning STES Raluy et al. [35] carried out a LCA of a central solar heating plant with seasonal storage and Tulus et al. [33] combined LCA with economic aspects.

Economic and environmental objectives are usually considered as conflicting targets. To solve this kind of problem, multi-objective optimization (MOO) techniques can be applied to obtain the Pareto optimal trade-off solutions for the pursued objectives [36–39].

This work integrates LCA and MOO in the modelling approach. It proposes a further research in the field of STES for passive single-family houses. The simulation is based on an existing and validated model [21]. A multi-objective optimization approach aims towards a systematic analysis of the size of solar collectors and seasonal storage to minimize the economic cost and environmental impact simultaneously.

2. PROBLEM STATEMENT

A passive house situated in Galway, Ireland with a solar assisted seasonal store (SASS) is simulated in TRNSYS 18. The model was validated for the original configuration. The objective is to further improve the existing design considering the sizing of the main components. Both solar collector area and storage size are the decision variables. Objective functions are the cost saving/economic cost and the environmental impact. The former is evaluated following the live cycle cost methodology. The environmental impact is evaluated by the life cycle assessment (LCA) using the ReCiPe 2008 methodology. The objective functions have to be optimized simultaneously to obtain the trade-off Pareto optimal solutions.

3. METHODOLOGY

The present work describes the integration of a TRNSYS model with an external optimization algorithm. The TRNSYS model is presented in detail by Clarke et al. [21]. The schematic representation of the process flow can be observed in Fig. IV-1.

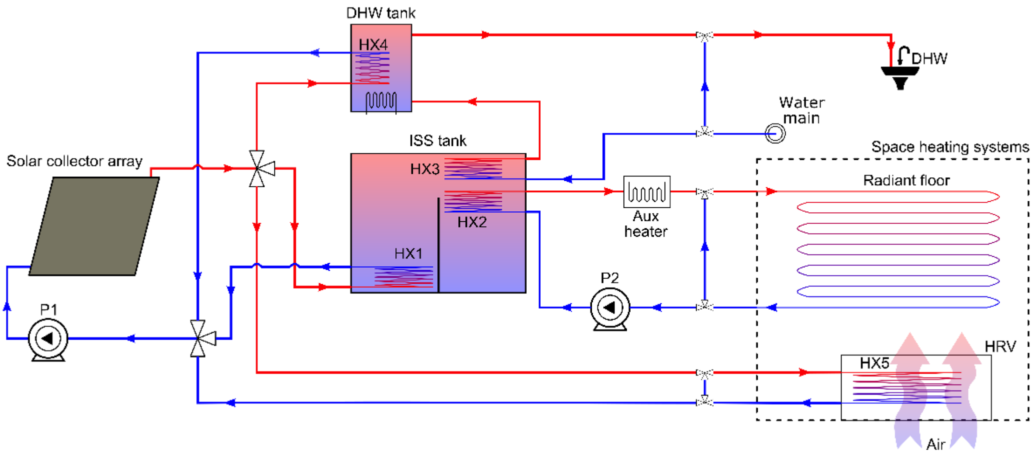

Fig. IV-1. Process flow diagram of the solar thermal combi-system with seasonal storage simulated in TRNSYS and validated in the Galway pilot plant.

4. CASE STUDY

Our study considers as base case a passive house with a seasonal store located in Galway, Ireland (Fig. IV-2). Measured data for 2010 were used for validation. Galway presents temperate maritime climate, and for the year 2010, the lowest monthly average temperature was 0ºC in December and the highest was 19ºC in June.

Fig. IV-2. Passive house in Galway (Ireland).

The total annual heat demand of the house was 2050 kWh (9.5 kWh/m^{2}a). Space heating demand was 1198 kWh, and domestic hot water accounted for 852 kWh. The home is equipped with a south facing 10.6 m2 solar thermal collector array inclined at 35º above the horizontal. This array was exposed to a total of 1160 kWh/m2 of solar irradiation over the course of 2010. Incoming solar radiation is used to heat a water/ethylene glycol mixture, which in turn heats domestic hot water and space heating via heat exchangers. Any heat that is not used directly is then stored by heating water in a 23 m^3 underground inter-seasonal storage tank (Fig. IV-3). Water was chosen as the storage medium. Details can be found in [20]. This configuration presents the base case of our model.

Concerning the economic analysis, we define an annual discount rate of 3%. All the equipment is supposed to have 25 years lifetime operation, except for the storage tank which will be amortized for 50 years. To define the electricity price for Ireland we used Eurostat price for 2018 which is 0.2407 €/kWh. We also assume an annual rate of inflation of 7.3% for the price of electricity. These taxes are supposed to be constant during the lifetime of the plant. The environmental impact is evaluated by the life cycle assessment (LCA) using the ReCiPe 2008 methodology [40].

Fig. IV-3. Inter-seasonal storage tank

5. EXPECTED RESULTS

At the moment of writing of this thesis, the aforementioned simulation model presents several convergence problems in some equipment units, such as the seasonal storage tank, control loops and downstream secondary units. We believe that this problem appeared due to the upgrading to TRNSYS 18 (the validated model provided to us by the co-authors was developed in TNSYS 16). The non-convergence of the Type 60d (storage tank) is a known problem and in the new version it has already been removed.

The next step will be to find and connect a different type for the storage tank, the same will have to be done with the other obsolete types used in the model. The updated model will have to be validated again and then we will be able to proceed with the optimization process.

Another problem of the TRNSYS model is the simulation times. It would take more than 5 minutes to perform a single simulation, translating this to the optimization process will take too much time to obtain the Pareto set. We believe that this is due to the complexity of the model and the big number of free variables which could be referenced to other variables in the model for simplicity. The other level of unnecessary calculations is the inclusion of the building in the simulation model. To simplify this, the demand data obtained from the building can be obtained after one-time simulation and included in the model as a data file. These steps should reduce the simulation time and consequently the overall optimization process.

We expect promising results which will be comparable to our previous results in a large scale. That is, due to the present financial situation, economically the optimized system may not be attractive, but the environmental part should achieve a significant reduction. We plan to compare these results with our previous works and extract conclusions about the different scales of such systems, going from large systems covering heat demands of a neighborhood to a small system covering the demand of single-family house. We expect to obtain some trends in that direction.

REFERENCES

[1] Klein SA et al. TRNSYS Version. 18, Solar Energy Laboratory, University of Wisconsin-Madison, Website: <http://sel.me.wisc.edu/ trnsys> 2004.

[2] Wetter M. GenOpt. Generic Optimization Program. User Manual. Berkeley Lab 2016:1–108.

[3] Kalogirou SA. Chapter twelve - Solar Economic Analysis. Sol. Energy Eng., Academic Press; 2009, p. 665–701. doi:10.1016/B978-0-12-374501-9.00012-1.

[4] ISO/TC 207/SC 5. ISO 14044:2006 Environmental management — Life cycle assessment — Requirements and guidelines 2006.

[5] IPCC. Climate Change 2014: Synthesis Report. Contribution of Working Groups I, II and III to the Fifth Assessment Report of the Intergovernmental Panel on Climate Change. Geneva, Switzerland: 2014. doi:10.1017/CBO9781107415324.

[6] IEA. Energy and Climate Change. World Energy Outlook Spec Rep 2015:1–200. doi:10.1038/479267b.

[7] Dalenbäck J. Central solar heating plants with seasonal storage: status report. Göteborg, Sweden: 1990.

[8] Marx R, Nußbicker-Lux J, Bauer D, Heidemann W, Drück H. Saisonale Wärmespeicher - Bauarten, Betriebsweise und Anwendungen. Chemie Ing Tech 2011;83:1994–2001. doi:10.1002/cite.201100064.

[9] Guadalfajara M, Lozano MA, Serra LM. Evaluation of the potential of large solar heating plants in Spain. Energy Procedia 2012;30:839–48. doi:10.1016/j.egypro.2012.11.095.

[10] Haghighat F. Applying Energy Storage in Building of the Future Best Practice for Architects and Engineers. 2013. doi:10.13140/RG.2.1.4477.3282.

[11] Pinel P, Cruickshank CA, Beausoleil-Morrison I, Wills A. A review of available methods for seasonal storage of solar thermal energy in residential applications. Renew Sustain Energy Rev 2011;15:3341–59. doi:10.1016/j.rser.2011.04.013.

[12] Ochs F, Heidemann W, Müller-Steinhagen H. Performance of Large-Scale Seasonal Thermal Energy Stores. J Sol Energy Eng 2009;131:041005.

doi:10.1115/1.3197842.

[13] Milewski J, Bujalski W. STES—Typical Scenarios for Heat Accumulator Cooperation. Energy Procedia 2014;50:414–20. doi:10.1016/j.egypro.2014.06.050.

[14] Mangold D, Schmidt T, Lottner V, Schimdt T, Mangold D, Müller-Steinhagen H, et al. Seasonal thermal energy storage in Germany. Futurestock 2003;14:1–7. doi:10.2749/101686604777963739.

[15] Bauer D, Marx R, Nußbicker-Lux J. German central solar heating plants with seasonal heat storage. Sol Energy 2010;84:612–23. doi:10.1016/j.solener.2009.05.013.

[16] Lundh M, Dalenbäck JO. Swedish solar heated residential area with seasonal storage in rock: Initial evaluation. Renew Energy 2008;33:703–11. doi:10.1016/j.renene.2007.03.024.

[17] Sibbitt B, McClenahan D, Djebbar R, Thornton J, Wong B, Carriere J, et al. The performance of a high solar fraction seasonal storage district heating system - Five years of operation. Energy Procedia 2012;30:856–65. doi:10.1016/j.egypro.2012.11.097.

[18] Persson J, Westermark M. Low-energy buildings and seasonal thermal energy storages from a behavioral economics perspective. Appl Energy 2013;112:975–80. doi:10.1016/j.apenergy.2013.03.047.

[19] Colclough S, Griffiths P, Smyth M. Solar Energy Storage – Critical Success Factors for Passive Houses in Ireland 2010:1–6.

[20] Colclough S. Thermal energy storage applied to the Passivhaus standard in the Irish climate. 2011.

[21] Clarke J, Colclough S, Griffiths P, McLeskey Jr. JT. A passive house with seasonal solar energy store: in situ data and numerical modelling. Int J Ambient Energy 2014;35:37–50. doi:10.1080/01430750.2012.759153.

[22] Colclough S, McGrath T. Net energy analysis of a solar combi system with Seasonal Thermal Energy Store. Appl Energy 2015;147:611–6. doi:10.1016/j.apenergy.2015.02.088.

[23] Colclough S, Griffiths P. Financial analysis of an installed small scale seasonal

thermal energy store. Renew Energy 2016;86:422–8. doi:10.1016/j.renene.2015.08.032.

[24] Hugo A. Computer simulation and life cycle analysis of a seasonal thermal storage system in a residential building. 2008. doi:10.1073/pnas.0703993104.

[25] Terziotti LT, Sweet ML, McLeskey Jr. JT. Modeling seasonal solar thermal energy storage in a large urban residential building using TRNSYS 16. Energy Build 2012;45:28–31. doi:10.1016/j.enbuild.2011.10.023.

[26] Wills AD. Design and co-simulation of a seasonal solar thermal system for a Canadian single – family detached house. 2013.

[27] Sweet MLML, McLeskey JT, Jr JM. Numerical simulation of underground Seasonal Solar Thermal Energy Storage (SSTES) for a single family dwelling using TRNSYS. Sol Energy 2012;86:289–300. doi:10.1016/j.solener.2011.10.002.

[28] Pahud D. Central solar heating plants with seasonal duct storage and short-term water storage: design guidelines obtained by dynamic system simulations. Sol Energy 2000;69:495–509. doi:10.1016/S0038-092X(00)00119-5.

[29] Guadalfajara M, Lozano M a. A, Serra LMM. Simple calculation tool for central solar heating plants with seasonal storage. Sol Energy 2015;120:72–86. doi:10.1016/j.solener.2015.06.011.

[30] Raab S, Mangold D, Müller-Steinhagen H. Validation of a computer model for solar assisted district heating systems with seasonal hot water heat store. Sol Energy 2005;79:531–43. doi:10.1016/j.solener.2004.10.014.

[31] Buoro D, Pinamonti P, Reini M. Optimization of a Distributed Cogeneration System with solar district heating. Appl Energy 2014;124:298–308. doi:10.1016/j.apenergy.2014.02.062.

[32] Durão B, Joyce A, Mendes JF. Optimization of a seasonal storage solar system using Genetic Algorithms. Sol Energy 2014;101:160–6. doi:10.1016/j.solener.2013.12.031.

[33] Tulus V, Boer D, Cabeza LF, Jiménez L, Guillén-Gosálbez G. Enhanced thermal energy supply via central solar heating plants with seasonal storage: A multi-objective optimization approach. Appl Energy 2016;181:549–61. doi:10.1016/j.apenergy.2016.08.037.

[34] Rey A, Zmeureanu R. Multi-objective optimization of a residential solar thermal combisystem. Sol Energy 2016;139:622–32. doi:10.1016/j.solener.2016.10.008.

[35] Raluy R, Serra L, Guadalfajara M, Lozano M. Life Cycle Assessment of Central Solar Heating Plants with Seasonal Storage. Energy Procedia 2014;48:966–76. doi:10.1016/j.egypro.2014.02.110.

[36] Carreras J, Boer D, Guillén-Gosálbez G, Cabeza LF, Medrano M, Jiménez L. Multi-objective optimization of thermal modelled cubicles considering the total cost and life cycle environmental impact. Energy Build 2015;88:335–46. doi:10.1016/j.enbuild.2014.12.007.

[37] Antipova E, Boer D, Cabeza LF, Guillén-Gosálbez G, Jiménez L. Multi-objective design of reverse osmosis plants integrated with solar Rankine cycles and thermal energy storage. Appl Energy 2013;102:1137–47. doi:10.1016/j.apenergy.2012.06.038.

[38] Salcedo R, Antipova E, Boer D, Jiménez L, Guillén-Gosálbez G. Multi-objective optimization of solar Rankine cycles coupled with reverse osmosis desalination considering economic and life cycle environmental concerns. Desalination 2012;286:358–71. doi:10.1016/j.desal.2011.11.050.

[39] Guillén-Gosálbez G, Mele FD, Grossmann IE. A Bi-Criterion Optimization Approach for the Design and Planning of Hydrogen Supply Chains for Vehicle Use. AIChE J 2010;56:650–67. doi:10.1002/aic.12024.

[40] Goedkoop M, Heijungs R, De Schryver A, Struijs J, van Zelm R, Huijbregts M, et al. ReCiPe 2008. A LCIA method which comprises harmonised category indicators at the midpoint and the endpoint level. Report I: Characterisation 2009:1–133. doi:http://www.lcia-recipe.net.

6. APPENDIX

In this appendix are presented the main input parameters of the TRNSYS 16 simulation model used trough the validation process.

Solar Pump (Type 3b)	Value	Units
Max Flow Rate	402	kg/hr
Fluid Specific Heat	3.6	kJ/kg.K
Max Power	36	kJ/hr
Conversion Coefficient	0.05	-
Power Coefficient(s)	0.5	-

Solar Collector (Type 1b)	Value	Units
Number in series	1	-
Collector Area	10.6	m^2
Fluid Specific Heat	3.6	kJ/kg.K
Efficiency Mode	1	-
Tested Flow Rate	40	kg/hr.m^2
Intercept Efficiency	0.65	-
Efficiency Slope	5.706	kJ/hr.m^2.K
Efficiency Curvature	0.007	kJ/hr.m^2.K^2
1st-order IAM	0.2	-
2nd-order IAM	0	-

DHW Tank (Type 60d)	Value	Units
Tank Volume	0.3	m^3
Tank Height	1.36	m
Height of Flow Inlet 1	0.1	m
Height of Flow Outlet 1	1.3	m
Fluid Specific Heat	4.19	kJ/kg.K
Fluid Density	1000	kg/m^3
Tank Loss Coefficient	3	kJ/hr.m^2.K
Fluid Thermal Conductivity	2.088	kJ/hr.m.K
Destratification Conductivity	0	kJ.hr.m.K
Boiling Temperature	100	C
Height of 1st aux heater	1.3	m
Height of 1st thermostat	0.75	m
Set point temp for element 1	60	C
Deadband for heating element 1	5	deltaC

Maximum heating rate of element 1	10800	kJ/hr
HX Fluid Indicator	3	-
Fraction of glycol	0.4	-
HX inside diameter	0.022	m
HX outside diameter	0.024	m
HX fin diameter	0.03	m
Total surface area of HX	1.2	m^2
Fins per meter for HX	300	-
HX length	4.5	m
HX wall conductivity	1440	kJ/hr.m.K
HX material conductivity	1440	kJ/hr.m.K
Height of HX inlet	0.2	m
Height of HX outlet	0.2	m
Nusselt constant for HX	0.5	-
Nusselt exponent for HX	0.25	-

HRV Duct Heater (Type 5e)	**Value**	**Units**
Specific Heat of Hot Side Fluid	3.6	kJ/kg.K
Specific Heat of Cold Side Fluid	1.005	kJ/kg.K
Overall Heat transfer coefficient of exchanger	311	kJ/hr.K
Cold Side flow rate	557	kg/hr

V GENERAL CONCLUSIONS

CONCLUSIONS

This work has been dedicated to developing simulation-based optimization models capable of assisting decision- and policy-makers in strive towards a sustainable future. Different simulation models of CSHPSS plants have been developed with an increase of complexity from the first case study to the others. Find below the summary of the knowledge gained from the study of the problems tackled in this thesis. Note that detailed discussions and conclusions related to every case study can be found in the corresponding chapter. The general conclusions are presented herein.

- Has been developed a multi-objective optimization approach to design complex central solar heating plants with seasonal storage taking into account the economic and environmental objectives simultaneously. The tool is intended to give support to the decision- and policy-makers.

- Generally speaking, all the investigated case studies display ranges of viability for CSHPSS installation in their respective regions taking into account the long-term utilization of the plant. The overall trend indicates that for the installation to be more profitable from the economic point of view, a better distribution of available and demanded energy is preferable (and this strongly depends on the climate conditions). On the other hand, from the environmental point of view all the cases showed great long-term reduction comparing to a natural gas system.

- The sensitivity analysis performed on the simulation-optimization model confirms fluctuations of around 10% in CSHPSS overall costs while increasing or decreasing the economic parameters up to 20%. Orders of magnitude higher dependency occurs in the total environmental impact of the CSHPSS while performing the same fluctuations in the economic parameters.

- Based on historically observed learning curves for the CSHPSS plants and the increasing trends in non-renewable energy costs, improved economic competitiveness is expected in the near future.

- The power of emerging simulation-based optimization methods has been proved in real-world case studies, therefore demonstrating their great potential in the application to computationally expensive, complex problems of the modern engineering.

- By the means of this work it has been proven that a sustainable development trajectory can be followed using the available tools. We have demonstrated that based on mathematical optimization models and methods, new decision-making support mechanisms can be developed to contribute towards the sustainable transition.

FUTURE WORK

Interesting new research lines were opened in the course of this work. Some of them have already drawn our attention; some others can potentially be the focus of future research works.

The variable scale of CSHPSS systems is an interesting topic. Potentially we could develop a model able to determine optimal demand sizes for a CSHPSS to become economically and environmentally attractive in the eye of the consumer. Our ongoing work will help us determine the viability of small scale, single-family systems, which can be the first step in a new research line.

Below we present potential research direction to be explored in the future:

- This thesis has contributed to two key structural transformations (energy and urban sustainability transformation), trying to tackle basically the climate change planetary boundary. Four other key structural transformations can be explored in the future to help the remaining planetary boundaries return into acceptable levels. These transformations are: i) food security transformation,

ii) population transformation, iii) biodiversity management transformation, iv) private and public governance transformation.

- The third sustainability pillar, social, was almost neglected in our research. Future works can incorporate social indicators as the third objective function. Although this task may seem challenging now due to the lack of standardized information on quantification of social aspects, new initiatives, like Social Life Cycle Assessment, are emerging and can become very attractive for a new research line.

- The deterministic nature of our models can be modified including all sorts of uncertainties in order to provide much more robust solutions in the future.

- Our CSHPSS models could be improved accounting for possible cooling demands from the consumers. This way the efficiency of the new system can potentially be increased, and overall costs and impacts can be gradually reduced.

- In the direction of mathematical programming research line stays the development of surrogate models computationally much cheaper to solve then our rigorous TRNSYS simulation models. Surrogate models can noticeably accelerate the optimization process, opening new horizons for optimization of simulation-based models.

VI APPENDICES

AUTHOR'S RESEARCH PROFILES (WITH UPDATED INFORMATION)

ORCID ID: *https://orcid.org/0000-0001-8774-9492*
SCOPUS ID: *57190865149*

LIST OF PUBLICATIONS

RESEARCH ARTICLES

Type: Research article in Scientific Journal
Status: Published (1 November 2016)
Title: ***"Enhanced thermal energy supply via central solar heating plants with seasonal storage: A multi-objective optimization approach"***
Full reference: **Elsevier Ltd., Applied Energy vol. 181 (2016) pp. 549–561 (ISSN: 0306-2619)**
Authors: Victor Tulus, Dieter Boer, Luisa F. Cabeza, Laureano Jiménez, Gonzalo Guillén-Gosálbez
Area/ SJR-2017: Energy/ 10 of 1212 (Q1), Engineering/ 33 of 6810 (Q1), Environmental science/ 24 of 1632 (Q1)
Impact Factor: 7.9
Citations: 24 (Google Scholar, 04/09/2018)

Type: Research article in Scientific Journal
Status: Submitted (September 2018)
Title: ***"Economic and environmental potentials for solar assisted central heating plants in the EU residential sector: Roadmap to the 2030 climate and energy EU targets"***
Journal: **Applied Energy**
Authors: Victor Tulus, Mohamed Hany Abokersh, Luisa F. Cabeza, Manel Vallès, Laureano Jiménez, Dieter Boer
Area/ SJR-2017: Energy/ 10 of 1212 (Q1), Engineering/ 33 of 6810 (Q1), Environmental science/ 24 of 1632 (Q1)
Impact Factor: 7.9
Citations: 0

BOOK CHAPTERS

V. Tulus, D. Boer, L. F. Cabeza, G. Guillén-Gosálbez, L. Jiménez
"Optimization of Thermal Energy Supply by Central Solar Heating Plants with Seasonal Storage"
2015 AIChE Annual Meeting Proceedings, 2015, Salt Lake City, USA, ISBN: 978-0-8169-1094-6

V. Tulus, D. Boer, L. F. Cabeza, G. Guillén-Gosálbez, L. Jiménez
"Potential of seasonal storage of thermal energy in Southern Europe"
EMChIE 2015 Conference Proceedings, 2015, Tarragona, Spain, ISBN: 978-84-8424-367-0

CONFERENCES

Oral communications

Title: ***"Multi-objective optimization of central solar heating plants with seasonal thermal energy storage"***
Authors: Victor Tulus, Luisa F. Cabeza, Laureano Jiménez, Gonzalo Guillén-Gosálbez, Álvaro de Gracia, Dieter Boer
Event: **10th World Congress of Chemical Engineering** (Barcelona, Spain. 1 - 5 October 2017)

Title: ***"Multi-objective optimization approach for a passive house with seasonal solar energy store"***
Authors: Victor Tulus, Shane Colclough, Philip Griffiths, Joshua Clarke, James T. McLeskey Jr., Laureano Jimenez, Dieter Boer
Event: **10º Congreso Nacional de Ingeniería Termodinámica** (Lleida, Spain. 28 - 30 June 2017)

Title: ***"Potential of seasonal storage of thermal energy in Southern Europe"***
Authors: Victor Tulus, Dieter Boer, Luisa F. Cabeza, Gonzalo Guillén-Gosálbez, Laureano Jiménez
Event: **7th European Meeting on Chemical Industry and Environment** (Tarragona, Spain. 10 – 12 June 2015)

Title: ***"Optimización multiobjetivo con TRNSYS: Aplicación a plantas solares de almacenamiento térmico estacional en edificios"***
Authors: Victor Tulus, Dieter Boer, Luisa F. Cabeza, Gonzalo Guillén-Gosálbez, Laureano Jiménez
Event: **9º Congreso Nacional de Ingeniería Termodinámica (**Cartagena, Spain. 3 – 5 June 2015)

Poster presentations

Title: ***"Optimization of Thermal Energy Supply by Central Solar Heating Plants with Seasonal Storage"***

Authors: Victor Tulus, Dieter Boer, Luisa F. Cabeza, Gonzalo Guillén-Gosálbez, Laureano Jiménez

Event: **2015 American Institute of Chemical Engineers (AIChE) Annual Meeting** (Salt Lake City, UT, USA. 8 – 13 November 2015)

MASTER THESES CO-SUPERVISION

Title: ***"Centrals solars tèrmiques amb emmagatzematge d'energia solar tèrmica. Viabilitat en distints climes"***

Author: Joan Pere Perelló Amengual

Supervisors: Dieter Boer, Victor Tulus

Master: Master of Industrial Engineering, Universitat Rovira i Virgili (2016-2017)

UNIVERSITAT
ROVIRA i VIRGILI